Imaging of the right ventricle in congenital heart disease

Hendrik G. Freling

Freling, H.G.
Imaging of the right ventricle in congenital heart disease

ISBN: 978-90-367-6705-7
ISBN: electronic version 978-90-367-6706-4

Cover & layout: H.G. Freling
Printed by: Gildeprint Drukkerijen, Enschede

rijksuniversiteit groningen

Imaging of the right ventricle in congenital heart disease

Proefschrift

ter verkrijging van de graad van doctor aan de
Rijksuniversiteit Groningen
op gezag van de
rector magnificus, prof. dr. E. Sterken
en volgens besluit van het College voor Promoties.

De openbare verdediging zal plaatsvinden op

woensdag 22 januari 2014 om 12.45 uur

door

Hendrik Gerardus Freling

geboren op 24 februari 1985
te IJsselstein

Promotor:
Prof. dr. D.J. van Veldhuisen

Copromotores:
Dr. T.P. Wilems
Dr. P.G. Pieper

Beoordelingscommissie:
Prof. dr. T. Ebels
Prof. dr. R.M.F. Berger
Prof. dr. A. de Roos

Financial support by the Dutch Heart Foundation for the publication of this thesis is gratefully acknowledged. The research described in this thesis was supported by a grant of the Dutch Heart Foundation (DHF-2013P129)

Further financial support is kindly provided by Fonds Radiologie, GUIDE, Medis medical imaging systems bv, Rijksuniversiteit Groningen, St Jude Medical, and Tafelronde 125 Zuid-Oost Drenthe (Matthijs Bakker, Hugo Bauerhuit, Marcel de Boer, Thijs Boersma, Hidde de Bruin, Harm Bruning, Marcel Brust, Arjen van Ess, Robin Mink, Roderick van Nie, Jeroen Schippers, Roderik Seubers, Simon van der Weerd, Friso Ypma)

Contents

1

General introduction and outline of the thesis

"The philosophies of one age have become the absurdities of the next, and the foolishness of yesterday has become the wisdom of tomorrow."

Sir William Osler

Historical perspective

The discovery of the anatomy and function of the right ventricle cannot be attributed to a single person nor to a single era. Over the centuries many erroneous ideas have been replaced with other, not necessarily correct, ideas. Religion and superstition dominated daily life for millennia and greatly influenced the perspective on the function of the heart and vessels. Moreover, many physicians were above all things theologians.

Ancient Greece

The first thorough description of right ventricular anatomy can be found in the Hippocratic Corpus, over 70 books written by Hippocrates (460-375 B.C.) and followers [1]. "The heart is an exceedingly strong muscle, 'muscle' in the sense not of 'tendon' but of a compressed mass of flesh. It contains in one circumference two separate cavities, one here, the other there. These cavities are quite dissimilar: the one on the right side lies face downwards, fitting closely against the other. By 'right' I mean of course the right of the left side, since it is on the left side that the whole heart has its seat. Furthermore this chamber is very spacious, and much more hollow than the other. It does not extend to the extremity of the heart, but leaves the apex solid, being as it were stitched on outside. The inside surface of both chambers is rough, as though slightly corroded; the left more so than the right"

The doctrine of Galen

Galen (131-201 A.D.), a brilliant physician, proved arteries contained blood and made a coherent concept of human physiology based on dissecting animals. He connected and integrated the vital functions of nutrition and respiration with the function of blood and the nervous system. As he was not aware of the presence of the circulation as we know it now, his description of the heart and vessel comprised two open-ended systems which provided one-time distribution of nutrients to the tissues. Absorbed food was made into blood containing 'nutritive spirits' by the liver. Veins, which all had their origin in the liver, distributed these 'nutritive spirits' throughout the entire body. He imagined the blood in the veins moved back and forth like tides of the sea. Part of the 'nutritive spirits' passed through invisible pores in the interventricular septum from the right to the left ventricle where it was mixed with air to form 'vital spirits'. 'Vital spirits', necessary for sustaining life and heat, were distributed by arteries. None of the blood entering the pulmonary artery arrived in the left side of the heart, but was

absorbed as nutrition by the lungs. So there was no separate systemic and pulmonary circulation in which arteries and veins were connected. Galen's theory on human physiology dominated Western medicine for fourteen centuries as he was seen as a divine man, the father of physicians. Furthermore, his theory was coherent and represented churchly doctrine.

Discovery of the circulation

At the end of the Middle Ages dissection of humans to study human anatomy and physiology was started once more and some physicians started questioning the authority of Galen. Michael Servatus (1511-1553) is considered the first to describe and publish the concept of the pulmonary circulation [2]. In fact he was the first European physician as three centuries before the pulmonary circulation was described by the Arab physician Ibn-an-Nafas [3]. His view on the pulmonary circulation was neglected and forgotten probably due to its heretical and original character. Michael Servatus described the pulmonary circulation in *De Christianismi Restitutio*. This was originally a theology work which intention was to prove the existence of the soul inside the blood [2]. "It (vital spirit) is a subtle spirit, generated by the power of heat, of yellow color and possessor of the power of the fire, so as to become a sort of lucid vapor of the purified blood, enclosing the elements of the water, the air and the fire. It is instantly produced inside the lungs by a mixture of inhaled air and subtle blood, while it is elaborated and communicated from the heart's right ventricle to the left one. This communication is not mediated via the median septum of the heart, as it is habitually thought; on the contrary, the subtle blood is transferred from the right ventricle, in a brilliant way, by following a long circuit through the lungs, which submits it into a transformation, in order for the blood to come out colored yellow: the arterial vein [pulmonary artery] transports it into the venous artery [pulmonary vein]. From that moment on, the blood is mixed in that very same venous artery with the inhaled air in order to become re-purified from all fuliginous materials, during this expiration. In this way, the entirety of this mixture is finally attracted by the left ventricle of the heart, during the diastole, to serve as a base for the vital spirit." *De Christianismi Restitutio* was the reason for condemning him to be burned at the stakes because it also preached nontrinitarianism and anti-infant baptism. Even in his last words he defied the inquisitor: "Oh Jesus, son of eternal God, have pity on me" [2].

Finally, William Harvey (1578-1657) explained the circulation and presented the determinant proofs in his thesis, *De Motu Cordis*, which established the foundation for the understanding of the systemic and pulmonary circulation [4].

He described the importance of right ventricular function: “Thus the right ventricle may be said to be made for the sake of transmitting blood through the lungs, not for nourishing them.” He knew his message would be controversial: “What remains to be said on the quantity and source of this transferred blood, is, even if carefully reflected upon, so strange and undreamed of, that not only do I fear danger to myself from the malice of a few, but I dread lest I have all men as enemies, so much does habit or doctrine (referring to Galen’s doctrine) once absorbed, driving deeply its roots, become second nature, and so much does reverence for antiquity influence all men. But now the die is cast, my hope is in the love of truth and in the integrity of intelligence.” The discovery of the circulation was received with great interest and accepted almost at once in his home country, England. On the mainland of Europe it won favor more slowly, however, before his death his concept was acknowledged by the medical profession [5].

Harvey’s followers have progressively completed the knowledge of cardiovascular physiology. However, up to the first half of the twentieth century there was almost no interest in the right ventricle. The main reason was the right ventricle was considered little more than a conduit for blood flow between the venous circulation and the pulmonary circulation [6]. Furthermore, how were they to investigate the right ventricle when there were almost no non-invasive tools to measure right ventricular function and volumes? This all changed with the emergence of cardiac surgery and new imaging modalities.

Anatomy and physiology

Septa divide the heart in a right- and left-sided compartment. The anulus fibrosus, a structure of dense connective tissue, subdivides each half of the heart into two cavities, the upper part being called atrium, the lower part ventricle. The morphology and structure of the right and left ventricle is substantially different as a result of the difference in origin of myocardial precursor cells and the vascular resistance of the pulmonary and systemic circulation [7,8]. Compared to the systemic circulation, the lungs are close to the heart and the pulmonary arteries and veins are relatively short and broad. This results in a low vascular resistance which can be easily overcome with a small increase in right ventricular pressure.

Compared to the left ventricle, the right ventricle has a complex geometry, with a triangular shape in the sagittal plane and a crescent shape in the coronal plane. The shape of a normal right ventricle can be imagined as a thin pouch that is wrapped around the thick ellipsoid left ventricle. Right ventricular mass is only one sixth of left ventricular mass. Functionally, the right ventricle can be divided into an inlet, outlet and apical coarsely trabeculated component. The inlet component consists of the tricuspid valve which is connected to its subvalvular apparatus. The subvalvular apparatus, comprising chordae tendineae and papillary muscles, prevents valve leaflets prolapsing into the atrium during ventricular contraction. The smooth walled muscular outlet, is separated from the inlet by a thick muscle, the crista supraventricularis, which arches from the anterolateral wall over the anterior leaflet of the tricuspid valve to the septal wall. At the lower septal segment of the crista supraventricularis, the septomarginal band originates and becomes continuous with the moderator band, which attaches to the lateral free wall and apex of the right ventricle [7].

Although the right ventricle is normally located on the right side of the heart and connected with the pulmonary circulation, this is not always the case in complex congenital heart disease. Several anatomic structures are distinctive features of the morphological right ventricle which can help differentiate the right from the left ventricle when imaging the heart. The right-sided atrioventricular valve has a trileaflet configuration with septal chordal and papillary insertions and a more apical hinge line of the septal leaflet relative to the anterior leaflet of the left-sided atrioventricular (mitral) valve. The right ventricular outflow tract is muscular and has no fibrous continuity with the atrioventricular valve. The apical trabeculae are much more coarsely than that of the left ventricle and the right ventricle has a moderator band [7].

Congenital heart disease

The emergence of cardiac surgery and advances in pediatric care dramatically increased the number of patients with complex congenital heart disease that survived into adulthood. Currently, the number of adults with complex congenital heart disease outnumber that of children [9]. In many patients with 'corrected' congenital heart disease the right ventricle has to perform under abnormal circumstances such as pressure or volume overload. The importance of the right ventricle became apparent after many of these patients developed short- and long- term complications. The normal healthy right ventricle performs under low pressures and is very compliant. The longitudinal orientation of most muscle fibers in the right ventricle results in a peristaltic contraction pattern that works as a bellows by pumping the blood against the interventricular septum towards the pulmonary artery. Although this mechanism generates low pressures, it is very efficient and can handle large changes in blood volume [7,8]. As the right and left ventricle share multiple muscle fibres, have a common interventricular septum and are constrained in the pericardial sac, both ventricles interact. In the normal heart, left ventricular contraction substantially contributes to rise in right ventricular pressure. Remodeling of the right ventricle in response to longstanding volume or pressure overload helps maintaining normal levels of cardiac output for a long period of time. Remodeling of the right ventricle involves a change in geometry of both ventricles with a progressively reduced diastolic left ventricular volume due to septal displacement and paradoxical systolic septal movement. This remodeling is detrimental for left ventricular output, especially during exercise [7,8]. Furthermore, in adulthood complications such as overt failure of the right ventricle, arrhythmias and sudden death often occur. Therefore, improving care in adult patients with congenital heart disease has in recent years focused on prevention of complications. Imaging of the right ventricle is indispensable in this setting. For example, most patients with 'repaired' tetralogy of Fallot have a volume overloaded right ventricle due to longstanding pulmonary regurgitation. This has been related to right ventricular dilation, right ventricular dysfunction, reduced left ventricular volumes, symptomatic heart failure, ventricular arrhythmia and sudden death [10-12]. Measurements of right and left ventricular volumes can guide timing of pulmonary valve replacement to relieve the volume overload and prevent these complications [13-17].

Cardiac imaging

Evaluation of right ventricular volumes and function is considered one of the cornerstones in the management of patients with 'repaired' congenital heart disease [10,11]. The right ventricle can be imaged with chest radiography, contrast angiography, radionuclide studies, computed tomography, echocardiography and cardiac magnetic resonance imaging. Preferably, imaging of right ventricular anatomy, volume and function is cheap, readily available, safe, accurate and reproducible. For serial measurements of the right ventricle during follow-up, imaging modalities that are invasive or use radiation are considered inappropriate. Therefore, echocardiography and cardiac magnetic resonance imaging are most frequently used in clinical practice [11].

The first modality to image the heart without radiation exposure was ultrasound. Although the existence of ultrasound was already recognized in bats in the 18th century, the development of cardiac ultrasound had to wait till the development of piezo-electric quartz crystals. In the 1950s, the first cardiac ultrasound was performed [18]. In the 1960s, progress was made in real-time two-dimensional echocardiography and now even three-dimensional ultrasound is available. Currently, two-dimensional echocardiography is the most frequently used modality to study the right ventricle as it is relatively cheap and readily available [19]. It excels in real-time visualization of small and mobile structures like valves. Since the heart is located in an angle with respect to the longitudinal axis of the body and is rotated slightly to the left, the ventral part of the heart consists mainly of right atrium and right ventricle. Although cardiac morphology can be visualized, this retrosternal position of the right ventricle limits echocardiographic visualization. Furthermore, the complex geometry of the right ventricle hampers reliable translation from two-dimensional diameters to volumes resulting in inaccurate measurements of right ventricular volume and function [20].

In 1946, the phenomenon of magnetic resonance was discovered which led to the development of nuclear magnetic resonance imaging [21,22]. Attenuation of tissues depends on the behavior of tissues when placed in an external magnetic field and exposed to radiofrequency radiation. In 1977, the first horizontal image through the human thorax was made, however, the acquisition time was to long to generate a qualitative good image of the heart [23]. With the introduction of ECG gating derived from nuclear radiology the first good quality cardiac images of the heart were generated in 1983. Nowadays, cardiac magnetic resonance is considered the gold standard for evaluation of cardiac volumes and function [24]. It is a cross-sectional technique that has the advantage of unrestricted fields of

view. Furthermore, with the newest sequences contrast between blood and muscle is outstanding. Measurements of right ventricular volumes and function do not rely on assumptions of geometry but uses slice summation to calculate volumes, which are highly accurate and reproducible. However, gold standard is not a synonym for perfect. The complex anatomy and morphology of the right ventricle result in less accurate and reproducible measurements compared to left ventricular measurements. Analyzing cardiac magnetic resonance derived images of the heart requires post-processing with extensive manual contouring, which is operator-dependent. Furthermore, part of the differences in right ventricular volumes and function reported in literature are the result of a difference in methodology and patient characteristics [24-26]. Therefore, interpretation and application of literature in clinical practice requires information to what extent results are influenced by methodology and patient characteristics.

Outline of the thesis

This thesis discusses imaging of the right ventricle in patients with congenital heart disease.

In many centers the right ventricular end-systolic and end-diastolic frame is selected independently from the left ventricular end-systolic and end-diastolic frame. Others state that independent selection of the right ventricular frame is unnecessary as the magnitude of the misrepresentation of right ventricular volumes and function is too small to be of clinical importance. In **Chapter 2** the magnitude of this misrepresentation is assessed.

An issue in post-processing is whether to consider trabeculae and papillary muscles part of measured right ventricular volumes or mass. Including trabeculations in the right ventricular blood volume makes analysis faster and more reproducible compared to excluding these trabeculations manually, however, right ventricular volumes will be overestimated. In Chapters 3, 4 and 5 this issue is addressed. **Chapter 3** validates a novel segmentation algorithm which semi-automatically excludes trabeculations and papillary muscles. **Chapter 4** studies the impact of right ventricular trabeculations and papillary muscles on measured right ventricular volumes and function in patients with repaired tetralogy of Fallot. **Chapter 5** shows the impact of right ventricular trabeculations and papillary muscles on measured volumes and function in patients with pressure overloaded right ventricles.

Chapter 6 evaluates the effects of right ventricular outflow tract obstruction on exercise capacity, right ventricular volumes, function and mass in adult patients with tetralogy of Fallot and volume overload due to pulmonary regurgitation. Recent studies demonstrated that patients with tetralogy of Fallot and combined pulmonary regurgitation and right ventricular outflow tract obstruction have smaller right ventricular volumes and higher ejection fraction compared to patients with isolated pulmonary regurgitation, however, the effect on exercise capacity is unknown.

Chapter 7 describes the study design and rationale of the 'Functional outcome and quality of life in adult patients with congenital heart disease and prosthetic valves (PROSTAVA) study'. Purpose of this prospective study is to describe the relation between prosthetic valve characteristics in adult patients with congenital heart disease on one hand and functional outcome, quality of life, the prevalence and predictors of prosthesis-related complications on the other hand. An addendum was added on measurements of right ventricular volumes and function in the PROSTAVA study.

References

[1] Cheng TO, (2001) Hippocrates and cardiology. Am Heart J 141:173-83.

[2] Stefanadis C, Karamanou M, Androutsos G, (2009) Michael Servetus (1511-1553) and the discovery of pulmonary circulation. Hellenic J Cardiol 50:373-8.

[3] Haddad SI, Khairallah AA, (1936) A Forgotten Chapter in the History of the Circulation of the Blood. Ann Surg 104:1-8.

[4] Thomas CT, (1928) Exercitatio Anatomica de Motu Cordis et Sanguinis in Animalibus by William Harvey with an English Translation and Annoatations by Chauncey D. Leake.

[5] Lindeboom GA, (2000) Inleiding tot de geschiedenis der geneeskunde. Erasmus Publishing.

[6] Dhainaut JF, Ghannad E, Dall'ava-Santucci J, (1988) The Obscure Right Ventricle - A Historical Review. In: Vincent J, editor. Update 1988. Springer Berlin Heidelberg.

[7] Haddad F, Hunt SA, Rosenthal DN, et al., (2008) Right ventricular function in cardiovascular disease, part I: Anatomy, physiology, aging, and functional assessment of the right ventricle. Circulation 117:1436-48.

[8] Haddad F, Doyle R, Murphy DJ, et al., (2008) Right ventricular function in cardiovascular disease, part II: pathophysiology, clinical importance, and management of right ventricular failure. Circulation 117:1717-31.

[9] Marelli AJ, Mackie AS, Ionescu-Ittu R, et al., (2007) Congenital heart disease in the general population: changing prevalence and age distribution. Circulation 115:163-72.

[10] Warnes CA, Williams RG, Bashore TM, et al., (2008) ACC/AHA 2008 Guidelines for the Management of Adults with Congenital Heart Disease: a report of the American College of Cardiology/American Heart Association Task Force on Practice Guidelines (writing committee to develop guidelines on the management of adults with congenital heart disease). Circulation 118:e714-833.

[11] Baumgartner H, Bonhoeffer P, De Groot NM, et al., (2010) ESC Guidelines for the management of grown-up congenital heart disease (new version 2010). Eur Heart J 31:2915-57.

[12] Gatzoulis MA, Balaji S, Webber SA, et al., (2000) Risk factors for arrhythmia and sudden cardiac death late after repair of tetralogy of Fallot: a multicentre study. Lancet 356:975-81.

[13] Therrien J, Provost Y, Merchant N, et al., (2005) Optimal timing for pulmonary valve replacement in adults after tetralogy of Fallot repair. Am J Cardiol 95:779-82.

[14] Buechel ER, Dave HH, Kellenberger CJ, et al., (2005) Remodelling of the right ventricle after early pulmonary valve replacement in children with repaired tetralogy of Fallot: assessment by cardiovascular magnetic resonance. Eur Heart J 26:2721-7.

[15] Oosterhof T, van Straten A, Vliegen HW, et al., (2007) Preoperative thresholds for pulmonary valve replacement in patients with corrected tetralogy of Fallot using cardiovascular magnetic resonance. Circulation 116:545-51.

[16] Frigiola A, Tsang V, Bull C, et al., (2008) Biventricular response after pulmonary valve replacement for right ventricular outflow tract dysfunction: is age a predictor of outcome? Circulation 118:S182-90.

[17] Geva T, (2011) Repaired tetralogy of Fallot: the roles of cardiovascular magnetic resonance in evaluating pathophysiology and for pulmonary valve replacement decision support. J Cardiovasc Magn Reson 13:9.

[18] Edler I, Hertz CH, (1954) Use of ultrasonic reflectoscope for continuous recording of movements of heart walls. Kurgl Fysiogr Sallad i Lund Forhandl 24.

[19] Rudski LG, Lai WW, Afilalo J, et al., (2010) Guidelines for the echocardiographic assessment of the right heart in adults: a report from the American Society of Echocardiography endorsed by the European Association of Echocardiography, a registered branch of the European Society of Cardiology, and the Canadian Society of Echocardiography. J Am Soc Echocardiogr 23:685,713; quiz 786-8.

[20] Kilner PJ, (2011) Imaging congenital heart disease in adults. Br J Radiol 84 Spec No 3:S258-68.

[21] Bloch F, Hansen WW, Packard M, (1946) Nuclear Induction. Phys.Rev. 69:127.

[22] Purcell EM, Torrey HC, Pound RV, (1946) Resonance Absorption by Nuclear Magnetic Moments in a Solid. Phys.Rev. 69:37-8.

[23] Damadian R, Goldsmith M, Minkoff L, (1977) NMR in cancer: XVI. FONAR image of the live human body. Physiol Chem Phys 9:97,100, 108.

[24] Kilner PJ, Geva T, Kaemmerer H, et al., (2010) Recommendations for cardiovascular magnetic resonance in adults with congenital heart disease from the respective working groups of the European Society of Cardiology. Eur Heart J 31:794-805.

[25] Fratz S, Schuhbaeck A, Buchner C, et al., (2009) Comparison of accuracy of axial slices versus short-axis slices for measuring ventricular volumes by cardiac magnetic resonance in patients with corrected tetralogy of fallot. Am J Cardiol 103:1764-9.

[26] Winter MM, Bernink FJ, Groenink M, et al., (2008) Evaluating the systemic right ventricle by CMR: the importance of consistent and reproducible delineation of the cavity. J Cardiovasc Magn Reson 10:40.

2

Improved cardiac MRI volume measurements in patients with tetralogy of Fallot by independent end-systolic and end-diastolic phase selection

Hendrik G. Freling
Petronella G. Pieper
Karin M. Vermeulen
Jeroen M. van Swieten
Paul E. Sijens
Dirk J. van Veldhuisen

Abstract

Objectives: To investigate to what extent cardiovascular MRI derived measurements of right ventricular (RV) volumes using the left ventricular (LV) end-systolic and end-diastolic frame misrepresent RV end-systolic and end-diastolic volumes in patients with tetralogy of Fallot (ToF) and a right bundle branch block.

Methods: Sixty-five cardiac MRI scans of patients with ToF and a right bundle branch block, and 50 cardiac MRI scans of control subjects were analyzed. RV volumes and function using the end-systolic and end-diastolic frame of the RV were compared to using the end-systolic and end-diastolic frame of the LV.

Results: Timing of the RV end-systolic frame was delayed compared to the LV end-systolic frame in 94% of patients with ToF and in 50% of control subjects. RV end-systolic volume using the RV end-systolic instead of LV end-systolic frame was smaller in ToF (median -3.3 ml/m^2, interquartile range -1.9 to -5.6 ml/m^2; $p < 0.001$) and close to unchanged in control subjects. Using the RV end-systolic and end-diastolic frame hardly affected RV end-diastolic volumes, while increasing the ejection fraction from 45 ± 7% to 48 ± 7% for patients with ToF ($p < 0.001$) rather than control subjects (54 ± 4%, both methods). QRS duration correlated positively with the changes in the RV end-systolic volume ($p < 0.001$) and RV ejection fraction obtained in ToF patients when using the RV instead of the LV end-systolic and end-diastolic frame ($p = 0.004$).

Conclusion: For clinical decision making in ToF patients RV volumes derived from cardiac MRI should be measured in the end-systolic frame of the RV instead of the LV.

PLoS One. 2013;8(1):e55462

Introduction

Evaluation of right ventricular (RV) volumes and function is crucial in the management of patients with congenital heart disease [1,2]. RV dysfunction is particularly a problem in patients with tetralogy of Fallot (ToF) due to longstanding massive pulmonary regurgitation. Irreversible RV dysfunction can be prevented by pulmonary valve replacement before a certain threshold value for RV end-systolic and end-diastolic volume is reached [3-7]. Cardiac magnetic resonance (CMR) imaging is the golden standard in the evaluation of RV volume and function, and plays an important role in the decision for pulmonary valve replacement in patients with ToF and pulmonary regurgitation [1-7].

To acquire accurate CMR derived volume measurements, correct selection of the RV end-systolic and end-diastolic frame may be important. In normal hearts, contraction of the RV lags slightly behind that of the left ventricle (LV) [8]. Most patients with ToF have a right bundle branch block (RBBB) which leads to intra- and interventricular dyssynchrony. This dyssynchrony significantly extends duration of RV contraction and delays timing of RV end-systole compared to the LV [7,9,10]. Additionally, timing of RV ejection and end-diastole may be delayed in patients with ToF [11,12]. In many centers the RV end-systolic and end-diastolic frame is selected independently from the LV end-systolic and end-diastolic frame [13,14]. However, the magnitude of the overestimation of RV end-systolic volume and underestimation of RV end-diastolic volume and ejection fraction is unknown. Therefore, others state that independent selection of the RV frame is unnecessary as the magnitude of the misrepresentation of RV volumes and function is too small to be of clinical importance.

The present study is the first to quantitatively document the influence of independent selection of the end-systolic and end-diastolic frame for the RV and LV, on RV volume measurements in a large group of patients with ToF and control subjects.

Materials and methods

Study population

Our institution's CMR database was searched to collect 65 of the most recent CMR scans of patients with ToF and 50 normal CMR scans performed in patients suspected for myocardial infarction (control subjects). Normal CMR scans were defined as normal anatomy, normal LV and RV contraction, normal LV and RV volumes and ejection fraction with no signs of infarction, and no valvular dysfunction [15]. Ischemia was ruled out by stress testing. In all patients electrocardiograms performed within 6 months to the CMR date were collected to evaluate rhythm and conductance disturbances. A RBBB was present when the longest manually measured QRS duration $\geq$ 100 ms in combination with a terminal R wave in lead V1 and V2, wide S wave in I and V6 on the electrocardiogram [16].

RBBB is defined as complete when the QRS duration $\geq$ 120 ms and defined as incomplete when the QRS duration is $\geq$100 ms and <120 ms [16]. CMR scans of patients with ToF were included when RBBB was the only conductance delay and no additional conductance delays were present. CMR scans of control subjects were excluded when conductance delays were present on the electrocardiogram [16].

This retrospective study was approved by the University Medical Center Groningen review board. Informed consent was not required according to the Dutch Medical Research Involving Human Subjects act.

Cardiac magnetic resonance imaging:

All subjects were examined on a 1.5-Tesla MRI system (Siemens Magnetom Sonata, Erlangen, Germany or Siemens Magnetom Avanto, Erlangen, Germany) using a 2 x 6 channel body-coil. After single-shot localizer images, for function analysis short axis cine loop images with breath holding in expiration were acquired using a retrospectively gated balanced steady state free precession sequence. Short axis slices were planned in end-diastole from two slices above the mitral valve plane to the apex. The following parameters were used: TR 2.7 ms, TE 1.1 ms, flip angle 80^{o}, field of view 320 mm, matrix 192 x 192 mm, 25 frames per cycle, slice thickness 6 mm, interslice gap 4 mm, voxel size 1.7 x 1.7 x 6 mm.

Image analysis was performed using commercially available software (QMass version 7.2., Medis, Leiden, The Netherlands). The end-systolic and end-diastolic frame was defined as the frame with the smallest and largest volume, respectively.These frames were selected by visual assessment independently for

the LV and RV. LV and RV contours were drawn manually by tracing the endocardial borders in every slice in the end-systolic and end-diastolic frame of the LV. Contour tracing was aided by reviewing the multiple phase scans in the movie mode. The papillary muscle and trabeculae were considered part of the cavum. Additionally, RV contours were drawn in the end-systolic and end-diastolic frame of the RV.

The basal slice was selected with aid of long-axis cine view images. The basal slice of the LV was defined as the most basal slice surrounded for at least 50% by the LV myocardium. When the pulmonary valve was visible in the RV basal slice, only the portion of the right ventricular outflow tract below the level of the pulmonary valve was included. For the inflow part of the RV, the blood volume was included when the ventricle wall was trabeculated and thick compared to the right atrium wall [15].

Stroke volume was defined as end-diastolic volume minus end-systolic volume. Ejection fraction was defined as stroke volume divided by end-diastolic volume.

Reproducibility

RV contours were first drawn in the visually selected end-systolic and end-diastolic frame of the RV. To minimize intraobserver variability, RV contours drawn in the end-systolic and end-diastolic frame of the RV were copied to the LV end-systolic and end-diastolic frame and then adjusted to this frame.

To obtain intra- and interobserver reproducibility, contours were drawn independently twice by the first observer and once by the second observer in 25 scans of patients with ToF and 25 scans of control subjects. The end-systolic and end-diastolic frame was selected independently twice by the first observer and once by the second observer. There were at least two weeks between repeated contour drawing by the first observer. Both observers had more than 2 years experience with RV contour drawing.

Statistical analyses

Descriptive statistics were calculated for all measurements as mean and standard deviation for normally distributed continuous variables, median with interquartile range (IQR) for skewed continuous variables and absolute numbers and percentages for dichotomous variables. Reproducibility was evaluated with the intraclass correlation coefficient (ICC). For normally distributed continuous variables a paired-samples Student's t-test and for skewed continuous variables a Wilcoxon test was used to compare RV volumes measured in the LV end-systolic

and end-diastolic frame with RV volumes measured in the RV end-systolic and end-diastolic frame. For normally distributed continuous variables an independent Student's T-test and for skewed continuous variables a Mann-Whitney test was used to compare the difference in RV volumes between normal scans and scans of patients with ToF when measuring RV volumes in the end-systolic and end-diastolic frame of the RV instead of the LV. The relation between QRS duration and change in RV volume and function when using the end-systolic and end-diastolic frame of the RV instead of the LV was analyzed using linear regression. The Statistical Package for the Social Sciences version 16.0 (SPSS Inc, Chicago, IL) was used for all statistical analyses. All statistical tests are two-sided and a P-value of less than 0.05 was considered statistically significant.

Results

Study population

Between January 2008 and January 2011, 65 CMR scans of patients with ToF (50 with complete RBBB, 15 with incomplete RBBB) and 50 normal CMR scans of control subjects were collected. Patients with ToF (37 male, 28 female; median age 28 years, IQR 21 to 37 years) were younger than control subjects (33 male, 17 female; median age 56 years, IQR 41 to 65 years), $p < 0.001$. QRS duration was longer in patients with ToF (145 ± 25 ms) than in control subjects (93 ± 9 ms), $p < 0.001$. Heart rate during the CMR scan was similar in patients with ToF (70 ± 12 bpm) and control subjects (73 ± 15 bpm), p = NS.

Timing of end-systole and end-diastole

The difference in frame selection of end-systole and end-diastole between the RV and LV is shown in table 1.

Table 1. End-systolic and end-diastolic frame selection of the RV compared to the LV.

RV – LV frame	End-systole		End-diastole	
	ToF	Control	ToF	Control
RV 3 frames earlier	0 (0)	0 (0)	2 (3)	0 (0)
RV 2 frames earlier	0 (0)	0 (0)	2 (3)	2 (4)
RV 1 frame earlier	0 (0)	0 (0)	14 (22)	14 (28)
No difference	4 (6)	25 (50)	38 (58)	34 (64)
RV 1 frame later	26 (40)	25 (50)	8 (12)	0 (0)
RV 2 frames later	28 (43)	0 (0)	0 (0)	0 (0)
RV 3 frames later	7 (11)	0 (0)	1 (2)	0 (0)

Data are expressed as number of patients (%). LV = left ventricle, RV = right ventricle, ToF = tetralogy of Fallot

Figure 1 shows the time-volume curve of the RV and LV of a patient with ToF and a complete RBBB. In almost all patients with ToF and half of control subjects the end-systolic frame of the RV was delayed compared to the LV. The resulting median difference in timing between the end-systolic frame of the RV and LV was larger in patients with ToF (median -53 ms, IQR -73 to -37 ms) than in control subjects (median -11 ms, IQR -32 to 0 ms), $p < 0.001$. Timing of the end-diastolic frame was not different between the RV and LV in most patients with ToF and control subjects. Also, the resulting median difference in timing between the ED

frame of the RV and LV frame was similar in patients with ToF (median 0 ms, IQR 0 to 36 ms) and control subjects (median 0 ms, IQR 0 to 32 ms), p = NS.

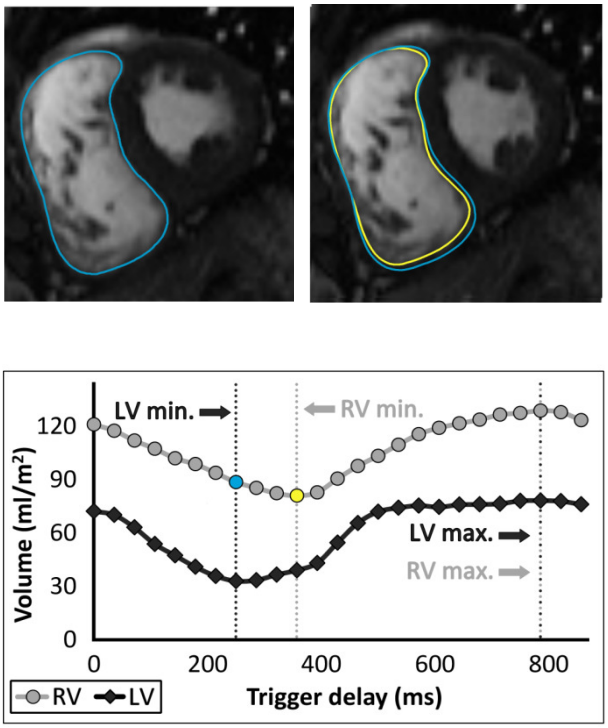

Figure 1. *Example of the LV and RV end-systolic frame and the corresponding time-volume curve. Two short axis images of the end-systolic frame of the LV (upper left) and RV (upper right), and the corresponding time-volume curve (below) in a patient with ToF and a complete RBBB. Timing of the RV end-systolic frame is 106 ms (3 frames) delayed compared to LV end-systolic frame. Measuring the RV end-systolic volume in the LV instead of the RV end-systolic frame results in a difference of 9 ml/m2. This is visible in the short-axis image of the RV end-systolic frame (upper right) in which the larger blue contour corresponds to the RV contour of the LV end-systolic frame (upper left) and the yellow contour to the RV contour of the RV end-systolic frame. Timing of the end-diastolic frame is the same for the RV and LV.*

Change in RV volume and function

Table 2 shows RV volumes and function measured in the end-systolic and end-diastolic frame of the LV and RV. Using the RV end-systolic instead of LV end-systolic frame in patients with ToF, mean RV end-systolic volume was reduced from 78 to 74 ml/m^2 ($p < 0.001$) while ejection fraction and stroke volume grew from 45 to 48% ($p < 0.001$) and from 62 to 66 ml/m^2, respectively ($p < 0.001$). ToF patient's changes in RV end-diastolic volume and the changes in any of these four parameters in the controls were very small, though still significant in paired data analysis. Figure 2 shows the difference in volumes and function when using the end-systolic and end-diastolic frame of the RV instead of the LV. The decrease in RV end-systolic volume was incremental when going from controls to patients with ToF and an incomplete RBBB to patients with ToF and a complete RBBB ($p<0.001$). In patients with ToF linear regression showed a significant association between QRS duration and change in RV end-systolic volume (B 3.37, CI 1.62 – 5.13, R^2 =

0.190, p < 0.001), and RV ejection fraction (B 4.25, CI 1.40 – 7.10, R^2 = 0.124, p = 0.004) when using the end-systolic and end-diastolic frame of the RV instead of the LV.

Table 2. RV volumes measured in the end-systolic and end-diastolic frame of the LV and RV.

	LV frame	RV frame	RV frame – LV frame	*P*
ToF				
RV ESV (ml/m^2)	77.8 ± 24.1	73.6 ± 23.0	-3.3 (-5.6 to -1.9)	<.001
RV EDV (ml/m^2)	139.6 ± 35.0	140.0 ± 35.0	0.0 (0.0 to 0.9)	<.001
RV EF (%)	44.8 ± 7.4	48.0 ± 6.9	2.8 (1.8 to 4.6)	<.001
RV SV (ml/m^2)	61.8 ± 16.4	66.4 ± 16.7	4.1 (2.6 to 5.8)	<.001
Control subjects				
RV ESV (ml/m^2)	35.1 ± 7.6	34.9 ± 7.6	0.0 (-0.4 to 0.0)	.003
RV EDV (ml/m^2)	75.2 ± 12.4	75.4 ± 12.3	0.0 (0.0 to 0.1)	.002
RV EF (%)	53.6 ± 4.1	54.0 ± 4.0	0.2 (0.0 to 0.7)	<.001
RV SV (ml/m^2)	40.1 ± 6.1	40.5 ± 6.1	0.2 (0.0 to 0.6)	<.001

Data are expressed as mean ± SD or median (IQR). EDV = end-diastolic volume, EF = ejection fraction, ESV = end-systolic volume, IQR = interquartile range LV = left ventricle, RV = right ventricle, SD = standard deviation, SV = stroke volume, ToF = tetralogy of Fallot

The increase of RV ejection fraction is mainly the result of decrease in end-systolic volume when using the end-systolic frame of the RV instead of the LV. Using the end-systolic frame of the RV instead of the LV resulted in a relative increase in ejection fraction of 7%, from 45 ± 7% to 48 ± 7%, in patients with ToF and of 1%, from 54 ± 4% to 54 ± 4%, in control subjects. The relative increase in ejection fraction and stroke volume by using the end-diastolic frame of the RV instead of the LV was <1% in both patients with ToF and control subjects.

In 17 (26%) patients with ToF the absolute increase of ejection fraction exceeded 5% (range 5-8%), figure 2C. In 39 (60%) patients with ToF ejection fraction fell short of the limit of 47% indicating abnormal RV function according to reference values [15]. When using the end-systolic frame of the RV instead of the LV frame, RV function changed to normal in 5 (13%) of these patients. None of the patients with an incomplete RBBB and an abnormal RV function showed improvement to normal values.

Reproducibility

Intra- and interobserver ICC for RV end-systolic volume, end-diastolic volume and ejection fraction was .98, .91, .87 and .98, .97, .95 in patients with ToF and .94, .93, .88 and .95, .97 and .89 in control subjects, respectively.

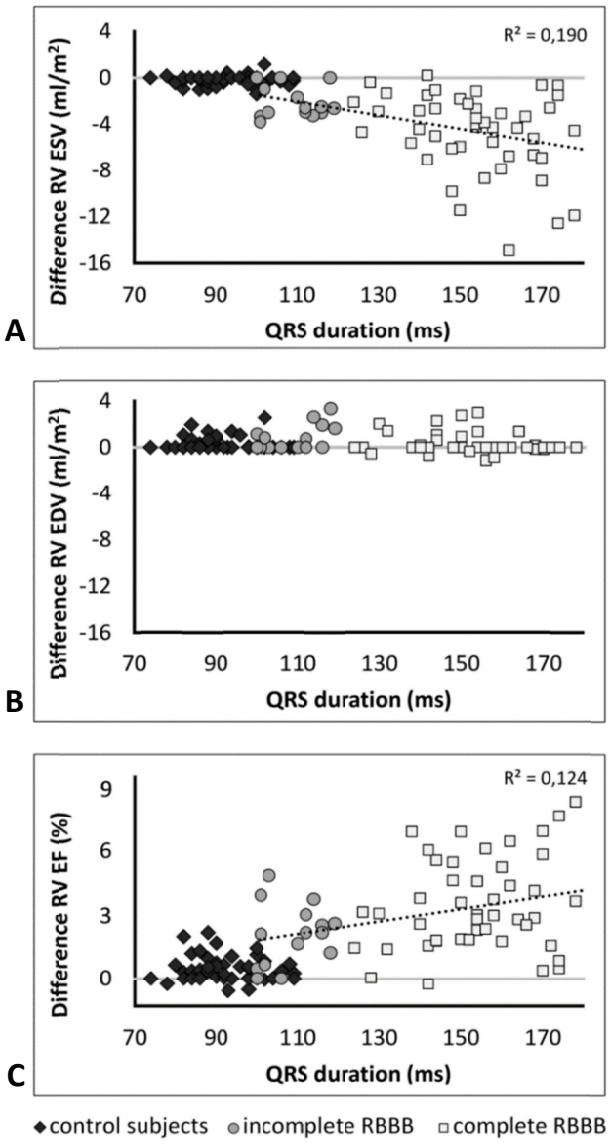

Figure 2. *Change in right ventricular volumes and function. Scatterplots of the change in RV end-systolic volume (A), end-diastolic volume (B) and ejection fraction (C) when using the end-systolic and end-diastolic frame of the RV instead of the LV. EDV = end-diastolic volume, EF = ejection fraction, ESV = end-systolic volume, LV = left ventricular, RBBB = right bundle branch block, RV = right ventricular, ToF = tetralogy of Fallot*

Discussion

Our study is the first to quantitatively demonstrate the difference in RV volumes and function between using the RV and LV end-systolic and end-diastolic frame. Performing cardiovascular MRI derived measurements of RV volumes using the LV end-systolic and end-diastolic frame, misrepresent RV end-systolic and end-diastolic volumes in many patients with ToF, especially in the frequent case of a complete RBBB. These findings can be of clinical importance in the evaluation of the RV in patients with ToF.

Previous echocardiographic and cardiovascular MRI studies reported on the electromechanical delay of the RV compared to the LV in patients with congenital heart disease and normal subjects [8-10,17,18]. The main focus of the echocardiographic studies was to assess intra- and interventricular dyssynchrony and their predictors. They showed that in patients with ToF RV free wall contraction lags behind LV free wall and interventricular septum contraction. Although they did not report on timing of end-systole, it can be expected that end-systole is also delayed. We showed that in most scans of patients with ToF, end-systole of the RV was more than one frame delayed compared to the LV. This was probably largely due to the longer QRS duration in patients with ToF and a complete RBBB. In control subjects the normal physiologically electromechanical delay of the RV could not be detected in every case as the delay was smaller than the time (mean 34 ± 7 ms) between two frames. Therefore, the end-systolic frame of the RV was in the same or one frame later than the end-systolic frame of the LV. In contrast to end-systole, timing of end-diastole of the RV and LV was similar in patients with ToF and control subjects.

One small (N=12) cardiovascular MRI study indicated that measuring RV volumes in the two frames preceding RV end-systole causes no clinically significant volume changes despite the observation that end-systole of RV and LV occur in different frames [19]. Our study has made clear that in end-systole the two previous frames have a larger volume. When there is a difference in timing of end-systole of the RV and LV with two or more frames, as is the case in most patients with ToF, this leads to a significant change in volume. When there is a difference in end-systole of the RV and LV in control subjects, this leads to a very small volume change only. QRS duration, unfortunately not documented in the above study [19], appears to be an important parameter as evidenced by the statistically significant correlation with the difference in end-systolic volume when using the end-systolic frame of the RV instead of the LV in patients with ToF obtained in this study. The correlation is weak, however, probably because of our inclusion of a group of

patients who are rather homogeneous in terms of QRS duration. In contrast to end-systole, in end-diastole the adjacent frames had a similar volume.

According to the guidelines of the ESC and ACC/AHA, indication for replacement of the pulmonary valve in patients with ToF and moderate/severe pulmonary regurgitation is based on several parameters including RV function [1,2]. It is important in this context that in 13% of the patients with ToF who were considered to have abnormal function (ejection fraction <47%) [15], ejection fraction increased to normal when using the end-systolic frame of the RV instead of the LV. The change in RV function was mainly due to the decrease in RV end-systolic volume when using the RV frame instead of the LV frame. Studies comparing RV volumes and function before and after pulmonary valve replacement have identified pre-operative threshold values for RV volumes after which volumes can return to normal [3-6]. None of these studies describe whether they selected the end-systolic and end-diastolic frame of the RV separately from the LV. The reported threshold for RV end-systolic volume above which RV volume does not return to normal after PVR varies between approximately 80 and 90 ml/m^2 [3-6]. When using a threshold for RV end-systolic volume of > 85 ml/m^2 [3], in our study 25 (39%) patients had volumes above this threshold when measuring RV volumes in the end-systolic frame of the LV. When using the end-systolic frame of the RV instead of the LV, the end-systolic volume dropped below this threshold in 7 (28%) patients. In some of these cases CMR measurements of RV volumes and function may prove to be decisive when considering reoperation. Therefore, RV volumes should be measured in end-systolic of the RV and not of the LV.

Limitations

Identifying tricuspid valve opening and closing in a 4-chamber or RV 2-chamber view may allow for more accurate selection of the end-systolic frame. However, in the 4-chamber view the opening and closing of the tricuspid valve was not always clearly visible and RV 2-chamber views were not acquired.

There are possible confounders for the difference in timing of end-systole between the studied groups, such as the difference in age, pulmonary stenosis and regurgitation, RV end-systolic and end-diastolic volume and underlying disease. However, it is unlikely that the difference in age will have influenced our results as age does not affect timing of contraction of the right and left ventricle [8]. Possibly, a stronger correlation would have been found between QRS duration and the difference in ejection fraction and end-systolic volume when using the end-systolic and end-diastolic frame of the RV instead of the LV when also patients with ToF and normal QRS duration had been included in this study. To investigate

the influence of QRS duration and RBBB more thoroughly, an additional group of patients with ToF and no conduction delays would be useful. However, these patients are rare and in our institution there are only three CMR scans of these patients available over the last three years [1].

Although we have shown that end-systolic volume of the RV in patients with ToF should be measured in the end-systolic frame of the RV instead of the LV, it is uncertain whether this applies to all patients with congenital heart diseases involving the right ventricle and a RBBB.

Conclusions

Independent selection of the end-systolic and end-diastolic LV and RV frame instead of using the LV end-systolic and end-diastolic frame for RV determinations, results in more accurate end-systolic RV volumes in patients with ToF and a RBBB. The differences are significant and correlate with QRS duration. For clinical decision making in patients with ToF and a RBBB, RV volumes should be measured in the end-systolic frame of the RV instead of the LV.

References

[1] Baumgartner H, Bonhoeffer P, De Groot NM, et al., (2010) ESC Guidelines for the management of grown-up congenital heart disease (new version 2010). Eur Heart J 31:2915-57.

[2] Warnes CA, Williams RG, Bashore TM, et al., (2008) ACC/AHA 2008 Guidelines for the Management of Adults with Congenital Heart Disease: a report of the American College of Cardiology/American Heart Association Task Force on Practice Guidelines (writing committee to develop guidelines on the management of adults with congenital heart disease). Circulation 118:e714-833.

[3] Therrien J, Provost Y, Merchant N, et al., (2005) Optimal timing for pulmonary valve replacement in adults after tetralogy of Fallot repair. Am J Cardiol 95:779-82.

[4] Buechel ER, Dave HH, Kellenberger CJ, et al., (2005) Remodelling of the right ventricle after early pulmonary valve replacement in children with repaired tetralogy of Fallot: assessment by cardiovascular magnetic resonance. Eur Heart J 26:2721-7.

[5] Oosterhof T, van Straten A, Vliegen HW, et al., (2007) Preoperative thresholds for pulmonary valve replacement in patients with corrected tetralogy of Fallot using cardiovascular magnetic resonance. Circulation 116:545-51.

[6] Frigiola A, Tsang V, Bull C, et al., (2008) Biventricular response after pulmonary valve replacement for right ventricular outflow tract dysfunction: is age a predictor of outcome? Circulation 118:S182-90.

[7] Geva T, (2011) Repaired tetralogy of Fallot: the roles of cardiovascular magnetic resonance in evaluating pathophysiology and for pulmonary valve replacement decision support. J Cardiovasc Magn Reson 13:9.

[8] Yu CM, Lin H, Ho PC, et al., (2003) Assessment of left and right ventricular systolic and diastolic synchronicity in normal subjects by tissue Doppler echocardiography and the effects of age and heart rate. Echocardiography 20:19-27.

[9] D'Andrea A, Caso P, Sarubbi B, et al., (2004) Right ventricular myocardial activation delay in adult patients with right bundle branch block late after repair of Tetralogy of Fallot. Eur J Echocardiogr 5:123-31.

[10] Mueller M, Rentzsch A, Hoetzer K, et al. (2010) Assessment of interventricular and right-intraventricular dyssynchrony in patients with surgically repaired tetralogy of Fallot by two-dimensional speckle tracking. Eur J Echocardiogr 11:786-92.

[11] Cullen S, Shore D, Redington A, (1995) Characterization of right ventricular diastolic performance after complete repair of tetralogy of Fallot. Restrictive physiology predicts slow postoperative recovery. Circulation 91:1782-9.

[12] van den Berg J, Wielopolski PA, Meijboom FJ, et al., (2007) Diastolic function in repaired tetralogy of Fallot at rest and during stress: assessment with MR imaging. Radiology 243:212-9.

[13] Maceira AM, Prasad SK, Khan M, et al., (2006) Reference right ventricular systolic and diastolic function normalized to age, gender and body surface area from steady-state free precession cardiovascular magnetic resonance. Eur Heart J 27:2879-88.

[14] Clarke CJ, Gurka MJ, Norton PT, et al., (2012) Assessment of the accuracy and reproducibility of RV volume measurements by CMR in congenital heart disease. JACC Cardiovasc Imaging 5:28-37.

[15] Alfakih K, Plein S, Thiele H, et al., (2003) Normal human left and right ventricular dimensions for MRI as assessed by turbo gradient echo and steady-state free precession imaging sequences. J Magn Reson Imaging 17:323-9.

[16] Mirvis DM, Goldberger AL, Electrocardiography. In: Bonow RO, Mann DL, Zipes DP, Libby P, Braunwald E, editors. Braunwald's Heart Disease. Saunders Elsevier, 2011.

[17] Frigiola A, Redington AN, Cullen S, et al., (2004) Pulmonary regurgitation is an important determinant of right ventricular contractile dysfunction in patients with surgically repaired tetralogy of Fallot. Circulation 110:II153-7.

[18] Sun AM, AlHabshan F, Cheung M, et al., (2011) Delayed onset of tricuspid valve flow in repaired tetralogy of Fallot: an additional mechanism of diastolic dysfunction and interventricular dyssynchrony. J Cardiovasc Magn Reson 13:43.

[19] Edwards R, Shurman A, Sahn DJ, et al., (2009) Determination of right ventricular end systole by cardiovascular magnetic resonance imaging: a standard method of selection. Int J Cardiovasc Imaging 25:791-6.

3

Improving the reproducibility of MR-derived left ventricular volume and function measurements with a semi-automatic threshold-based segmentation algorithm

Karolien Jaspers
Hendrik G. Freling
Kees van Wijk
Elisabeth I. Romijn
Marcel J.W. Greuter
Tineke P. Willems

Abstract

Purpose: To validate a novel semi-automatic segmentation algorithm for MR-derived volume and function measurements by comparing it with the standard method of manual contour tracing.

Methods: The new algorithms excludes papillary muscles and trabeculae from the blood pool, while the manual approach includes these objects in the blood pool. An epicardial contour served as input for both methods. Multiphase 2D steady-state free precession short axis images were acquired in 12 subjects with normal heart function and in a dynamic anthropomorphic heart phantom on a 1.5T MR system. In the heart phantom, manually and semi-automatically measured cardiac parameters were compared to the true end-diastolic volume (EDV), end-systolic volume (ESV) and ejection fraction (EF). In the subjects, the semi-automatic method was compared to manual contouring in terms of difference in measured EDV, ESV, EF and myocardial volume (MV). For all measures, intra- and inter-observer agreement was determined.

Results: In the heart phantom, EDV and ESV were underestimated for both the semi-automatic . As the papillary muscles were excluded from the blood pool with the semi-automatic method, EDV and ESV were approximately 20 ml lower in the patients, whereas EF was approximately 16 % higher. Intra- and inter-observer agreement was overall improved with the semi-automatic method compared to the manual method. Correlation between manual and semi-automatic measurements was high (EDV: R = 0.99, ESV: R = 0.96; EF: R = 0.80, MV: R = 0.99).

Conclusion: The semi-automatic method could exclude endoluminal muscular structures from the blood volume with significantly improved intra- and inter-observer variabilities in cardiac function measurements compared to the conventional, manual method, which includes endoluminal structures in the blood volume.

Int J Cardiovasc Imaging. 2013 Mar;29(3):617-23

Introduction

Quantification of left ventricular (LV) volumes and mass is important for the diagnostic and prognostic assessment in a variety of cardiovascular diseases [1,2]. The golden standard for assessment of these quantities is cardiovascular magnetic resonance (CMR) imaging, due to its high reproducibility and accuracy [3,4]. The current clinical practice is to manually draw epicardial and endocardial contours in the end-diastolic and end-systolic phase of the cardiac cycle. The inclusion of the papillary muscles in the blood volume introduces a considerable bias in the measured volumes and ejection fraction [5]. This bias is generally accepted, as manually excluding the papillary muscles by drawing non-convex endocardial contours is even more time consuming and has demonstrated a higher intra- and inter-observer variability [6].

However, reliable determination of trabecular volumes can be clinically relevant in patients with left ventricular hypertrophy [7] or in patients with noncompaction cardiomyopathy [8-10]. In these cases, automated segmentation of blood and muscle could not only provide faster and more objective analysis, but may also yield more accurate estimations of cardiac volumes and function than the manual method. Several automated segmentation techniques have been proposed, ranging from semi-automatic to fully automated [11-16]. They were, however, not designed to separately assess trabecular and papillary muscle volumes.

The purpose of our study was to validate a novel semi-automatic segmentation algorithm by comparing it with the standard method of manual contour tracing. In an anthropomorphic heart phantom, the accuracy of volume and function measurement was assessed. In twelve subjects with normal cardiac function, the effect of including papillary muscles and trabeculae in the myocardial volume was investigated, and intra- and inter-observer agreement was assessed.

Materials and methods

Heart phantom

A dynamic anthropomorphic heart phantom (Shelley Medical Imaging Technologies, London, Ontario, Canada) was used to compare the semi-automatic and manual method in terms of accuracy.

The heart phantom was made of a hydrogel filled with water, placed in a water-filled tank. The phantom was connected to a mechanical pump that mimics the cyclic filling and emptying of the heart. The ejection fraction (EF) was set at 61% (end-diastolic volume (EDV): 69 ml, end-systolic volume (ESV): 27 ml). During acquisition, the heart rate was 44 beats per minute. The phantom has distinct boundaries between the cavities and the wall, and does not include any trabeculations nor papillary muscles.

Subjects

Analysis was performed on normal CMR scans obtained from twelve subjects suspected of myocardial infarction. Normal CMR scans were defined as normal anatomy, normal contractibility, normal volumes and function with no signs of infarction. This retrospective study was approved by the University Medical Center Groningen review board and informed consent was not required according to the Dutch Medical Research Involving Human Subjects act.

Image acquisition

Heart phantom

Imaging was performed on a clinical 1.5 tesla scanner (Sonata, Siemens Healthcare, Erlangen, Germany) equipped with a body array coil. A 2D steady-state free precession (SSFP) sequence was used to acquire a series of multiphase short axis images of the heart. The number of cardiac phases was 25, and 12 slices with slice thickness 6 mm and interslice gap of 4 mm were acquired. Total TR was 40 ms, TE 1.2 ms and the flip angle was 80°. Matrix size was 144 × 192, and pixel size 1.7 × 1.7 mm.

Subjects

The subjects were positioned in a supine position in a 1.5T scanner (Avanto, Siemens Healthcare, Erlangen, Germany) with a 6-element body matrix coil. The protocol included multiple single-slice SSFP series with 25 cardiac phases. The single slice images were positioned along the short axis of the left ventricle. To cover the entire heart, 15 images with slice thickness 6 mm and interslice gap of 4

mm were acquired. Total TR was 45 ms, TE 1.3 ms and the flip angle was 80°. Matrix size depended on subject size, and pixel size was 1.8 × 1.8 mm^2.

Image analysis

Image analysis was performed manually by using QMass MR (version 7.2, Medis, Leiden, The Netherlands) and semi-automatically by using QMass MR research edition (Medis, Leiden, The Netherlands).

Slice selection: The end-systolic and end-diastolic frames were selected by visual assessment. The basal slice was selected with the aid of long-axis cine view images. The basal slice of the LV was defined as the most basal slice surrounded for at least 50% by the LV myocardium. Slices at the apex were included when blood was clearly visible. Contours were drawn manually by tracing the endocardial and epicardial borders in every slice in end-systole and end-diastole. Contour tracing was aided by reviewing the multiple phase scans in the movie mode.

Manual method: For the manual method, the EDV and ESV were defined as the total volume of voxels within the endocardial contour in the end-diastolic and end-systolic phase, respectively. The myocardial volume (MV) was defined as the total volume of voxels between the epicardial and epicardial contours in the end-diastolic phase. The manual method included papillary muscles and trabeculae in the endocardial contour and therefore the blood volume (see Figure 1a and c).

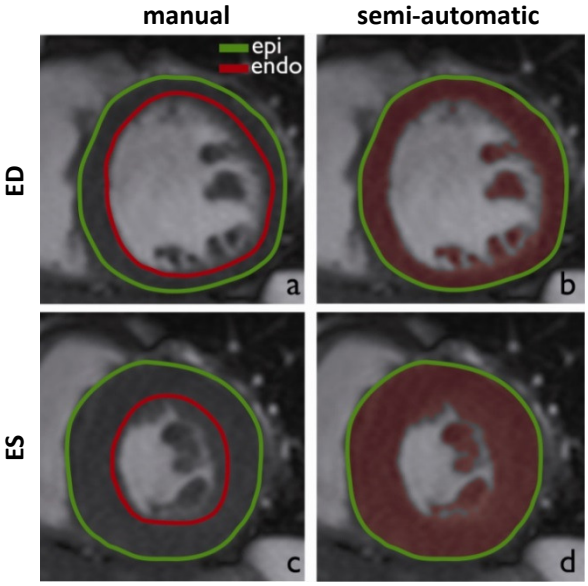

Figure 1. *Segmentation according to the manual (panels a and c) and semi-automatic method (panels b and d) for the end-diastolic and end-systolic phase (ED and ES, respectively). For the manual method, epi- and endocardial contours (green and red lines, respectively) are drawn. For the semi-automatic method, within the epicardial contour voxels are classified as either muscle (red) or blood (grey).*

Semi-automatic method: The epicardial contour served as input for the semi-automatic method. As the semi-automatic threshold-based segmentation algorithm was an integral part of QMass, both methods used the same epicardial contour. Within the epicardial contour, voxels were classified as either blood or muscle based on their signal intensity. A detailed description of the segmentation procedure can be found in Appendix I. The EDV and ESV were defined as the total volume of voxels classified as blood within the epicardial contour. The MV was defined as the total volume of voxels classified as muscle within the epicardial contour in the end-diastolic phase. With the semi-automatic method, the papillary muscles and trabeculae were excluded from the blood volume. For both methods, the ejection fraction (EF) was defined as:

$$EF = \frac{EDV - ESV}{EDV} \cdot 100\% \qquad (1)$$

Heart phantom: The deviation from the ground truth of both methods was evaluated by comparing the EDV, ESV and EF with the predefined parameters of the heart phantom. Contours were drawn by five observers, who were blinded for each others results.

Subjects: To assess inter-observer agreement, contours were drawn by two observers, who both repeated their measurements for intra-observer agreement evaluation. Observer 1 had several years of experience and Observer 2 was inexperienced. The observers were blinded for the outcomes of the other observer and their previous measurements. The observers drew in the same amount of slices, such that the comparison would be purely between methods and not on how many slices each observer chose to include.

Statistical analysis

Statistical analysis was performed in SPSS (SPSS 18, Chicago IL, USA) For the heart phantom study, a paired Wilcoxon signed rank test was used to assess the difference in EDV, ESV and EF between the manual and semi-automatic method. To see whether there was a significant difference between the ground truth and measured values, a one-sample Wilcoxon signed rank test was applied.

For the subject study, the difference in measured EDV, ESV, MV and EF between the manual and semi-automatic method was tested with a paired Wilcoxon signed rank test, using the average of the four observations for each subject. The correlation between both methods was assessed with the Pearson's correlation coefficient.

The intra-observer agreement coefficient (AC_{intra}) between paired observations was calculated for each observer:

$$AC_{intra} = 100 \cdot \left(1 - \frac{2 \cdot |Obs_1 - Obs_2|}{Obs_1 + Obs_2}\right) \qquad (2)$$

For each observer, the median AC_{intra} was computed. Similarly, the inter-observer agreement coefficient AC_{inter} was computed. For each observer, the average of the two paired observations was used. The difference in median AC between the manual and semi-automatic method was tested with a paired Wilcoxon signed rank test. Effects were considered significant for $p < 0.05$.

Results

Heart phantom

Compared to the ground truth (ESVgt = 27 ml), the ESV was underestimated with both the manual (median: 21.7; range: 18.4 – 22.6 ml; p = 0.04) and semi-automatic method (median: 22.7 ml; range: 21.1 – 25.1 ml; p = 0.04). For the EDV (EDVgt: 69 ml), a significant underestimation between measured volume and ground truth was found for the manual method (median: 65.1 ml; range: 61.6 – 66.0 ml; p = 0.04), but not for the semi-automatic method (median: 67.8 ml; range: 66.0 – 69.4 ml; p = 0.09).

Underestimation of the EDV and ESV resulted in an overestimation of EF (ground truth: 61 %) for both the manual (median: 67.2 %; range: 65.3 – 70.1 %; p = 0.04) and semi-automatic method (median: 66.8 %; range: 63.9 – 68.0 %; p = 0.04).

Subjects

The correlation between the semi-automatic and manual method was high for all parameters (EDV: R = 0.993, ESV: R = 0.958; EF: R = 0.800, MV: R = 0.991, see Figure 2).

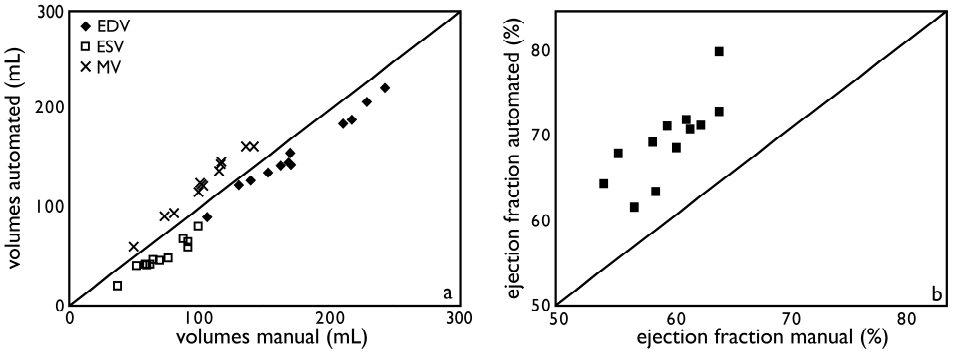

Figure *2* *Correlation between the semi-automatic and manual method for (panel a) the end-diastolic and end-systolic volumes (ESV (open squares) and EDV (black diamonds), respectively) and myocardial volume (MV, crosses), as well as (panel b) the ejection fraction.*

With the semi-automatic method, the EDV and ESV were lower compared to the manual method (p < 0.01). The median difference between semi-automatic and manual method, which reflected the volume of trabeculae and papillary muscles,

was 20 ml (range: 9 – 29 ml) for the EDV and 23 ml (range: 14 – 34 ml) for the ESV. The difference in end-diastolic MV between the semi-automatic and manual method was equal to the difference in EDV. With the semi-automatic method, the estimated ejection fraction was approximately 16% higher ($p < 0.01$) compared to the manual method (range: 8 – 24 %).

Overall, observer agreement was higher for the semi-automatic method compared to the manual method (Figure 3). For the inexperienced observer 2, the semi-automatic method gave a significantly higher intra-obsever agreement coefficient for both the EDV ($p = 0.03$) and ESV ($p < 0.05$). In contrast, for the experienced observer no difference in AC_{intra} was found for the EDV ($p = 0.53$) or ESV ($p = 0.08$). AC_{inter} of the semi-automatic method was significantly improved for the semi-automatic method compared to the manual method for the ESV ($p = 0.04$), but not for the EDV ($p = 0.24$).

For the ejection fraction, the semi-automatic method yielded a higher AC_{inter} ($p = 0.03$) and AC_{intra} ($p < 0.01$ for observer 1 and $p = 0.01$ for observer 2) compared to the manual method. The intra-observer agreement for the myocardial volume determined with the semi-automatic method was significantly improved for the inexperienced observer ($p = 0.01$), but not for the experienced observer ($p = 0.17$). AC_{inter} for MV was higher for the semi-automatic method compared to the manual method ($p < 0.01$).

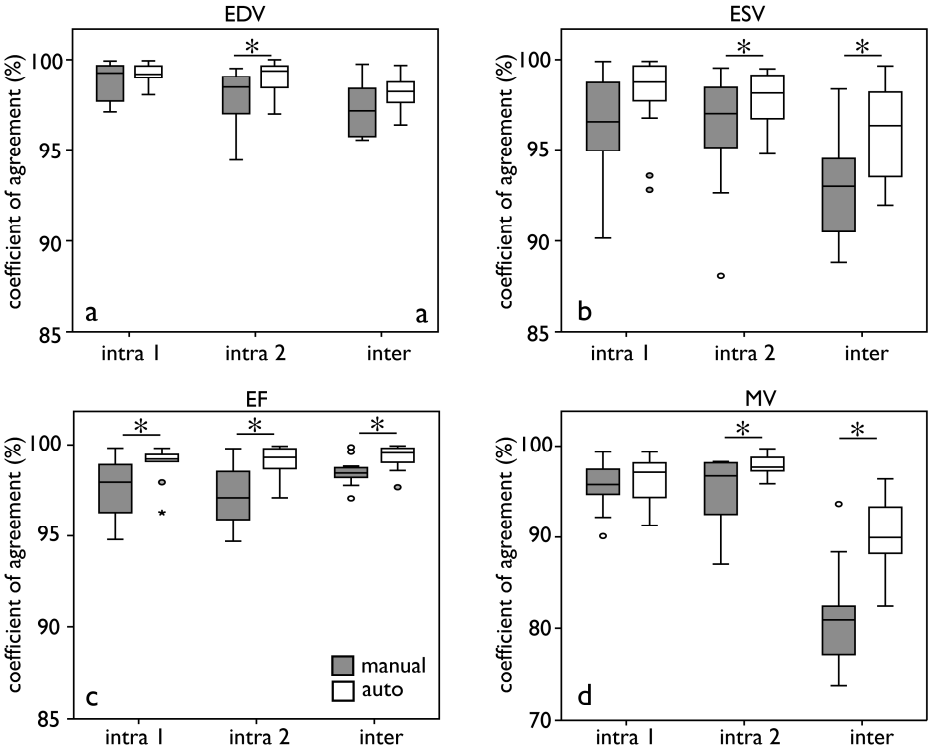

Figure 3. *Intra- and inter-observer coefficients of agreement for the manual (grey) and semi-automatic method (white) for the end-diastolic (EDV, panel a), end-systolic (ESV, panel b), ejection fraction (EF, panel c) and myocardial volumes (panel d) . Observer 2 is the inexperienced observer. * indicate a significant difference between the manual and semi-automatic method ($p < 0.05$)*

Discussion

In this study, a semi-automatic segmentation algorithm has been presented which segments blood and muscle within a user-provided epicardial contour. The algorithm was tested on CMR data of a dynamic heart phantom with known volumes, and in subjects with normal heart function.

An important feature of the semi-automatic segmentation procedure was that the papillary muscles and trabeculae were included in the myocardial volume rather than in the blood volume. In the subject study, this led to notably lower EDVs and ESVs with the semi-automatic method compared to the manual method. It also has a pronounced effect on the ejection fractions, which were considerably higher for the semi-automatic method. In this study, all ejection fractions found with either method were within the normal range, and the recorded difference would not be relevant for clinical decision-making. However, other studies have demonstrated that including the papillary muscles and trabeculae in the myocardial volume can have consequences for patient management [17], especially in patients with myocardial hypertrophy [7]. Further research is needed to indicate which measure is clinically most relevant.

Variations in drawing the contours was the main source of intra- and inter-observer variations in both the semi-automatic and manual method. However, for the semi-automatic method only the epicardial contour was required. Compared to the endocardial contour, the epicardial contour is generally less user-dependent, because the contrast between myocardium and surrounding tissues is usually higher. Moreover, delineation of the endocardial contour was in most subjects complicated by the presence of papillary muscles and trabeculae. This was especially true for the ESV, where the endoluminal muscular structures lied against the myocardial border. As a result, observer agreement was significantly improved for the semi-automatic method compared to the manual method.

For the phantom, both the manual and semi-automatic method underestimated the volumes. The discrepancy between true and measured volumes may be caused by the exclusion of the most basal slice from the total volume. Due to partial volume effects, no pure blood was present in this slice. Inclusion would have led to overestimation of the blood volumes. Moreover, because the delineation of the endocardial contour was less pronounced, it might have increased the inter-observer variation for both the manual and semi-automatic method.

In the phantom study, the semi-automatic method gave slightly larger blood volumes than the manual method. This may indicate that the threshold value of 70

% is too high for this situation. Whether this is only true for the heart phantom, which in this experiment had a higher blood-myocardium contrast than a real heart remains to be investigated.

Conclusion

With the semi-automatic method, endoluminal muscular structures could be excluded from the blood volume with significantly improved intra- and inter-observer agreement in cardiac function measurements compared to the conventional, manual method.

References

[1] Koren MJ, Devereux RB, Casale PN, et al., (1991) Relation of left ventricular mass and geometry to morbidity and mortality in uncomplicated essential hypertension. Ann Intern Med 114:345-52.

[2] Solomon SD, Anavekar N, Skali H, et al., (2005) Influence of ejection fraction on cardiovascular outcomes in a broad spectrum of heart failure patients. Circulation 112:3738-44.

[3] Dewey M, Muller M, Eddicks S, et al., (2006) Evaluation of global and regional left ventricular function with 16-slice computed tomography, biplane cineventriculography, and two-dimensional transthoracic echocardiography: comparison with magnetic resonance imaging. J Am Coll Cardiol 48:2034-44.

[4] Pattynama PM, Lamb HJ, van der Velde EA, et al., (1993) Left ventricular measurements with cine and spin-echo MR imaging: a study of reproducibility with variance component analysis. Radiology 187:261-8.

[5] Sievers B, Kirchberg S, Bakan A, et al., (2004) Impact of papillary muscles in ventricular volume and ejection fraction assessment by cardiovascular magnetic resonance. J Cardiovasc Magn Reson 6:9-16.

[6] Papavassiliu T, Kuhl HP, Schroder M, et al., (2005) Effect of endocardial trabeculae on left ventricular measurements and measurement reproducibility at cardiovascular MR imaging. Radiology 236:57-64.

[7] Janik M, Cham MD, Ross MI, et al., (2008) Effects of papillary muscles and trabeculae on left ventricular quantification: increased impact of methodological variability in patients with left ventricular hypertrophy. J Hypertens 26:1677-85.

[8] Chin TK, Perloff JK, Williams RG, et al., (1990) Isolated noncompaction of left ventricular myocardium. A study of eight cases. Circulation 82:507-13.

[9] Oechslin EN, Attenhofer Jost CH, Rojas JR, et al., (2000) Long-term follow-up of 34 adults with isolated left ventricular noncompaction: a distinct cardiomyopathy with poor prognosis. J Am Coll Cardiol 36:493-500.

[10] Fernandez-Golfin C, Pachon M, Corros C, et al., (2009) Left ventricular trabeculae: quantification in different cardiac diseases and impact on left ventricular morphological and functional parameters assessed with cardiac magnetic resonance. J Cardiovasc Med (Hagerstown) 10:827-33.

[11] Codella NC, Weinsaft JW, Cham MD, et al., (2008) Left ventricle: automated segmentation by using myocardial effusion threshold reduction and intravoxel computation at MR imaging. Radiology 248:1004-12.

[12] Furber A, Balzer P, Cavaro-Menard C, et al., (1998) Experimental validation of an automated edge-detection method for a simultaneous determination of the endocardial and epicardial borders in short-axis cardiac MR images: application in normal volunteers. J Magn Reson Imaging 8:1006-14.

[13] Graves MJ, Berry E, Eng AA, et al., (2000) A multicenter validation of an active contour-based left ventricular analysis technique. J Magn Reson Imaging 12:232-9.

[14] Lynch M, Ghita O, Whelan PF, (2006) Automatic segmentation of the left ventricle cavity and myocardium in MRI data. Comput Biol Med 36:389-407.

[15] van Geuns RJ, Baks T, Gronenschild EH, et al., (2006) Automatic quantitative left ventricular analysis of cine MR images by using three-dimensional information for contour detection. Radiology 240:215-21.

[16] van der Geest RJ, Lelieveldt BP, Angelie E, et al., (2004) Evaluation of a new method for automated detection of left ventricular boundaries in time series of magnetic resonance images using an Active Appearance Motion Model. J Cardiovasc Magn Reson 6:609-17.

[17] Weinsaft JW, Cham MD, Janik M, et al., (2008) Left ventricular papillary muscles and trabeculae are significant determinants of cardiac MRI volumetric measurements: effects on clinical standards in patients with advanced systolic dysfunction. Int J Cardiol 126:359-65.

[18] Farnebäck G, (2002) Polynomial Expansion for Orientation and Motion Estimation.

[19] Otsu N, (1979) A Threshold Selection Method from Gray-Level Histograms. Systems, Man and Cybernetics, IEEE Transactions on 9:62-6.

[20] Spreeuwers LJ, Bangma SJ, Meerwaldt RJHW, et al. (2005), Detection of Trabeculae and Papillary Muscles in Cardiac MR Images. 2005:415-8.

Appendix I

The semi-automatic segmentation method (QMass MR research edition, Medis, Leiden, The Netherlands) was based on the signal intensity distribution of MR images. The technique of normalized convolution [18] is used to estimate the spatially varying blood and muscle intensities within a user-provided epicardial contour. The voxel intensity is defined by a first order model with six variables:

$$I(x,y) = (1 - w(x,y)) \cdot (I_m(x,y) + w(x,y) \cdot I_b(x,y) \quad (1)$$

with:

$$\text{Muscle: } I_m(x,y) = a_0 + a_1x + a_2y \quad (2)$$
$$\text{Blood: } I_b(x,y) = b_0 + b_1x + b_2y$$

where a_0, a_1, a_2, b_0, b_1 and b_2 are constants that vary among scans according to the grey value distribution of the image within the epicardial contour. $I_m(x,y)$ and $I_b(x,y)$ represent the approximation of the intensity of muscle and blood, respectively, at the position (x,y) (see Figure A). The constants are obtained with an iterative optimization procedure, during which the weight $w(x,y)$ is initialized to either 1 or 0 using the Otsu threshold method [19]. The procedure is stopped when the classification $w > 0.5$ is unaltered between iterations or when the number of iterations exceeds ten.

Assuming a linear relationship between the fraction of blood and the intensity of the voxel ($I(x,y)$), the weight $w(x,y)$ represents the fraction of blood in the voxel.

$$w(x,y) = \frac{I(x,y) - I_m(x,y)}{I_b(x,y) - I_m(x,y)} \quad (3)$$

A binary classification is obtained by thresholding $w(x,y)$. If $w(x,y)$ is higher than the threshold value, the voxel is considered pure blood, otherwise it is defined as pure muscle. In this experiment the threshold value was set to 70%. Blood volume measures are obtained by multiplying the number of voxels classified as blood with the voxel volume.

Note that this method does not distinct trabeculations from papillary muscle and as such stands out from methods that do specifically target the papillary muscles (See e.g. [20].

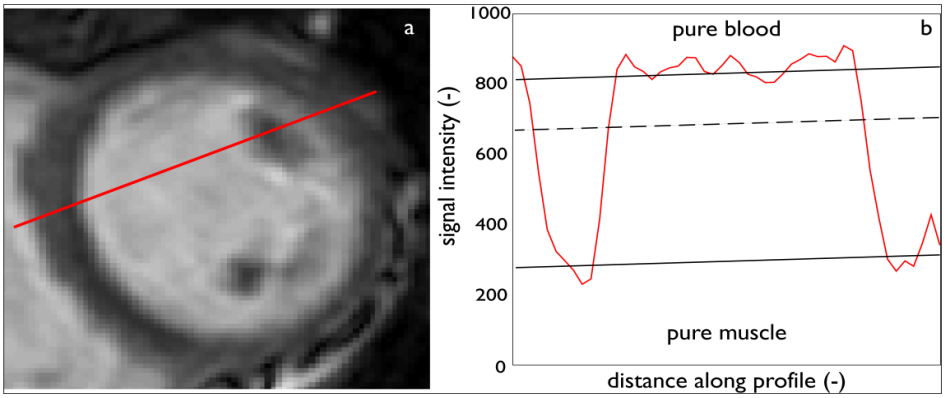

Figure A Segmentation procedure. *Panel a shows a short axis view of the heart. The signal intensities along the red line in panel a are represented in panel b. The algorithm fits two planes (represented by the solid black lines) through the highest (blood) and lowest (muscle) signal intensities within the epicardium. A threshold plane was defined at 70 % between the two intensity planes. Voxels with signal intensities above this threshold are considered pure blood, and voxels with signal intensities below this threshold are considered to be pure muscle.*

4

Impact of right ventricular endocardial trabeculae on volumes and function assessed by CMR in patients with tetralogy of Fallot

Hendrik G. Freling
Kees van Wijk
Karolien Jaspers
Petronella G. Pieper
Karin M. Vermeulen
Jeroen M. van Swieten
Tineke P. Willems

Abstract

Purpose: To assess the impact of right ventricular (RV) trabeculae and papillary muscles on measured volumes and function assessed by cardiovascular magnetic resonance imaging in patients with repaired tetralogy of Fallot.

Methods: Sixty-five patients with repaired tetralogy of Fallot underwent routine cardiovascular magnetic resonance imaging. Endocardial and epicardial contours were drawn manually and included trabeculae and papillary muscles in the blood volume. Semi-automatic threshold-based segmentation software excluded these structures. Both methods were compared in terms of end-diastolic, end-systolic and stroke volume, ejection fraction and mass. Observer agreement was determined for all measures.

Results: Exclusion of trabeculae and papillary muscle in the RV blood volume decreased measured RV end-diastolic volume by 15% (from 140 ± 35 ml/m^2 to 120 ± 32 ml/m^2) compared to inclusion, end-systolic volume by 21% (from 74 ± 23 ml/m^2 to 59 ± 20 ml/m^2), stroke volume by 9% (from 66 ± 16 ml/m^2 to 60 ± 16 ml/m^2) and relatively increased ejection fraction by 7% (from 48 ± 7% to 51 ± 8%) and end-diastolic mass by 79% (from 28 ± 7 g/m^2 to 51 ± 10 g/m^2), $p<.01$. Excluding trabeculae and papillary muscle resulted in an improved interobserver agreement compared to including these structures (coefficient of agreement of 87% vs 78%, $p < .01$)

Conclusions: Trabeculae and papillary muscle significantly affect measured RV volumes, function and mass. Semi-automatic threshold-based segmentation software can reliably exclude trabeculae and papillary muscles from the RV blood volume.

Int J Cardiovasc Imaging. 2013 Mar;29(3):625-31

Introduction

Tetralogy of Fallot (ToF) is the most common congenital heart disease involving the right ventricle (RV). Important complications during follow-up after repair for ToF are RV volume overload. Longstanding volume overload can result in irreversible RV dilation and dysfunction which can be prevented by timely replacing the pulmonary valve [1-5]. Furthermore, many patients have some amount of pressure overload caused by residual outflow tract obstruction, stenosis of a pulmonary artery branch or stenosis of a valve prosthesis. Therefore, evaluation of the RV is essential in the follow-up of patients with ToF [6,7].

Guidelines advise cardiac magnetic resonance imaging (CMR) as the primary imaging modality for evaluation of RV volumes and function [6,7]. Consensus is lacking on whether to consider trabeculae and papillary muscles as part of measured RV volumes [8-10]. Including trabeculae and papillary muscles in RV volumes results in larger measured volumes compared to measurements with exclusion of these structures. In healthy subjects and patients without congenital heart disease, the influence of trabeculae and papillary muscle on RV volumes is too small to be of clinical importance [9]. The increase in papillary muscle and trabeculae can be large in patients with a systemic right ventricle [10]. However, no studies have addressed the influence of papillary muscle and trabeculae on measured RV volumes in patients with repaired ToF. Studies in patients with ToF including trabeculae and papillary muscles in the RV blood volume report larger RV volumes and lower RV mass than studies excluding these structures [11-14]. Therefore, knowledge of the quantity of trabeculae and papillary muscles and the possibility to estimate this amount could be of clinical importance in patients with ToF.

The primary objective of our study was to determine the trabecular volume of the RV and the reliability by which it can be measured in patients with repaired ToF. The second objective was to create a mathematical model that describes the relation between the RV volumes with and without inclusion of trabeculae and papillary muscle in the RV blood volume.

Materials and methods

Patients

The study population consisted of 65 patients with repaired ToF. All patients underwent CMR examination between January 2008 and January 2011. In 60 (92%) patients primary indication for CMR was follow-up of RV volumes and pulmonary flow parameters, in 3 (5%) patients sudden decrease in exercise capacity, in 1 (2%) patient new onset of ventricular tachycardia and in 1 (2%) patient poor echocardiographic image quality. In 24 (37%) patients clinical symptoms were present: subjective reduced exercise capacity in 14 (22%) patients, history of supraventricular tachycardia in 5 (8%) patients and history of ventricular tachycardia in 5 (8%) patients. Other patient characteristics are shown in table 1.

This retrospective study was approved by the University Medical Center Groningen review board and informed consent was not required according to the Dutch Medical Research Involving Human Subjects act.

Table 1 Patient characteristics

Characteristic	
Male	37 (57)
Age (years)	30 ± 10
Body surface area (m^2)	1,86 ± 0,19
Age at total repair (years)	1.76 (0.89 – 5,05)
Pulmonary valve replacement	15 (23)
Pulmonary regurgitation fraction (%)	34 (15 – 45)
Pulmonary regurgitation volume (ml/m^2)	18 (7 – 30)
Pulmonary valve peak flow velocity (cm/s)	187 ± 75

Data are mean ± standard deviation, median (IQR), or number of subjects (%)

CMR image acquisition

All subjects were examined on a 1.5-Tesla MRI system (Siemens Magnetom Sonata, Erlangen, Germany or Siemens Magnetom Avanto, Erlangen, Germany) using a 2 x 6 channel body-coil. After single-shot localizer images, short axis cine loop images with breath holding in expiration were acquired using a retrospectively gated balanced steady state free precession sequence. Parallel imaging was employed using GRAPPA (GeneRalized Autocalibrating Partially Parallel Acquisition). To improve image intensity uniformity Prescan Normalize was

used. Short axis slices were planned in end-diastole from two slices above the mitral valve plane to the apex. The following parameters were used: TR 2.7 ms, TE 1.1 ms, flip angle 80^{o}, matrix 192 x 192 mm, 25 frames per cycle, slice thickness 6 mm, interslice gap 4 mm, voxel size 1.7 x 1.7 x 6 mm.

Two-dimensional velocity encoded MRI flow measurements perpendicular and directly cranial to the pulmonary valve was performed to quantify flow velocity and volumes. Encoded velocity was 200 cm/s which was increased in steps of 50 cm/s in case of aliasing.

CMR image analysis

Image analysis was performed manually by using QMass MR (version 7.2, Medis, Leiden, The Netherlands) and semi-automatically by using QMass MR research edition (Medis, Leiden, The Netherlands).

The end-systolic and end-diastolic frames of the RV were selected by visual assessment. The basal slice was selected with aid of long-axis cine view images. When the pulmonary valve was visible in the RV basal slice, only the portion of the right ventricular outflow tract below the level of the pulmonary valve was included. The inflow part of the RV was included in the RV volume. The RV inflow part was distinguished from the right atrium by recognizing the trabeculated and thick right ventricular wall compared to the thin right atrial wall [15]. RV contours were drawn manually by tracing the endocardial and epicardial borders in every slice in end-systole and end-diastole. Contour tracing was aided by reviewing the multiple phase scans in the movie mode.

Two methods were used to measure RV volumes, function and mass (see figure 1). Method 1 excluded papillary muscle and trabeculae from the RV blood volume by using semi-automatic threshold-based segmentation software. Method 2 included these structures in the endocardial contour and therefore the blood volume. The semi-automatic threshold-based segmentation software was based on the signal intensity distribution of MR images. The voxels within the epicardial contour were classified as either blood or muscle according to their signal intensity, taking into account spatial variations in signal intensity. Based on their signal intensity, trabeculae and pappilary muscles were included in the myocardial volume. Users had the possibility to manually change the threshold level of signal intensities above which voxels are depicted as blood for every slice. Selecting and deselecting individual voxels was possible, for example in case of artefacts due to mechanical pulmonary valve prosthesis. As the semi-automatic threshold-based segmentation software was an integral part of QMass, both methods used the

same endocardial and epicardial contours. A more detailed description of the segmentation procedure can be found in Appendix I of Chapter 3.

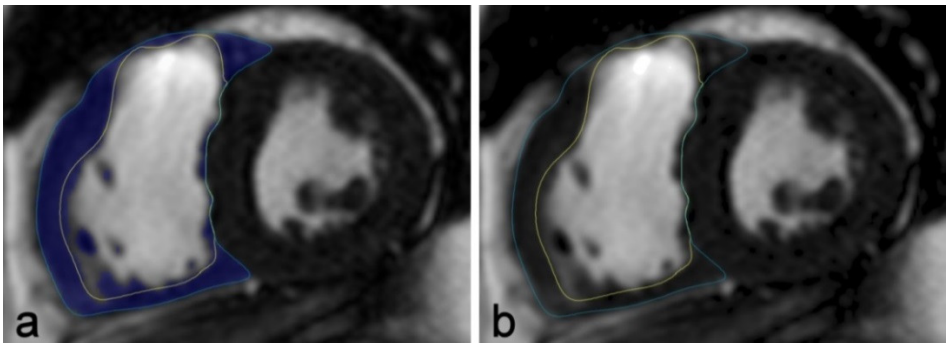

Figure 1. *Two methods were used to measure RV volumes. In Method 1, trabeculae and papillary muscle were excluded from the right ventricular volume with use of semi-automatic threshold-based segmentation software (a). In Method 2, trabeculae and papillary muscle were included in the right ventricular volume (b).*

Stroke volume was defined as end-diastolic volume minus end-systolic volume. Ejection fraction was defined as stroke volume divided by end-diastolic volume. Mass is derived from myocardial volume after multiplying by the density of cardiac muscle, 1.05 g/cm^3. All volumes were indexed for Body Mass Index.

To obtain agreement between observers, 25 randomly selected CMR scans were analysed by a second independent observer. For agreement within one observer, the same 25 scans were analysed a second time by the first observer with an interval of at least two weeks between the first and second analysis.

Statistical analyses

The Statistical Package for the Social Sciences version 16.0 (SPSS Inc, Chicago, IL) was used for all statistical analyses. All statistical tests are two-sided and a P-value of less than .05 was considered statistically significant.

Descriptive statistics were calculated as mean and standard deviation for normally distributed continuous variables, median with interquartile range (IQR) for non-normally distributed continuous variables and absolute numbers and percentages for dichotomous variables. The manual and semi-automatic methods were compared in terms of RV volume, mass and function by using the paired-samples Student's t-test.

The intraobserver agreement coefficient (AC_{intra}) between paired observations was calculated for both observers:

$$AC_{intra} = 100 \cdot \left(1 - \frac{2 \cdot |Obs_1 - Obs_2|}{Obs_1 + Obs_2}\right) \qquad (1)$$

For the first observer, the median AC_{intra} was computed. The interobserver agreement coefficient AC_{inter} was also determined. For both observers, the average of the two paired observations was used. The difference in median AC between the manual and semi-automatic method was assessed with a paired Wilcoxon signed rank test.

Linear regression was used to examine the relationship between RV volume measurements when including and excluding trabeculae and papillary muscles.

Results

RV volumes and function

Exclusion (Method 1) instead of inclusion (Method 2) of trabeculae and papillary muscle in the RV blood volume resulted in a significant change in measured RV volumes and function. When Method 1 was compared to Method 2, end-diastolic volumes were 15 ± 4% (from 140 ± 35 ml/m^2 to 120 ± 32 ml/m^2), end-systolic volumes 21 ± 5% (from 74 ± 23 ml/m^2 to 59 ± 20 ml/m^2) and stroke volumes 9 ± 5% (from 66 ± 16 ml/m^2 to 60 ± 16 ml/m^2) smaller ($p < .01$). Ejection fractions were 7 ± 4% (from 48 ± 7% to 51 ± 8%) and the end-diastolic masses were 79 ± 21% (from 28 ± 7 g/m^2 to 51 ± 10 g/m^2) larger ($p < .01$). The difference in RV end-diastolic volumes, RV end-systolic volumes, RV ejection fraction and RV end-diastolic mass between Method 1 and Method 2 increased as volumes, ejection fraction and mass became larger (see figure 2). Exclusion of trabeculae and papillary muscle took an average of 67 ± 16 seconds extra time compared to inclusion of these structures.

Observer agreement

The intra- and interobserver reproducibility data are shown in table 2. Observer agreement was high in all measurements with exception of RV mass. Method 1 resulted in a significantly higher AC_{intra} and AC_{inter} for RV mass ($p < .01$). The AC_{intra} for RV end-diastolic volume was significantly higher for Method 2 ($p = .02$).

Model

The amount of trabeculae increased with increasing end-diastolic and end-systolic volumes. Based on this relationship the following model was created:

$$RV_{excl} = a \cdot RV_{incl} + b \qquad (2)$$

RV_{excl} and RV_{incl} were RV volumes in which the trabeculae and papillary muscles were excluded and included, respectively. For end-diastolic volumes the constant *a* and *b* from equation 2 were .90 (95% CI .87 to .94) and -7.04 ml/m^2 (95% CI -2.29 to -11.79 ml/m^2), respectively. For end-systolic volumes, *a* was .87 (95% CI .84 to .90) and *b* -5.30 ml/m^2 (95% CI -2.64 to -7.96 ml/m^2).

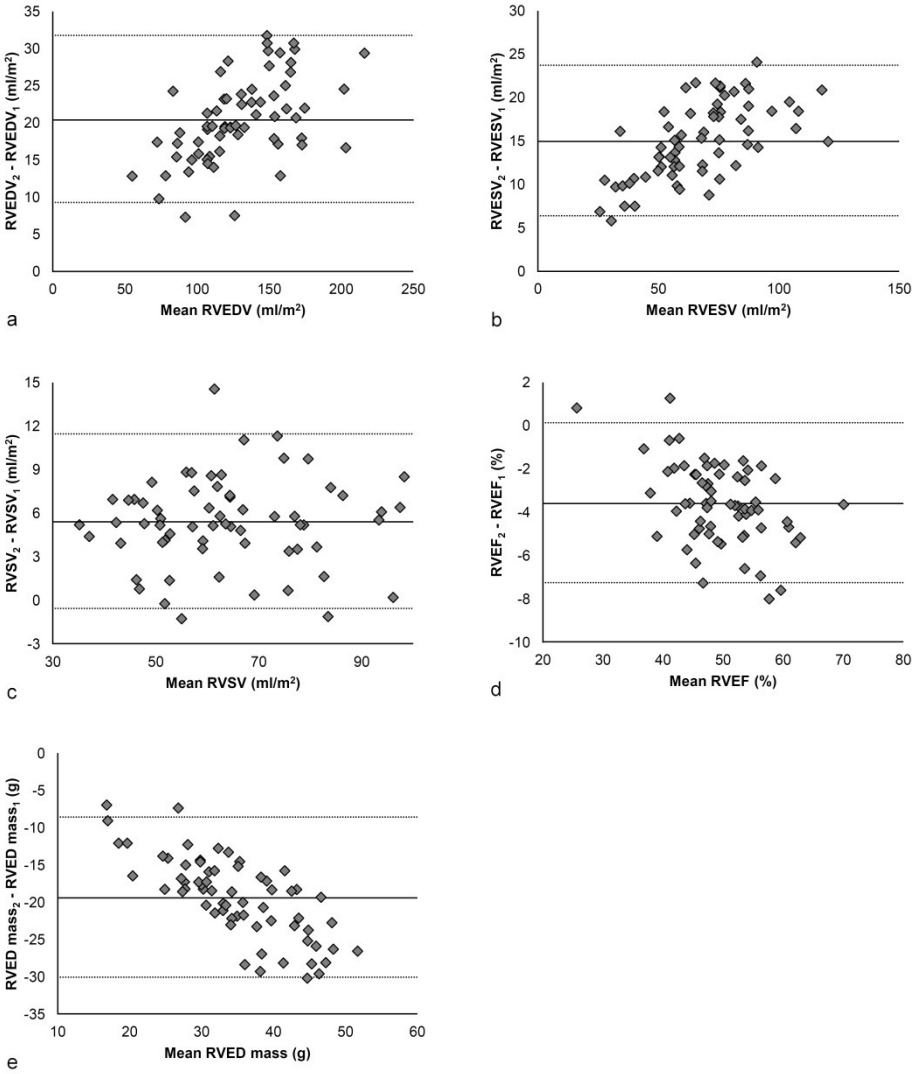

Figure 2. *Bland-Altman plots visualizing the differences between Method 1 and Method 2 for measurements of (a) right ventricular end-diastolic volume, (b) right ventricular end-systolic volume, (c) right ventricular stroke volume, (d) right ventricular ejection fraction and (e) right ventricular end-diastolic mass. The X-axis depicts the mean value of Method 1 and Method 2 for each parameter. The Y-axis depicts the difference in measurements between Method 1 and Method 2. The continuous line represents the mean difference between Method 1 and Method 2 for each measurement and the dotted line represents the mean difference ± 1.96 standard deviations between Method 1 and Method 2. RVED mass = right ventricular end-diastolic mass, RVEDV = right ventricular end-diastolic volume, RVEF = right ventricular ejection fraction, RVESV = right ventricular end-systolic volume, RVSV = right ventricular stroke volume.*

Table 2 Interobserver and intraobserver coefficients of agreement of right ventricular volume and function measurements for Method 1 and Method 2

	RVEDV	RVESV	RVSV	RVEF	RV mass
Interobserver					
Method 1					
Mean diff. ± SD	0.4 ± 7.7	-0.5 ± 6.5	0.6 ± 3.8	0.4 ± 3.9	-2.2 ± 8.8
95% CI	-14.7 to 15.5	-13.3 to 12.2	-6.9 to 8.1	-7.2 to 8.0	-19.4 to 15.0
AC (%)	96	95	93	95	87
Method 2					
Mean diff. ± SD	1.1 ± 10.7	2.4 ± 7.3	-0.6 ± 4.5	-1.5 ± 3.8	-2.8 ± 7.0
95% CI	-19.9 to 22.2	-11.9 to 16.6	-9.5 to 8.3	-9.0 to 6.0	-16.5 to 11.0
AC (%)	95	94	91	95	78
P Value	.43	.86	.21	.56	<.01
Intraobserver					
Method 1					
Mean diff. ± SD	5.1 ± 6.8	4.2 ± 5.4	0.4 ± 3.4	-1.2 ± 3.6	1.9 ± 4.4
95% CI	-8.3 to 18.5	-6.4 to 14.9	-6.3 to 7.2	-8.3 to 5.8	-6.8 to 10.6
AC (%)	95	95	95	97	93
Method 2					
Mean diff. ± SD	2.7 ± 7.1	3.9 ± 7.2	-0.7 ± 3.3	-1.8 ± 3.6	4.6 ± 3.3
95% CI	-11.2 to 16.6	-10.0 to 18.0	-7.1 to 5.7	-8.8 to 5.2	-1.9 to 11.1
AC (%)	97	96	93	96	85
P Value	.02	.19	.72	.40	<.01

Volumetric data are expressed in ml/m^2, and mass in g/m^2. 95% CI = 95% confidence interval, AC = agreement coefficient, diff = difference, Method 1 = exclusion of papillary muscle and trabeculae from the RV blood volume, Method 2 = inclusion of papillary muscle and trabeculae in the RV blood volume, RV mass = right ventricular end-diastolic mass, RVEDV = right ventricular end-diastolic volume, RVEF = right ventricular ejection fraction, RVESV = right ventricular end-systolic volume, RVSV = right ventricular stroke volume, SD = standard deviation

Discussion

Our study is the first to show the impact of trabeculae and papillary muscle on RV volume measurements in a large group of patients with repaired tetralogy of Fallot. Semi-automatic threshold-based segmentation software provided a reproducible method to differentiate myocardium from blood. Compared to including papillary muscle and trabeculae from the RV blood volume, exclusion of the papillary muscle and trabeculae in the RV blood volume resulted in significantly decreased end-systolic and end-diastolic volumes and increased ejection fraction and mass. Manually delineating RV trabeculae and papillary muscles has a low reproducibility in patients with increased trabeculae and is time-consuming [10]. Therefore, many studies in patients with ToF have included these structures in the blood volume. Our study showed that with semi-automatic threshold-based segmentation software it is possible to differentiate myocardium from blood with a high reproducibility, which is in line with a previous report [11]. This creates the possibility to measure RV blood volume without inclusion of trabeculae and papillary muscles. Inclusion or exclusion of trabeculae and papillary muscles can have a profound effect on the measured volumes and mass. Our study showed a decrease of 21% in end-systolic volume and 15% in end-diastolic volume when these structures were excluded from the RV blood pool. The change in measured RV mass was very large with an increase of 79%.

Most patients with repaired ToF are considered to mainly have a volume-overloaded. We expected the trabeculae to blood volume ratio to be much less in our patients with ToF than reported in patients with systemic RVs. However, compared to patients with systemic RVs in a study by Winter et al., the change in volume was similar in patients with repaired ToF for end-diastolic volume (15% for both groups) and smaller for the end-systolic volume (21% vs 27%) when trabeculae and papillary muscle were excluded from the RV blood pool [10]. It is difficult to compare our results with those from the study by Winter et al. as they delineated trabeculae and papillary muscles manually to differentiate blood from muscle, instead of semi-automatic with threshold-based segmentation software. In our study, no direct comparison was made between these two methods because of the aforementioned disadvantages of manually delineating trabeculae and papillary muscles [10].

Although the amount of trabeculae and papillary muscles should be the same in end-systole and end-diastole, stroke volume was 6 ml/m^2 larger when including compared to excluding these structures. A possible explanation is that the amount of trabeculae in end-systole was underestimated. Discriminating trabeculae from

RV wall is difficult in end-systole due to compression of the trabeculae against the RV wall. Therefore, contour tracing was aided by reviewing the multiple phase scans in the movie mode. Based on movement and position of the trabeculae during the entire heart cycle, it was possible to interpolate the position of the endocardial contour. Some of the trabeculae were possibly considered to be RV wall in end-systole and not in end-diastole. Another explanation is that the amount of trabeculae was overestimated in end-diastole. Trabeculae can be better distinguished from the RV wall in end-diastole. However, this will result in more voxels containing both blood and trabeculae and too much of these voxels were possibly considered to be trabuculae and not blood.

The existing RV reference values are based on RV volumes including trabeculae and papillary muscles. When papillary muscles and trabeculae are excluded from the blood volume, use of these reference values is no longer valid. Until new reference values are developed in which the trabeculae and papillary muscles are excluded, it is possible to use the proposed model in patients with ToF to allow comparison with the old reference values. The same applies to the application of threshold values. An important threshold is the use of RV end-diastolic volume for timing pulmonary valve replacement in patients with ToF [1-5]. The reported thresholds range from 82 to 90 ml/m^2 for end-systolic volume and 150 to 170 ml/m^2 for end-diastolic volumes. Some of these differences may be explained by including or excluding trabeculae and papillary muscles in the measured volumes. Unfortunately, only one of these studies reported whether they included RV trabeculae and papillary muscles in the measured volumes [2].

Limitations and future perspectives

A gold standard for the amount of endocardial trabeculae of the RV is lacking. Therefore, a validation in vivo was not possible. However, exclusion of trabeculae and papillary muscle should be theoretically more accurate as these structures are part of the myocardium and not blood.

In our study, measurements of RV volumes and function were highly reproducibility. However, an axial orientation could have resulted in an even higher reproducibility and also a higher accuracy in patients with a severely dilated RV [16,17].

Our study was limited to patients with repaired ToF as this is the most common severe congenital heart disease in adult patients. To determine the influence of trabeculae in the RV volume in other patient groups, more research is required. Our study showed that semi-automatic threshold-based segmentation software is a valuable tool for further research in this area.

Conclusion

RV endocardial trabeculae significantly influence measured RV volumes and mass. Exclusion compared to inclusion of trabeculae and papillary muscle in the RV blood volume results in a significantly decrease in measured end-systolic and end-diastolic volume and increase in measured ejection fraction and mass. Semi-automatic threshold-based segmentation software can exclude trabeculae and papillary muscles from the RV blood volume in a reproducible manner. Currently used ranges and thresholds for congenital heart disease patients should be re-established, as new threshold-based algorithms will become available in clinical practice.

References

[1] Therrien J, Provost Y, Merchant N, et al., (2005) Optimal timing for pulmonary valve replacement in adults after tetralogy of Fallot repair. Am J Cardiol 95:779-82.

[2] Buechel ER, Dave HH, Kellenberger CJ, et al., (2005) Remodelling of the right ventricle after early pulmonary valve replacement in children with repaired tetralogy of Fallot: assessment by cardiovascular magnetic resonance. Eur Heart J 26:2721-7.

[3] Oosterhof T, van Straten A, Vliegen HW, et al., (2007) Preoperative thresholds for pulmonary valve replacement in patients with corrected tetralogy of Fallot using cardiovascular magnetic resonance. Circulation 116:545-51.

[4] Frigiola A, Tsang V, Bull C, et al., (2008) Biventricular response after pulmonary valve replacement for right ventricular outflow tract dysfunction: is age a predictor of outcome? Circulation 118:S182-90.

[5] Geva T, (2011) Repaired tetralogy of Fallot: the roles of cardiovascular magnetic resonance in evaluating pathophysiology and for pulmonary valve replacement decision support. J Cardiovasc Magn Reson 13:9.

[6] Baumgartner H, Bonhoeffer P, De Groot NM, et al., (2010) ESC Guidelines for the management of grown-up congenital heart disease (new version 2010). Eur Heart J 31:2915-57.

[7] Warnes CA, Williams RG, Bashore TM, et al., (2008) ACC/AHA 2008 Guidelines for the Management of Adults with Congenital Heart Disease: a report of the American College of Cardiology/American Heart Association Task Force on Practice Guidelines (writing committee to develop guidelines on the management of adults with congenital heart disease). Circulation 118:e714-833.

[8] Kilner PJ, Geva T, Kaemmerer H, et al., (2010) Recommendations for cardiovascular magnetic resonance in adults with congenital heart disease from the respective working groups of the European Society of Cardiology. Eur Heart J 31:794-805.

[9] Sievers B, Kirchberg S, Bakan A, et al., (2004) Impact of papillary muscles in ventricular volume and ejection fraction assessment by cardiovascular magnetic resonance. J Cardiovasc Magn Reson 6:9-16.

[10] Winter MM, Bernink FJ, Groenink M, et al., (2008) Evaluating the systemic right ventricle by CMR: the importance of consistent and reproducible delineation of the cavity. J Cardiovasc Magn Reson 10:40.

[11] Beerbaum P, Barth P, Kropf S, et al., (2009) Cardiac function by MRI in congenital heart disease: impact of consensus training on interinstitutional variance. J Magn Reson Imaging 30:956-66.

[12] Mooij CF, de Wit CJ, Graham DA, et al., (2008) Reproducibility of MRI measurements of right ventricular size and function in patients with normal and dilated ventricles. J Magn Reson Imaging 28:67-73.

[13] Samyn MM, Powell AJ, Garg R, Sena L, et al., (2007) Range of ventricular dimensions and function by steady-state free precession cine MRI in repaired tetralogy of Fallot: right ventricular outflow tract patch vs. conduit repair. J Magn Reson Imaging 26:934-40.

[14] Davlouros PA, Kilner PJ, Hornung TS, et al., (2002) Right ventricular function in adults with repaired tetralogy of Fallot assessed with cardiovascular magnetic resonance imaging: detrimental role of right ventricular outflow aneurysms or akinesia and adverse right-to-left ventricular interaction. J Am Coll Cardiol 40:2044-52.

[15] Alfakih K, Plein S, Thiele H, et al., (2003) Normal human left and right ventricular dimensions for MRI as assessed by turbo gradient echo and steady-state free precession imaging sequences. J Magn Reson Imaging 17:323-9.

[16] Clarke CJ, Gurka MJ, Norton PT, et al., (2012) Assessment of the accuracy and reproducibility of RV volume measurements by CMR in congenital heart disease. JACC Cardiovasc Imaging 5:28-37.

[17] Fratz S, Schuhbaeck A, Buchner C, et al., (2009) Comparison of accuracy of axial slices versus short-axis slices for measuring ventricular volumes by cardiac magnetic resonance in patients with corrected tetralogy of fallot. Am J Cardiol 103:1764-9.

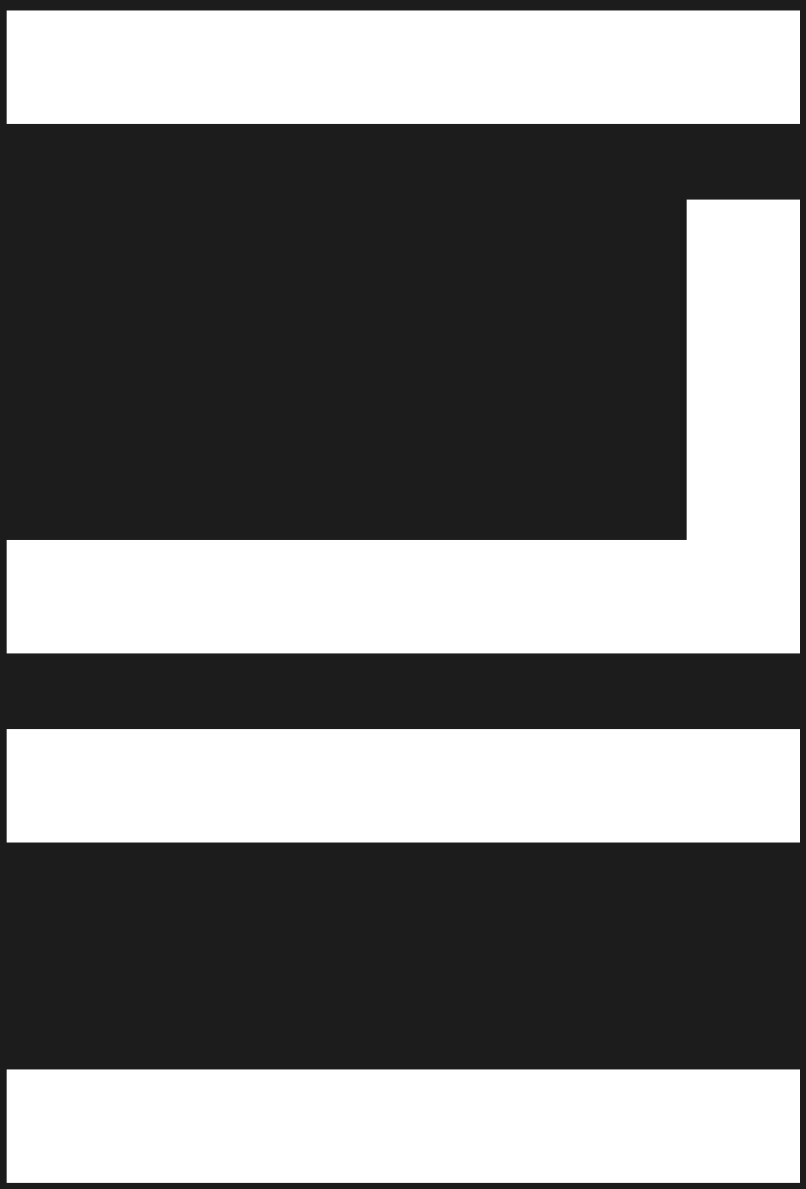

5

Pressure overloaded right ventricles: a multicenter study on the importance of trabeculae in right ventricular function measured by CMR

Mieke M.P. Driessen
Vivan J.M. Baggen
Hendrik G. Freling
Petronella G. Pieper
Arie P. van Dijk
Pieter A. Doevendans
Repke J. Snijder
Marco C. Post
Folkert J. Meijboom
Gertjan Tj. Sieswerda
Tim Leiner
Tineke P. Willems

Abstract

Objectives: Cardiac magnetic resonance imaging (CMR) is the preferred method to measure right ventricular (RV) volumes and ejection fraction (RVEF). This study aimed to determine the impact of trabeculae and papillary muscles on RV volumes and function in patients with pressure overloaded RVs and its reproducibility using semi-automatic software.

Material and methods: Eighty patients with pressure overloaded RVs (pulmonary hypertension, transposition of the great arteries after arterial switch operation and after atrial switch procedure and repaired tetralogy of Fallot) and 20 healthy controls underwent short-axis multislice cine CMR. End-diastolic volume (EDV), end-systolic volume, RV mass and RVEF were measured using 2 methods and compared using paired samples T-test. First, manual contour tracing of RV endo- and epicardial borders was performed. Thereafter, trabeculae were excluded from the RV blood volume using semi-automatic pixel-intensity based software. Twenty-five datasets were re-analyzed, to assess intra- and interobserver agreement.

Results: Exclusion of trabeculae resulted in significantly decreased EDV; ranging from a decrease of -5.7 ± 1.7 ml/m^2 in healthy controls to -29.2 ± 6.6 ml/m^2 in patients after atrial switch procedure. RVEF significantly increased in all groups, ranging from an absolute increase of 3.4 ± 0.8% in healthy controls up to 10.1 ± 2.3% in patients after atrial switch procedure. Observer agreement was high for all measurements.

Conclusions: In patients with pressure overloaded RVs exclusion of trabeculae from the blood volume results in a significant change in RV volumes, RVEF and RV mass and is highly reproducible when semi-automatic pixel-intensity based software is used.

Accepted in Int J Cardiovasc Imaging

Introduction

Both in patients with pulmonary hypertension (PH) and in patients with different types of congenital heart disease (CHD), the right ventricle (RV) performs under increased pressure loading. The RV adapts by hypertrophying, however at a certain point the RV is unable to cope with the increased pressures and RV failure will ensue. Consequently, RV function is an important determinant of prognosis and of therapeutic strategy in these patients. For instance, in patients with pulmonary valvular (PV) stenosis, timing of intervention is partly dependent on RV function [1]. In patients with PH, deterioration of RV ejection fraction (RVEF), increased RV end-diastolic volume (RVEDV) and stroke index are associated with poor outcome [2,3]. Furthermore, for patients with systemic RV after atrial switch operation, decline in RV function is one of the most important clinical problems. Therefore RV volumes and function are used frequently in follow-up of these patients, making accurate and reproducible measurements highly important.

As 2D and also 3D echocardiography of the RV remain less accurate and reproducible than cardiac magnetic resonance imaging (CMR), the latter is still considered to be the reference standard for the quantification of RV volumes and EF [4-7]. Whether trabeculae and papillary muscles should be included or excluded from the blood volume is subject of debate. Throughout literature both methods are used [2,8-10]. However, in many studies it is not clearly described whether trabeculae and papillary muscles were included or excluded from the RV blood volume [11-14]. The impact of trabeculae is assumed to be small in healthy individuals, but Winter et al. showed that exclusion of trabeculae from the RV blood volume resulted in a substantial difference of RVEDV, RV end-systolic volume (RVESV) and RVEF in patients with a systemic right ventricle[15]. Although theoretically more accurate, Winter et al. also showed that manual tracing of trabeculae has low reproducibility and therefore can be considered less favorable for longitudinal follow-up [5,15].

Freling et al. recently reported that semi-automatic pixel-intensity based segmentation software is able to exclude trabeculae and papillary muscles from the RV blood volume with high reproducibility in tetralogy of Fallot (ToF) patients with volume overloaded RVs. Moreover, this resulted in a substantial difference in RV volumes and RVEF compared to the standard method which includes these structures in the RV blood volume [16]. However, impact and reproducibility of excluding trabeculae and papillary muscles with this semi-automatic software in patient groups with RV pressure overload has not been investigated.

The purpose of the current study was to determine the impact of trabeculae and papillary muscles on RV volumes and function as assessed by CMR in different patient groups with pressure overloaded RVs and to determine the reproducibility of this methodology when semi-automatic pixel-intensity based software is used.

Methods

Study design and population

One hundred patients were included in the analysis (median age 36.2 years, 51% male). Four groups of 20 adult patients with pressure overloaded RV's were analyzed: patients with pre-capillary PH, patients with right ventricular outflow tract obstruction (RVOTO) after arterial switch operation (ASO) for transposition of the great arteries (TGA), patients with repaired ToF and patients with TGA and atrial switch procedure (Mustard or Senning operation). A reference group of 20 healthy controls was also included.

Pre-capillary PH was defined as a mean pulmonary artery pressure of ≥ 25 mmHg and a pulmonary capillary wedge pressure of ≤ 15 mmHg in accordance with ESC/ESR guidelines [17]. All patients with PH had an established diagnosis of either chronic thrombo-embolic PH or idiopathic PH. In all patients RV systolic pressure (RVSP) was measured using Doppler echocardiography on the day of CMR investigation. RVSP was measured using the peak velocity of tricuspid insufficiency plus estimated right atrial pressure. Patients with repaired ToF were included if a RVSP of ≥ 36 mmHg was measured by Doppler echocardiography [18]. Patients after ASO were included if RVSP measured by Doppler echocardiography was ≥ 36 mmHg or if, using Doppler echocardiography, a mild or moderate RVOTO was measured, defined as a maximum gradient of ≥ 25 mmHg. For patients with TGA and atrial switch procedure systolic blood pressure was used to determine RVSP. Basic patient characteristics for each patient group are illustrated in table 1.

In this retrospective study, MR images from two tertiary referral hospitals were analyzed. One centre contributed 59 patient CMR datasets and 20 control subjects. The second centre provided the remaining 21 patient CMR datasets. The datasets in this study were obtained between May 2008 and July 2012. Prior to analysis, all patient and control data were encoded to preserve anonymity. All CMR datasets were acquired in a routine clinical setting and anonymized for analysis. The medical ethics committees waived the need for informed consent.

CMR imaging protocol

Datasets were obtained using commercially available 1.5 T MR imagers (Ingenia R4.1.2; Philips Healthcare, Best, The Netherlands [n = 79]; Magnetom Sonata, Siemens Healthcare; [n = 7] and Magnetom Avanto; Siemens Healthcare, Erlangen, Germany [n = 14]). For all studies dedicated chest or torso phased array parallel-imaging capable surface coils were used with 12-28 elements. CMR images were acquired during repeated end-expiratory breath holds. Cine images were acquired

using a retrospectively gated balanced steady state free precession sequence with 25-30 cardiac phases per cardiac cycle. Slice thickness varied between 6-8 mm with an interslice gap of 0 - 4 mm. Sequences included multi-slice, multi-phase cine short-axis, longitudinal four-chamber, vertical two-chamber and RV outflow views. The multi-slice cine short-axis acquisitions were planned from above the mitral valve up to and including the cardiac apex. The following ranges of other scan parameters was used: TR 2.7 - 3.4 ms; TE 1.1 - 1.7 ms; flip angle 80^{o} – 90^{o}; matrix 171 - 192; voxel size: 1.25 x 1.25 x 8.0 mm and 1.7 x 1.7 x 6.0 mm. Parallel imaging factors varied between 0 - 3.

Table 1. Patient characteristics

	PH ***n* = 20**	**ASO** ***n* = 20**	**ToF** ***n* = 20**	**Atrial Switch** ***n* = 20**	**Controls** ***n* = 20**
Male gender (*n* (%))	7 (35)	11 (55)	11 (55)	12 (60)	10 (50)
Age (year) *	55.0 ± 14.1	24.9 ± 4.0	29.1 ± 7.8	33.0 ± 6.3	36.7 ± 10.1
BSA (m^2) *	1.93 ± 0.18	1.88 ± 0.18	1.87 ± 0.19	1.96 ± 0.21	1.88 ± 0.21
RVESP (mmHg) #	54 (37-65) *n = 20*	40 (37-53) *n = 15*	45 (41-50) *n = 20*	120(106-125) *n = 20*	-
RVOT (mmHg) #	-	35 (29-42) *n = 8*	33 (30-40) *n = 15*	-	4 (3-8) *n = 20*

 # Data presented as median (IQR) , Data presented as mean ± SD. ASO = arterial switch operation, BSA = body surface area, PH = pulmonary hypertension, RVESP = right ventricular esnd-systolic pressure, RVOT = right ventricular outflow tract, ToF = tetralogy of Fallot.*

CMR image analysis

Image analysis was performed using Qmass MR Research edition version 7.4.14.0 (Medis, Leiden, the Netherlands) [16]. Segmentation was performed on end-diastolic and end-systolic phases only. End-diastolic and end-systolic phases were selected by visual assessment as the phase with the largest and smallest RV cavity sizes, taking into account the longitudinal four-chamber, vertical two-chamber and RV outflow tract as reference views. If visual assessment was difficult, multiple frames were contoured to determine the correct end-diastolic or end-systolic phase. Using a previously described RV analysis protocol the RV epicardial and endocardial contours were manually traced from the most apical to the most basal short-axis slice [19]. Only the portion of the outflow tract below the pulmonary valve was included in the blood volume in the basal slice in which the pulmonary

valve was visible. If more than 50% of the tricuspid annulus or atrium was visible in a basal slice the valve area was excluded from the blood volume. Epi- and endocardial contours overlapped at valve borders and septum as the septum was considered part of the left ventricle. For patients with systemic RV, the septum was included in the myocardial mass of the RV.

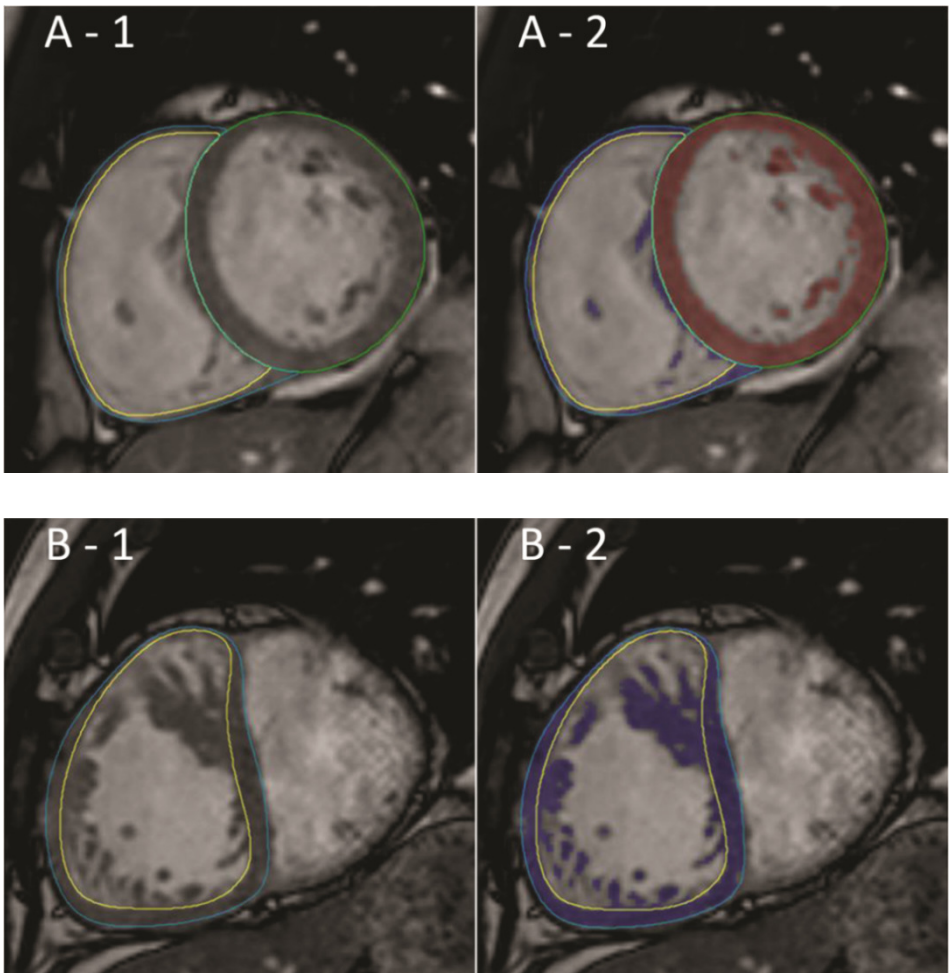

Figure 1. *RV contours and semi-automatic selection of trabeculae.Two methods of measuring RV volumes in a healthy control (A) and patient after atrial switch procedure (B). Method 1: inclusion trabeculae in the blood volume (A-1 and B-1); Method 2: exclusion of trabeculae from the blood volume, using identical endocardial contours (A-2 and B-2).*

Based on the methodology described above, two methods were used for determining RV volumes, function and mass. With method 1 trabeculae and

papillary muscles were included in the blood volume. With method 2, trabeculae and papillary muscles were excluded from the blood volume (Figure 1). Selection of trabeculae and papillary muscles was done using a semi-automatic threshold-based segmentation software. The segmentation software is based on the signal intensity distribution of MR images and has been described in detail by Freling et al [16]. In brief, voxels within the epicardial contour are classified as either blood or muscle according to their signal intensity, taking into account spatial variations in signal intensity. Based on this algorithm, trabeculae and papilary muscles were excluded from the blood volume and included in the myocardial volume. It is a possibility to manually change the thresholds for every slice, in order to select the same trabeculae in end- diastole and end-systole. Observers selected only trabeculae with signal intensity similar to the intensity of right ventricular myocardium. Selection and deselection of individual voxels was also possible in case of artifacts due to nonlaminar flow.

For both methods RV volumetric parameters were calculated by the sums of the traced contours multiplied by slice thickness in all short-axis slices. For method 1 the volume of trabeculae and papillary muscles were included in the RV blood volume and for method 2 they were excluded from the blood volume. Stroke volume (SV) was defined by the difference between end diastolic volume (EDV) and end systolic volume (ESV). All volumetric data were indexed for body surface area (BSA), which was calculated using the Dubois-Dubois formula ($0.20247 \times \text{Height(m)}^{0.725} \times \text{Weight(kg)}^{0.425}$). EF was calculated by SV/ EDV * 100%. For method 1 myocardial volume was defined as epicardial minus the endocardial contour, for method 2 end-diastolic trabecular volume was added to the myocardial volume. RV mass was quantified by multiplying the specific density of myocardium (1.05 g/ml) with the end-diastolic myocardial volume.

Reproducibility

Intraobserver reproducibility of both methods was assessed by re-analyzing 5 randomly selected CMR datasets from every patient group, as well as the healthy control subjects by the primary observer. In total 25 datasets were reanalyzed. To determine interobserver variability a second observer re-analyzed the same 25 datasets. Observers were blinded for earlier results and there was an interval of at least two weeks between the first and second analysis. The observers had equal experience in RV volumetric analysis and received the same training for Qmass MR research edition.

Statistical analysis

Continuous data were expressed as median and interquartile range (IQR) or mean value ± standard deviation (SD) as appropriate. Mean differences ± SD between method 1 and 2 was calculated for RVEDV/m^2, RVESV/m2, RVSV/m^2, RVEF and RV mass/m^2, using Paired Student's T-test. Differences in RVEDV/m^2, RVESV/m^2 and RVEF found in the patient groups were compared to the healthy control group using a one-way ANOVA with posthoc Dunnett's test. For the one-way ANOVA data underwent logarithmic transformation if necessary (i.e. if homogeneity of variances was inequal). P-values of <0.05 were considered statistically significant.

Intra- and interobserver agreement were assessed using Bland-Altman plots and intraclass correlation coefficients (ICC). Paired Student's T-test was used to test for significant differences between observer 1 and 2 and between the first and second measurements of observer 1. Mean differences ± SD for all measurements were calculated. All data analysis was performed in IBM SPSS statistics version 20.0 (IBM SPSS, Chicago, IL).

Results

Exclusion of trabecular volume

RVEDV/m^2, RVESV/m^2, RV EF and RV mass measured including (method 1) and excluding (method 2) RV trabeculae from the RV blood volume (method 2) are listed in table 2. For all patient groups and for healthy controls, exclusion of trabeculae and papillary muscles from the blood volume resulted in significantly decreased RVEDV/m^2 and RVESV/m^2 and a significantly increased RVEF (table 2).

Table 2. RV volume, mass and ejection fraction measured with inclusion (method 1) and exclusion of trabeculae from the RV blood volume (method 2).

		PH	ASO	ToF	Atrial switch	Controls
RVEDV	M 1	117.4 ± 31.8	99.4 ± 23.3	147.0 ± 42.5	139.9 ± 33.6	96.9 ± 18.9
(ml/m^2)	M 2	105.1 ± 28.4	88.3 ± 21.2	124.8 ± 38.0	110.7 ± 28.7	91.2 ± 17.8
	Diff	*-12.3 ± 4.6**	*-11.1 ± 3.3**	*-22.2 ± 6.0**	*-29.2 ± 6.6**	*-5.7 ± 1.7**
RVESV	M 1	75.4 ± 30.0	50.1 ± 13.3	85.5 ± 27.8	85.9 ± 26.2	47.5 ± 11.5
(ml/m^2)	M 2	62.7 ± 25.9	39.2 ± 11.3	63.7 ± 23.2	57.1 ± 21.7	41.6 ± 10.5
	Diff	*-12.7 ± 4.8**	*-10.9 ± 3.3**	*-21.8 ± 6.0**	*-28.8 ± 6.5**	*-5.9 ± 1.5**
RVSV	M 1	42.0 ± 7.9	49.3 ± 11.7	61.5 ± 19.4	54.0 ± 14.9	49.4 ± 8.6
(ml/m^2)	M 2	42.4 ± 8.0	49.2 ± 11.5	61.0 ± 19.6	53.6 ± 14.7	49.6 ± 8.6
	Diff	*-0.4 ± 0.6***	*-0.2 ± 0.6*	*-0.4 ± 0.8***	*-0.4 ± 0.9*	*0.2 ± 0.5*
RVM	M 1	18.5 ± 5.5	20.1 ± 5.0	25.4 ± 7.1	43.3 ± 9.1	13.0 ± 3.0
(gr/m^2)	M 2	31.4 ± 9.8	31.1 ± 7.5	48.7 ± 12.3	73.9 ± 15.4	19.0 ± 4.2
	Diff	*12.9 ± 4.9**	*11.0 ± 4.8**	*23.3 ± 6.3**	*30.6 ± 6.9**	*6.0 ± 1.8**
RVEF	M 1	37.2 ± 8.5	49.6 ± 5.0	42.1 ± 6.9	39.2 ± 7.8	51.3 ± 3.8
(%)	M 2	41.9 ± 9.1	55.8 ± 5.1	49.4 ± 12.3	49.3 ± 9.7	54.7 ± 4.1
	Diff	*4.7 ± 1.6**	*6.1 ± 1.7**	*7.2 ± 1.7**	*10.1 ± 2.3**	*3.4 ± 0.8**

*Data are presented as mean ± SD. *p < 0,001 using paired Student's T-test; ** p < 0.05 using paired Student's T-test. ASO = arterial switch operation, M = Method, PH = pulmonary hypertension, RVEDV = right ventricular end-diastolic volume, RVEF = right ventricular ejection fraction, RVESV = right ventricular end-systolic volume, RVM = right ventricular mass, RVSV = right ventricular stroke volume, ToF = tetralogy of Fallot.*

Also a significant difference in RVSV/m^2 was found. However, for all populations the mean difference in RVSV was very small, <0.5 mL/m^2. The differences between both methods were most pronounced in the patients after atrial switch procedure and least pronounced in the PH patients, with mean absolute differences in EF of 10.1 ± 2.3% and 4.7±1.6%, respectively. In healthy controls an absolute increase in RVEF of 3.4 ± 0.8% was measured. By excluding trabeculae volume from the blood volume, and including them with RV mass, this parameter also significantly increased in all groups (table 2). Of note, the differences in EDV/m^2, EDV/m^2, RVEF and RV mass were significantly larger in all patients groups compared to the healthy controls (p<0.01).

Reproducibility

For both methods inter- and intraboserver agreement was high in all measurements, as illustrated by high ICCs with small limits of agreement (table 3 & figure 2). For both methods, RVEDV, RVESV and RV mass showed significant differences between repeated measurements. However, mean differences were small and considered not clinically relevant. In figure 2, Bland-Altman plots show interobserver variability for RVESV, RVEDV and RVEF for both methods. For RVEDV, RVESV and RV mass the limits of agreement were narrower when trabeculae and papillary muscles were excluded from the RV blood volume (method 2).

Table 3. Inter- and intraobserver agreement

		Interobserver (obs 2 – obs 1^I)			Intraobserver (obs 1^{II} – obs 1^I)		
		ICC	Mean diff ± SD	P-value	ICC	Mean diff ± SD	P-value
RVEDV (mL/m^2)	M 1	0.981	-2.4 ± 6.7	0.089	0.990	2.8 ± 5.1	0.012
	M 2	0.987	1.8 ± 4.5	0.059	0.985	3.0 ± 5.0	0.006
RVESV (mL/m^2)	M 1	0.970	-2.3 ± 5.2	0.039	0.982	1.1 ± 4.2	0.209
	M 2	0.974	1.7 ± 3.5	0.027	0.969	1.0 ± 3.8	0.194
RVEF (%)	M 1	0.934	0.9 ± 2.6	0.086	0.965	0.4 ± 1.8	0.241
	M 2	0.934	-0.5 ± 2.6	0.354	0.954	0.6 ± 2.2	0.189
RVM (gr/m^2)	M 1	0.965	5.8 ± 3.5	0.000	0.983	0.5 ± 2.3	0.283
	M 2	0.993	1.4 ± 2.6	0.012	0.990	0.3 ± 3.2	0.694

P-value obtained using paired student T-test. M = Method, Obs 2 = second observer, Obs 1^I = first measurement of primary observer, Obs 1^{II} = second measurement of primary observer, RVEDV = right ventricular end-diastolic volume, RVEF = right ventricular ejection fraction, RVESV = right ventricular end-systolic volume, RVM = right ventricular mass

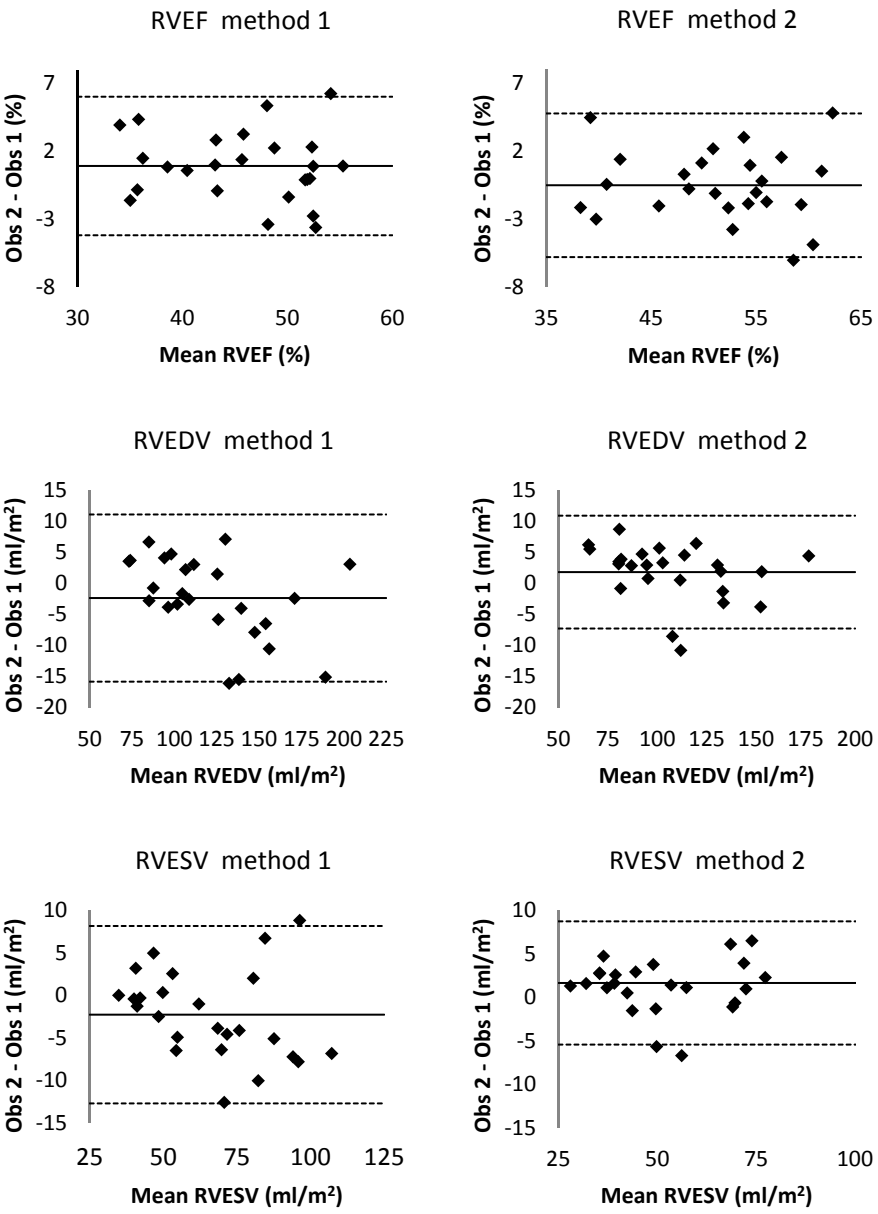

Figure 2. *Bland-Altman plots for method 1 and method 2 Bland-Altman plots showing the mean value of both observers on the x-axis and absolute differences between the observers on the y-axis for each paired observation. Limits of agreement are defined as ± 2 SD. Obs = observer, RVEDV = right ventricular end-diastolic volume, RVEF = right ventricular ejection fraction, RVESV = right ventricular end-systolic volume.*

Discussion

Exclusion of trabeculae and papillary muscles resulted in substantial alterations of RV volumes, RVEF and RV mass in a wide range of patient populations with pressure overloaded RVs. Furthermore, we found that these differences in RV parameters vary widely depending on the exact condition underlying RV overload. Although prior studies already established this fact in general terms, the major impediment to widespread adoption of this method in clinical practice was the lack of a fast and reproducible way to measure the exact amount of RV trabeculae and papillary muscles. We found that exclusion of RV trabeculae using semi-automatic pixel-intensity based software resulted in fast and highly reproducible RV measurements. This is opposed to manual tracing of trabeculae which has previously been shown to be unreliable [15,20].

Accurate and reproducible measurement of RV volume and function is mandatory because of the prognostic and therapeutic consequences in patients with PAH and CHD [1,3,21,22]. The impact of excluding trabeculae from the RV blood volume was previously illustrated in patients with systemic RVs and ToF with volume overloaded RVs [15,23]. The current study underscores that exclusion of trabeculae has a substantial impact on RV volumes, RVEF and RV mass in CHD and PAH patients with RV pressure overload. Healthy controls also exhibited significant differences in all RV measurements, but these were significantly smaller compared to the differences observed in patient groups. Consequently, RV volume and function in most patients will be closer to the normal range after trabeculae are excluded from the RV blood volume.

To date the major obstacles to exclude trabeculae and papillary muscles from the RV blood volume have been the time investment of performing manual tracing of these structures and the low reproducibility [15,20]. In the current study we found that using semi-automatic threshold-based segmentation software results in improved accuracy of RV volumetric measurements with high reproducibility. Because in- or exclusion of trabeculae from the RV blood volume has a major impact on RV parameters as measured with CMR, studies using different methodologies are incomparable. Several major studies in CHD patients differ on the point of in- or excluding RV trabeculae and papillary muscles from the RV blood volume [3,4,11,12,20,22,24] or are not clear about which methodology was used [13,14]. Application of the method described in this study may be a step forward to achieve uniformity of RV volumetric measurements, which is important to compare the effect of interventions aimed at preserving or improving RV function.

When comparing the current study to prior studies investigating the impact of trabeculae and papillary muscles on RV volume and function, some important differences can be observed. Winter et al. studied 29 patients with systemic right ventricles and found an increase in RVEF of 7.4± 3.9 % compared to 10.1 ± 2.3 % in our report. In contrast to our results, which are based on semi-automated pixel-intensity based segmentation, manual exclusion of trabeculae was substantially less reproducible in the study of Winter et al [15]. Moreover, both our study as well as the study by Freling et al. reported a higher reproducibility for RVEDV, RVESV and RV mass using this semi-automatic method to exclude trabeculea compared to only endocardial contour tracing [23]. We attribute this finding to observer variation in handling of trabeculae adjacent to the endocardial border, which can result in small differences for endocardial contour tracing, which will be rectified if all trabeculae are excluded. Sievers et al. studied the effect of trabeculae on RV volumes in healthy controls and reported a difference in RVEF of only 1.72% compared to 3.4 ± 0.8% in our study, however baseline RVEDV values also differed considerably with ours, indicating that these study populations are not comparable [25]. Freling et al. investigated ToF patients with volume overloaded RV's using the same software package as described in the current study and found a similar increase in RVEF of 7 ± 4 %, versus 7 ± 2% in our study [23].

The current study only focused on one of the possible sources of error in RV volumetric assessement with CMR. An important source of error remains basal slice selection and delineation of the tricuspid valve. A short-axis orientation for RV volumetric measurement was used in this study as this is standard practice in our hospitals. Axial orientation, however, might result in higher reproducibility than short-axis orientation in CHD patients with severely dilated RVs, decreasing the difficulty of valve delineation in the basal slices [26,27]. To minimize errors at the tricuspid and pulmonic valve, images were cross linked to RV 2-chamber, 4-chamber and RV outflow tract views. Furthermore only a small portion of the patients had severely dilated RVs, therefore it is unlikely that the slice orientation would have resulted in important differences for the current study. The impact and reproducibility of the semi-automatic software used in the current study will likely be similar in axial slice orientation, as the software is not restricted by geometric assumptions and uses signal intensity to select trabeculae. Finally, another source of error might be inadequate selection of the RV end-systolic frame. In daily practice both RV and LV ESV are often assessed in the LV end-systolic frame. However in patients with CHD, who often have right bundle branch block, timing of the RV end-systolic frame can be delayed compared to the LV end-

systolic frame [28]. We choose RV end-diastolic and end-systolic phase based solely on RV cavity size.

This study is unable to determine whether in- or excluding trabeculae best represents true RV volumes, as a gold standard in vivo is lacking. However, theoretically exclusion of trabeculae is more accurate as they do not contribute to RVEDV and RVESV.

Conclusion

Exclusion of trabeculae and papillary muscles has a substantial impact on measured RV volumes, mass and EF. The magnitude of the differences varied between patient groups and was significantly larger in all patient groups when compared to healthy controls. Semi-automatic pixel-intensity based software provides a highly reproducible way to exclude these structures.

References

[1] Baumgartner H, Bonhoeffer P, De Groot NM, et al., (2010) ESC Guidelines for the management of grown-up congenital heart disease (new version 2010). Eur Heart J 31:2915-57.

[2] van de Veerdonk MC, Kind T, Marcus JT, et al.(2011) Progressive right ventricular dysfunction in patients with pulmonary arterial hypertension responding to therapy. J Am Coll Cardiol 58:2511-9.

[3] van Wolferen SA, Marcus JT, Boonstra A, et al., (2007) Prognostic value of right ventricular mass, volume, and function in idiopathic pulmonary arterial hypertension. Eur Heart J 28:1250-7.

[4] Valsangiacomo Buechel ER, Mertens LL, (2012) Imaging the right heart: the use of integrated multimodality imaging. Eur Heart J 33:949-60.

[5] Kilner PJ, Geva T, Kaemmerer H, et al., (2010) Recommendations for cardiovascular magnetic resonance in adults with congenital heart disease from the respective working groups of the European Society of Cardiology. Eur Heart J 31:794-805.

[6] van der Zwaan HB, Geleijnse ML, McGhie JS, et al., (2011) Right ventricular quantification in clinical practice: two-dimensional vs. three-dimensional echocardiography compared with cardiac magnetic resonance imaging. Eur J Echocardiogr 12:656-64.

[7] Iriart X, Montaudon M, Lafitte S, et al., (2009) Right ventricle three-dimensional echography in corrected tetralogy of fallot: accuracy and variability. Eur J Echocardiogr 10:784-92.

[8] Beerbaum P, Barth P, Kropf S, et al., (2009) Cardiac function by MRI in congenital heart disease: impact of consensus training on interinstitutional variance. J Magn Reson Imaging 30:956-66.

[9] Rominger MB, Bachmann GF, Pabst W, et al., (1999) Right ventricular volumes and ejection fraction with fast cine MR imaging in breath-hold technique: Applicability, normal values from 52 volunteers, and evaluation of 325 adult cardiac patients. Journal of Magnetic Resonance Imaging 10:908-18.

[10] Lorenz CH, Walker ES, Morgan VL, et al., (1999) Normal human right and left ventricular mass, systolic function, and gender differences by cine magnetic resonance imaging. J Cardiovasc Magn Reson 1:7-21.

[11] Oosterhof T, van Straten A, Vliegen HW, et al., (2007) Preoperative thresholds for pulmonary valve replacement in patients with corrected tetralogy of Fallot using cardiovascular magnetic resonance. Circulation 116:545-51.

[12] Therrien J, Provost Y, Merchant N, et al., (2005) Optimal timing for pulmonary valve replacement in adults after tetralogy of Fallot repair. Am J Cardiol 95:779-82.

[13] Lidegran M, Odhner L, Jacobsson LA, et al., (2000) Magnetic resonance imaging and echocardiography in assessment of ventricular function in atrially corrected transposition of the great arteries. Scand Cardiovasc J 34:384-9.

[14] Lee C, Kim YM, Lee C, et al., (2012) Outcomes of Pulmonary Valve Replacement in 170 Patients With Chronic Pulmonary Regurgitation After Relief of Right Ventricular Outflow Tract Obstruction: Implications for Optimal Timing of Pulmonary Valve Replacement. J Am Coll Cardiol 60:1005.

[15] Winter MM, Bernink FJ, Groenink M, et al., (2008) Evaluating the systemic right ventricle by CMR: the importance of consistent and reproducible delineation of the cavity. J Cardiovasc Magn Reson 10:40.

[16] Freling HG, van Wijk K, Jaspers K, et al., (2012) Impact of right ventricular endocardial trabeculae on volumes and function assessed by CMR in patients with tetralogy of Fallot. Int J Cardiovasc Imaging.

[17] Galie N, Hoeper MM, Humbert M, et al., (2009) Guidelines for the diagnosis and treatment of pulmonary hypertension: the Task Force for the Diagnosis and Treatment of Pulmonary Hypertension of the European Society of Cardiology (ESC) and the European Respiratory Society (ERS), endorsed by the International Society of Heart and Lung Transplantation (ISHLT). Eur Heart J 30:2493-537.

[18] Rudski LG, Lai WW, Afilalo J, et al., (2010) Guidelines for the echocardiographic assessment of the right heart in adults: a report from the American Society of Echocardiography endorsed by the European Association of Echocardiography, a registered branch of the European Society of Cardiology, and the Canadian Society of Echocardiography. J Am Soc Echocardiogr 23:685,713; quiz 786-8.

[19] Prakken NH, Velthuis BK, Vonken EJJ, et al., (2008) Cardiac MRI: Standardized Right and Left Ventricular Quantification by Briefly Coaching Inexperienced Personnel. Open Magn Reson J 1:104-11.

[20] Papavassiliu T, Kuhl HP, Schroder M, et al., (2005) Effect of endocardial trabeculae on left ventricular measurements and measurement reproducibility at cardiovascular MR imaging. Radiology 236:57-64.

[21] Warnes CA, (2009) Adult congenital heart disease importance of the right ventricle. J Am Coll Cardiol 54:1903-10.

[22] Knauth AL, Gauvreau K, Powell AJ,et al., (2008) Ventricular size and function assessed by cardiac MRI predict major adverse clinical outcomes late after tetralogy of Fallot repair. Heart 94:211-6.

[23] Freling HG, van Wijk K, Jaspers K, et al., (2013) Impact of right ventricular endocardial trabeculae on volumes and function assessed by CMR in patients with tetralogy of Fallot. Int J Cardiovasc Imaging 29:625-31.

[24] Helbing WA, Rebergen SA, Maliepaard C,et al., (1995) Quantification of right ventricular function with magnetic resonance imaging in children with normal hearts and with congenital heart disease. Am Heart J 130:828.

[25] Sievers B, Kirchberg S, Bakan A,et al., (2004) Impact of papillary muscles in ventricular volume and ejection fraction assessment by cardiovascular magnetic resonance. J Cardiovasc Magn Reson 6:9-16.

[26] Clarke CJ, Gurka MJ, Norton PT, et al., (2012) Assessment of the accuracy and reproducibility of RV volume measurements by CMR in congenital heart disease. JACC Cardiovasc Imaging 5:28-37.

[27] Fratz S, Schuhbaeck A, Buchner C, et al., (2009) Comparison of accuracy of axial slices versus short-axis slices for measuring ventricular volumes by cardiac magnetic resonance in patients with corrected tetralogy of fallot. Am J Cardiol 103:1764-9.

[28] Freling HG, Pieper PG, Vermeulen KM, et al., (2013) Improved cardiac MRI volume measurements in patients with tetralogy of fallot by independent end-systolic and end-diastolic phase selection. PLoS One 8:e55462.

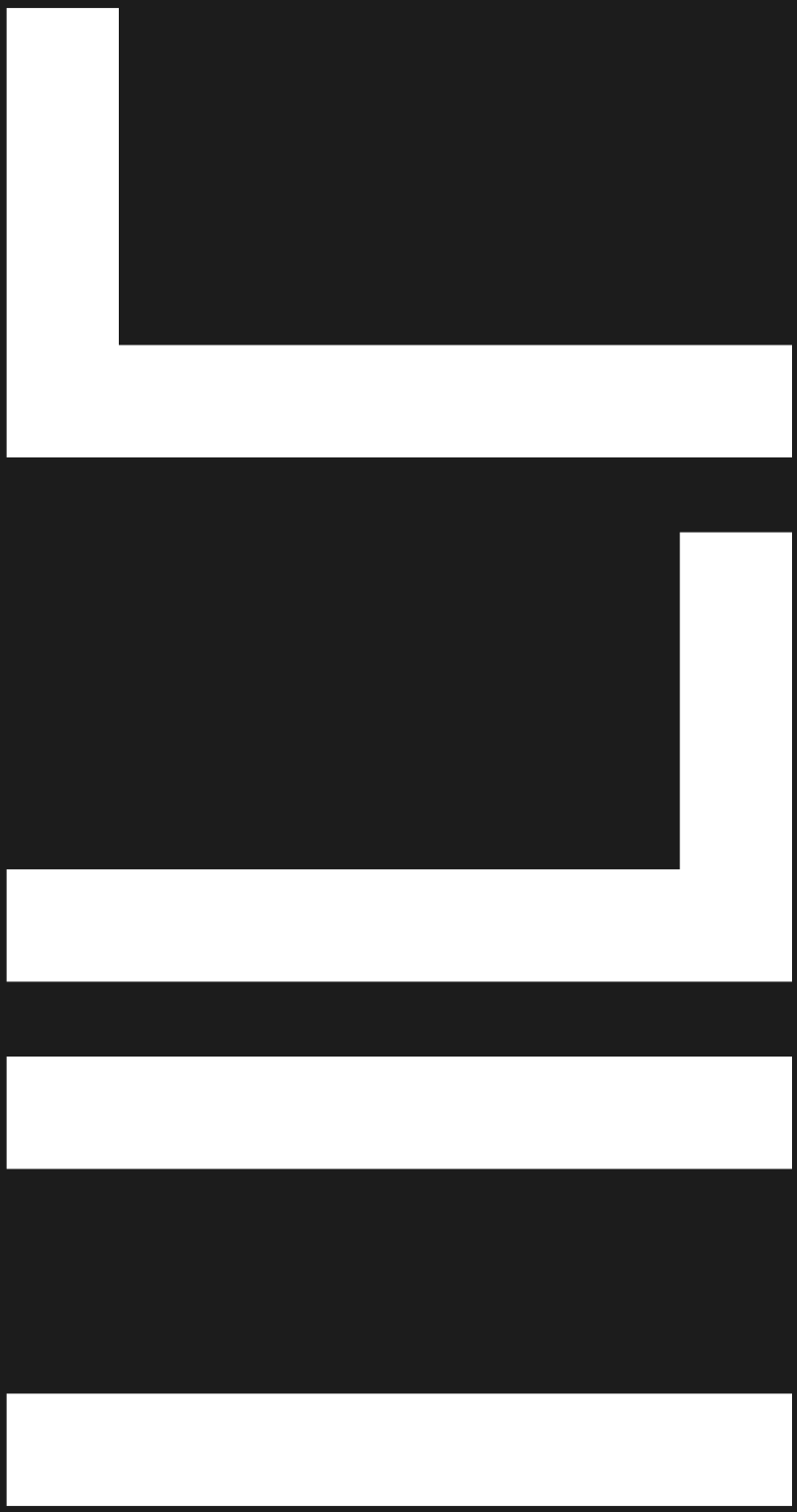

6

Effect of right ventricular outflow tract obstruction on right ventricular volumes and exercise capacity in patients with repaired tetralogy of Fallot

Hendrik G. Freling
Tineke P. Willems
Joost P. van Melle
Ymkje J. van Slooten
Beatrijs Bartelds
Rolf M.F. Berger
Dirk J. van Veldhuisen
Petronella G. Pieper

Abstract

Background: Patients with tetralogy of Fallot (ToF) and combined right ventricular (RV) outflow tract obstruction (RVOTO) and pulmonary regurgitation (PR) have compared to patients without RVOTO more favorable RV volumes and function. Unknown is whether RVOTO is also associated with improved exercise capacity.

Methods: Cardiac magnetic resonance imaging, echocardiography and exercise tests were compared between 12 patients with and 30 patients without RVOTO (Doppler peak RVOT gradient (RVOT-PG) $\geq$ 30 mmHg).

Results: Patients with RVOTO had smaller RV end-systolic (50 ± 16 versus 64 ± 18 ml/m^2) and end-diastolic volumes (117 ± 24 versus 135 ± 28 ml/m^2) and higher RV mass (52 ± 14 versus 42 ± 11 ml/m^2) than patients without RVOTO, $p < .050$. RV ejection fraction did not differ significantly between patients with and without RVOTO (58% ± 8% versus 53% ± 7%), $p = 0.051$. Degree of PR, left ventricular volumes and function were not different between both groups. Patients with RVOTO had a significant lower peak oxygen uptake (25 ± 3 versus 32 ± 8 ml/kg/min) and percentage of predicted peak oxygen uptake (63% ± 7% versus 79% ± 14%) than patients without RVOTO, $p < 0.001$. In multivariate analysis RVOT-PG was the only independent predictor of exercise capacity.

Conclusions: Exercise capacity is lower in patients with compared to patients without RVOTO despite more favourable RV volumes at rest and comparable degree of pulmonary regurgitation. Therefore, exercise capacity should be considered in addition to RV volumes and function in patients with ToF and PR.

Accepted in Am J Cardiol

Background

Most adult patients with repaired tetralogy of Fallot (ToF) have longstanding pulmonary regurgitation (PR). PR results in chronic right ventricular (RV) volume overload, and has been related to RV dilation, RV dysfunction, symptomatic heart failure, ventricular arrhythmia and sudden death [1-3].

In addition to PR, many patients have residual RV outflow tract obstruction (RVOTO) resulting in some amount of pressure overload. Animal studies demonstrated that RVOTO may limit the negative impact of PR on RV size and myocardial contractility. Increase in cardiac output during dobutamine infusion was not different between animals with PR and animals with combined RVOTO and PR [4,5]. This suggests that despite smaller RV volumes with higher myocardial contractility, patients with combined RVOTO and PR may not have better exercise capacity than patients with isolated PR. Indeed, despite smaller RV size in patients with ToF and combined RVOTO and PR as demonstrated in recent studies, New York Heart Association functional class did not differ compared to patients with isolated PR [6,7] However, since functional class is known to be poorly correlated with objective exercise capacity [8,9], it remains unclear what the effect of RVOTO is on exercise capacity.

Therefore, we performed a study to evaluate the effects of RVOTO on exercise capacity, RV volumes and RV function in adult patients with repaired ToF and volume overload due to PR.

Methods

Patients

This retrospective study was approved by the University Medical Center Groningen review board. Informed consent was not required according to the Dutch Medical Research Involving Human Subjects act.

Our institute's cardiac magnetic resonance (CMR) imaging database contained 123 patients with repaired ToF without a pulmonary valve replacement. We included patients in whom adequate echocardiographic examination, exercise testing and CMR imaging were performed within 6 months of each other (n = 48; 39%) and no clinical relevant event occurred in the meantime. All examinations are part of routine follow up in our center. Patients with significant regurgitation or stenosis of other valves than the pulmonary valve and residual intracardiac shunts were excluded (n = 5). The remaining 42 patients were divided into two groups: 12 patients with combined PR and RVOTO and 30 patients with PR and no RVOTO. RVOTO was defined as a Doppler peak pressure gradient across the RVOT of > 30 mm Hg.

Cardiac magnetic resonance imaging

All subjects were examined on a 1.5-Tesla MRI system (Siemens Magnetom Sonata, Erlangen, Germany or Siemens Magnetom Avanto, Erlangen, Germany) using a 2 x 6 channel body-coil. After single-shot localizer images, short axis cine loop images with breath holding in expiration were acquired using a retrospectively gated balanced steady state free precession sequence. The following parameters were used: TR 2.7 ms, TE 1.1 ms, flip angle 80^{o}, matrix 192 x 192 mm, 25 frames per cycle, slice thickness 6 mm, interslice gap 4 mm, voxel size 1.7 x 1.7 x 6 mm.

Two-dimensional velocity encoded MRI flow measurements perpendicular and directly cranial to the pulmonary valve was performed to quantify flow velocity and volumes.

Cardiac magnetic resonance image analysis

Analysis of CMR images has been described previously [10-12]. In summary, image analysis was performed semi-automatically by using QMass MR research edition (Medis, Leiden, The Netherlands). LV and RV contours were drawn manually by tracing the endo- and epicardial borders in every slice in the end-systolic and end-diastolic frame. The end-systolic phase of the RV was selected independently from the LV. Papillary muscles and trabeculae were excluded from the RV blood volume

and included in the mass. Stroke volume was calculated by subtracting the end-systolic volume from the end-diastolic volume. Ejection fraction was obtained by dividing stroke volume by end-diastolic volume.

Analysis of MRI flow measurements was performed using QFlow version 5.2 (Medis, Leiden, The Netherlands. Contours were drawn manually in all 30 phases. PR was quantified as PR fraction and PR volume. All ventricular volumes were indexed for body surface area.

Echocardiography

Continuous-wave Doppler was used to determine the maximum velocity across the RV outflow tract. The RV outflow tract gradient was calculated with use of the simplified Bernoulli equation. The presence of restrictive physiology was defined as forward flow across the pulmonary valve during end-diastole. The tricuspid and left-sided valves were reviewed for significant stenosis or regurgitation. All patients were screened for the presence of residual intracardiac shunts.

Exercise testing

A treadmill cardiopulmonary exercise test was performed in all patients. Workload was incremented at regular intervals with a combination of speed and grade. Because the expected maximum workload was relatively low in most patients, a modified Bruce protocol was used in which workload starts at a relatively low level and increases more gradually than in the standard Bruce protocol [13]. At the first stage speed was 1.7 miles/hour and incline 0%, at the second stage the same speed and 5% incline, and the third stage corresponded to the first stage of the Bruce protocol. Cardiopulmonary exercise testing ended when patients reached their peak oxygen uptake (VO_2), could not keep up with the treadmill speed, breathing reserve dropped and O_2 heart rate decreased, or discontinuation was indicated for safety reasons. Peak Vo_2 was calculated as the average VO_2 for the two highest measurements at peak exercise and expressed as millilitre per minute per kilogram and as percentage of predicted maximum VO_2. Respiratory exchange ratio was computed as carbon dioxide production/VO_2. Exercise tests were only included if the patient reached the anaerobic threshold, defined as having a respiratory exchange ratio > 1.0.

Analysis

Descriptive statistics were calculated for all measurements as mean and standard deviation for normally distributed continuous variables, median with 25^{th} and 75^{th} percentile for skewed continuous variables and absolute numbers and percentages

for dichotomous variables. Differences in characteristics between patient groups were analyzed using Student's T-test for normally distributed continuous variables and Mann-Whitney U-test for skewed continuous variables. Fisher's Exact Test was used for comparison of categorized variables. Univariate linear regression analysis was performed to determine which variables were significantly related to percentage of predicted peak VO_2. Variables included were patient characteristics (age at exercise testing, gender), operative characteristics (age at repair, usage of transannular patch), imaging parameters (CMR measurements of RV volume and function and left ventricular function, degree of PR, presence of restrictive physiology and peak pressure gradient across the RVOT) and QRS duration. In multivariate analysis we evaluated independent predictors of peak VO_2. Only variables statistically significant ($p < .050$) in univariate analysis were included in the multivariate analysis (backward stepwise regression method). The Statistical Package for the Social Sciences version 20.0 (SPSS Inc, Chicago, IL) was used for all statistical analyses. All statistical tests are two-sided and a P-value of less than .050 was considered statistically significant.

Results

Patient characteristics

Patient characteristics were not different between both groups except peak gradient across the RVOT (Table 1). Twenty-five (60%) patients were male. Mean age at the study was 32 ± 9 years. Previous palliative shunt was performed in 9 (21%) patients. ToF repair was performed between March 1972 and July 1993 and median age at repair was 2.7 (25^{th} – 75^{th} percentile, 1.3 – 5.7) years. During repair 22 (54%) patients received a transannular patch. All patients were in NYHA class I at time of evaluation for this study, except one patient with isolated PR who was in NYHA class II. Mean QRS duration was 136 ± 26 ms and all patients had a right bundle branch block. Restrictive physiology was present in 14 (37%) patients and could not be determined due to inadequate Doppler signals in 4 (10%) patients. Peak pressure gradient across the RVOT on Doppler echocardiography was 24 ± 14 mmHg, and was 42 ± 9 mmHg in patients with combined RVOTO and PR and 16 ± 6 mmHg in patients with isolated PR, p <.001.

Table 1. Patients' characteristics

	Isolated PR (N=30)	**Combined RVOTO + PR (N=12)**	**P**
Male	15 (50)	10 (83)	.081
Age at repair (years)	2.5 (1.3 – 5.5)	3.9 (1.8 – 5.9)	.449
Age at study (years)	30 ± 9	34 ± 9	.246
Previous palliative shunt	6 (20)	3 (25)	.699
Transannular patch	14 (47)	8 (73)*	.173
NYHA class			1.000
class I	29 (97)	12 (100)	
class II	1 (3)	0 (0)	
Peak gradient RVOT (mmHg)	16 ± 6	42 ± 9	<.001
Restrictive physiology	10 (37)**	4 (36)**	1.000
QRS duration (ms)	137 ± 26	132 ± 30	.579

** Details of the operative procedure could not be retrieved of one patient. ** Presence of restrictive physiology could not be determined in four patients, one patient with and three patients without RVOTO. Data are presented as number of patients (%), mean ± standard deviation or median (25th-75th percentile). NYHA = New York Heart Association, PR = pulmonary regurgitation, RVOT = right ventricular outflow tract, RVOTO = right ventricular outflow tract obstruction, ToF = tetralogy of Fallot*

CMR

Patients with combined RVOTO and PR had statistically significant smaller RV end-systolic and end-diastolic volumes and higher RV mass than patients with isolated PR, p <.050. The higher RV ejection fraction in patients with combined RVOTO and PR compared to patients with isolated PR was not statistically significant, p = .051. Number of patients with PR regurgitation fraction > 20%, severity of PR, LV end-systolic, end-diastolic and stroke volume, and LV ejection fraction were not different between both groups (Table 2).

Table 2. Results of cardiac magnetic resonance imaging

	All ToF (N = 42)	Isolated PR (N =30)	Combined RVOTO + PR (N = 12)	P
PR percentage (%)	36 ± 15	34 ± 15	38 ± 16	.456
PR >20%	36 (86)	25 (83)	11 (92)	.655
PR volume (ml/m^2)	26 ± 15	26 ± 14	27 ± 17	.820
RVESV (ml/m^2)	60 ± 18	64 ± 18	50 ± 16	.021
RVEDV (ml/m^2)	130 ± 28	135 ± 28	117 ± 24	.049
RVSV (ml/m^2)	70 ± 15	71 ± 15	67 ± 14	.448
RVEF (%)	54 ± 7	53 ± 7	58 ± 8	.051
RVM (ml/m^2)	45 ± 13	42 ± 11	52 ± 14	.019
LVESV (ml/m^2)	38 ± 9	39 ± 8	37 ± 10	.552
LVEDV (ml/m^2)	87 ± 13	88 ± 12	84 ± 13	.398
LVSV (ml/m^2)	48 ± 7	49 ± 8	47 ± 6	.483
LVEF (%)	56 ± 6	56 ± 6	57 ± 6	.674
LVM (ml/m^2)	53 ± 8	52 ± 8	55 ± 8	.174

Data are presented as number of patients (%) or mean ± standard deviation. LEDV = left ventricular end-diastolic volume, LVEF = left ventricular ejection fraction, LVESV = left ventricular end-systolic volume, LVM = left ventricular mass, LVSV = left ventricular stroke volume, PR = pulmonary regurgitation, RVEDV = right ventricular end-diastolic volume, RVEF = right ventricular ejection fraction, RVESV = right ventricular end-systolic volume, RVM = right ventricular mass, RVSV = right ventricular stroke volume, RVOTO = right ventricular outflow tract obstruction, ToF = tetralogy of Fallot

Exercise capacity

Mean time between CMR and exercise testing was 1.9 ± 7.6 weeks. Patients with combined RVOTO and PR had a significant lower percentage of predicted peak VO_2 than patients with isolated PR, p < .001. Exercise capacity was impaired, defined as peak VO_2 < 85% of the predicted value, in all patients with combined RVOTO and

PR, and in 20 (67%) patients with isolated PR, p = .040. Heart rate at rest was not significantly different between both groups. The lower maximum heart rate and lower percentage of predicted maximum heart rate in patients with combined RVOTO and PR compared to patients with isolated PR was not statistically significant, (Table 3).

Table 3. Results of cardiopulmonary exercise testing

	All ToF (N=42)	Isolated PR (N=30)	Combined RVOTO + PR (N=12)	P
Rest heart rate (bpm)	77 ± 11	77 ± 11	76 ± 11	.800
MHR (bpm)	170 ± 21	174 ± 17	162 ± 26	.144
MHR (% of predicted normal values)	90 ± 9	92 ± 7	87 ± 12	.186
Peak VO_2 (ml/kg/min)	30 ± 8	32 ± 8	25 ± 3	<.001
% of predicted peak VO_2	74 ± 15	79 ± 14	63 ± 7	<.001
Respiratory exchange ratio	1.11 ± 0.07	1.11 ± 0.07	1.12 ± 0.08	.491

Data are presented as mean ± standard deviation. MHR = maximum heart rate, RVOTO = right ventricular outflow tract obstruction, ToF = tetralogy of Fallot, VO2 = oxygen uptake

Univariate analysis showed a statistically significant relation between percentage of predicted peak VO_2 and peak pressure gradient across the RVOT (Figure 1) and RV end-diastolic volume. In multivariate analysis peak pressure gradient across the RVOT was the only independent predictor of exercise capacity (Table 4).

Table 4. Univariate and multivariate predictors of percentage of predicted peak oxygen uptake

	Univariate RC ± SE	P	Multivariate RC ± SE	P
Peak gradient (mmHg)	-0.49 ± 0.15	.002	-0.49 ± 0.15	.002
Constant			86.93 ± 4.10	-
RVEDV (ml/m^2)	0.17 ± 0.08	.034		NS

Data are regression coefficients ± standard errors. R2 for the multiple regression model of percentage of predicted peak VO2 was .212. RC = regression coefficient, RVEDV = right ventricular end-diastolic volume

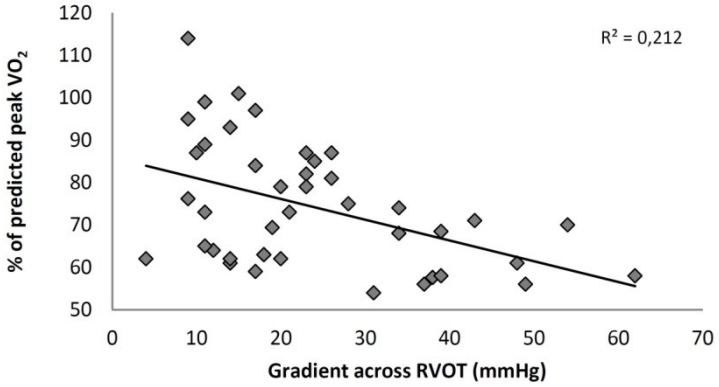

Figure 1. Correlation of percentage of predicted peak oxygen uptake and gradient across the right ventricular outflow tract. RVOT = right ventricular outflow tract, VO_2 = oxygen uptake

Discussion

Our study is the first to demonstrate in patients with repaired ToF that combined RVOTO and PR is associated with reduced exercise capacity despite more favourable RV volumes at rest. Furthermore, peak pressure gradient across the RVOT was the only independent predictor of percentage of predicted peak VO_2.

Experimental studies in growing swine have demonstrated that combined RVOTO and PR resulted in more RV hypertrophy, and less dilatation of the RV compared to isolated PR [4,5]. Our and other studies in patients with repaired ToF confirmed that patients with combined RVOTO and PR had smaller RV volumes compared to patients with isolated PR, despite comparable degree of PR [6,7,14]. Some studies proposed that decreased diastolic compliance resulting from RVOTO-induced hypertrophy prevents severe RV dilatation due to limiting PR [7,14]. However, we and others found no difference in PR between patients with and without RVOTO [6,7]. The RV hypertrophy and decreased compliance might have protective properties against RV dilatation, however, the exact mechanism of protection against RV dilatation remains unknown. Although smaller RV volumes and higher ejection fraction have been considered markers for better RV performance in patients with repaired ToF, our results suggest that adaptations of the RV in response to RVOTO do not result in increase cardiac output during exercise.

During exercise, cardiac output increases to deliver the required oxygen and nutrients to the muscles. Increase in cardiac output is mainly a result of changes in preload, afterload, contractility and heart rate [15]. A healthy untrained person can increase cardiac output a little over fourfold, and a well-trained athlete can increase output about sixfold [15]. However, increase in cardiac output during exercise is decreased in patients with repaired ToF [16]. As the left ventricle and RV are in series, cardiac output of the left ventricle is most likely limited because of reduced RV output. Under normal circumstances the RV is an energetic efficient pump because of the low pressure in the pulmonary circulation [17,18]. In patients with repaired ToF and PR energetic inefficiency exists due to enlarged stroke volume which for a large part flows back into the RV. Additionally, often intra- and interventricular dyssynchrony cause suboptimal coordination of RV contraction [19]. RV dilatation results in a changed geometry of both ventricles with reduced diastolic LV volume due to septal displacement and paradoxical systolic septal movement, which further reduces cardiac output [17,18].

Furthermore, when a patient has additional RVOTO, more kinetic energy is required to overcome the obstruction. This induces RV hypertrophy and increases

contractile force allowing the RV to generate higher pressures. The simplified Bernouilli equation states that pressure gradient = 4 x [flow / area]^2. As a result, the increase in pressure during exercise can be quite high given that gradients are a square function of flow. The increased contractile force in patients with combined RVOTO and PR might not be sufficient to adequately increase cardiac output during strenuous exercise.

Additionally, RV hypertrophy and degenerative myocardial changes after longstanding pressure overload could be detrimental for RV compliance and diastolic function. Previous studies have discussed that restrictive physiology, visible as forward flow during diastole, is associated with smaller RV volumes and improved exercise performance. Like a previous report, we found no difference in frequency of restrictive physiology between patients with combined RVOTO and PR compared to patients with isolated PR [7]. Furthermore, in our study presence of restrictive physiology was not correlated with measured exercise capacity. However, this does not rule out that patients with combined RVOTO and PR have more often or more severe diastolic dysfunction during exercise. Last, in our data there was a trend towards a lower heart rate response during exercise in patients with combined RVOTO and PR which further reduces the ability to increase output. Therefore, poorer RV function during exercise in patients with combined RVOTO and PR is most likely caused by insufficient systolic function, reduced diastolic function, reduced heart rate or a combination of those.

When pulmonary valve replacement is performed timely in patients with ToF and PR, RV volumes will normalize and irreversible RV dysfunction is prevented [20,21]. Therefore, timing of pulmonary valve replacement is increasingly being based on CMR derived RV volume measurements [22]. As patients with additional RVOTO have smaller RV volumes, pulmonary valve replacement will be performed less frequently in these patients [23]. Whether optimal timing of pulmonary valve replacement to prevent irreversible RV dysfunction in patients with combined RVOTO and PR should be guided by RV volumes in the same way as in patients with isolated PR is unknown. Since volumes remain smaller in patients with additional RVOTO, while our results suggest that exercise capacity is more impaired than in patients with isolated PR, it can be postulated that patients with combined RVOTO and PR should require different criteria to guide the timing of pulmonary valve replacement. Possibly exercise capacity should be given more weight while RV volumes may be less important. However, whether more timely pulmonary valve replacement would have a beneficial effect on exercise capacity remains unknown.

Study limitations

In our study total repair was performed in different decennia. The trend is to perform total repair at an increasingly younger age. This shortens the period the patient is subjected to systemic hypoxia and RV pressure overload. Furthermore, current surgical strategies to relieve pulmonary stenosis during repair of ToF aim at limiting the amount of future PR and mild residual stenosis is accepted. Because of the retrospective nature of our study in combination with the long time between repair of ToF and our study, we have insufficient data concerning the time of onset of RVOTO. It is unknown whether RVOTO has been present since repair of ToF or evolved later. We have no CMR or echocardiographic data during exercise at our disposal, therefore we can only speculate about the cause of the difference in exercise capacity between patients with and without additional RVOTO.

The number of patients in our study with combined RVOTO and PR is relatively small and the degree of RVOTO was only moderate. A larger, preferable prospective, study should be performed to confirm whether our results can be extrapolated to patients in which total repair was performed using current surgical strategies.

Conclusion

Currently, timing of pulmonary valve replacement in patient with ToF and PR is mainly guided by RV volumes and to a lesser degree exercise capacity. However, patients with combined RVOTO and PR have reduced exercise capacity despite more favourable RV volumes at rest compared to patients without RVOTO. Therefore, exercise testing as well as CMR imaging should be interpreted in conjunction with the presence of RVOTO. Whether current guidelines on timing of pulmonary valve replacement need to be revised for patients with combined RVOTO and PR, giving exercise capacity a more prominent role, should be the subject of future studies.

References

[1] Warnes CA, Williams RG, Bashore TM, et al., (2008) ACC/AHA 2008 Guidelines for the Management of Adults with Congenital Heart Disease: a report of the American College of Cardiology/American Heart Association Task Force on Practice Guidelines (writing committee to develop guidelines on the management of adults with congenital heart disease). Circulation 118:e714-833.

[2] Baumgartner H, Bonhoeffer P, De Groot NM, et al., (2010) ESC Guidelines for the management of grown-up congenital heart disease (new version 2010). Eur Heart J 31:2915-57.

[3] Gatzoulis MA, Balaji S, Webber SA, et al., (2000) Risk factors for arrhythmia and sudden cardiac death late after repair of tetralogy of Fallot: a multicentre study. Lancet 356:975-81.

[4] Kuehne T, Gleason BK, Saeed M, et al., (2005) Combined pulmonary stenosis and insufficiency preserves myocardial contractility in the developing heart of growing swine at midterm follow-up. J Appl Physiol 99:1422-7.

[5] Kuehne T, Saeed M, Gleason K, et al., (2003) Effects of pulmonary insufficiency on biventricular function in the developing heart of growing swine. Circulation 108:2007-13.

[6] Yoo BW, Kim JO, Kim YJ, et al., (2012) Impact of pressure load caused by right ventricular outflow tract obstruction on right ventricular volume overload in patients with repaired tetralogy of Fallot. J Thorac Cardiovasc Surg 143:1299-304.

[7] Spiewak M, Biernacka EK, Malek LA, et al., (2011) Right ventricular outflow tract obstruction as a confounding factor in the assessment of the impact of pulmonary regurgitation on the right ventricular size and function in patients after repair of tetralogy of Fallot. J Magn Reson Imaging 33:1040-6.

[8] Gratz A, Hess J, Hager A, (2009) Self-estimated physical functioning poorly predicts actual exercise capacity in adolescents and adults with congenital heart disease. Eur Heart J 30:497-504.

[9] Rogers R, Reybrouck T, Weymans M, et al., (1994) Reliability of subjective estimates of exercise capacity after total repair of tetralogy of Fallot. Acta Paediatr 83:866-9.

[10] Freling HG, Pieper PG, Vermeulen KM, et al., (2013) Improved cardiac MRI volume measurements in patients with tetralogy of fallot by independent end-systolic and end-diastolic phase selection. PLoS One 8:e55462.

[11] Freling HG, van Wijk K, Jaspers K, et al., (2013) Impact of right ventricular endocardial trabeculae on volumes and function assessed by CMR in patients with tetralogy of Fallot. Int J Cardiovasc Imaging 29:625-31.

[12] Jaspers K, Freling HG, van Wijk K, et al., (2013) Improving the reproducibility of MR-derived left ventricular volume and function measurements with a semi-automatic threshold-based segmentation algorithm. Int J Cardiovasc Imaging 29:617-23.

[13] American Thoracic Society, American College of Chest Physicians, (2003) ATS/ACCP Statement on cardiopulmonary exercise testing. Am J Respir Crit Care Med 167:211-77.

[14] Latus H, Gummel K, Rupp S, et al., (2013) Beneficial effects of residual right ventricular outflow tract obstruction on right ventricular volume and function in patients after repair of tetralogy of fallot. Pediatr Cardiol 34:424-30.

[15] Hall JE, Guyton and Hall textbook of medical physiology. Saunders, 2010.

[16] Valente AM, Gauvreau K, Assenza GE, et al., (2013) Rationale and design of an International Multicenter Registry of patients with repaired tetralogy of Fallot to define risk factors for late adverse outcomes: the INDICATOR cohort. Pediatr Cardiol 34:95-104.

[17] Haddad F, Hunt SA, Rosenthal DN, et al., (2008) Right ventricular function in cardiovascular disease, part I: Anatomy, physiology, aging, and functional assessment of the right ventricle. Circulation 117:1436-48.

[18] Haddad F, Doyle R, Murphy DJ, et al., (2008) Right ventricular function in cardiovascular disease, part II: pathophysiology, clinical importance, and management of right ventricular failure. Circulation 117:1717-31.

[19] D'Andrea A, Caso P, Sarubbi B, et al., (2004) Right ventricular myocardial activation delay in adult patients with right bundle branch block late after repair of Tetralogy of Fallot. Eur J Echocardiogr 5:123-31.

[20] Cheung EW, Wong WH, Cheung YF, (2010) Meta-analysis of pulmonary valve replacement after operative repair of tetralogy of Fallot. Am J Cardiol 106:552-7.

[21] Oosterhof T, van Straten A, Vliegen HW, et al., (2007) Preoperative thresholds for pulmonary valve replacement in patients with corrected tetralogy of Fallot using cardiovascular magnetic resonance. Circulation 116:545-51.

[22] Geva T, (2011) Repaired tetralogy of Fallot: the roles of cardiovascular magnetic resonance in evaluating pathophysiology and for pulmonary valve replacement decision support. J Cardiovasc Magn Reson 13:9.

[23] van der Hulst AE, Hylkema MG, Vliegen HW, et al., (2012) Mild residual pulmonary stenosis in tetralogy of fallot reduces risk of pulmonary valve replacement. Ann Thorac Surg 94:2077-82.

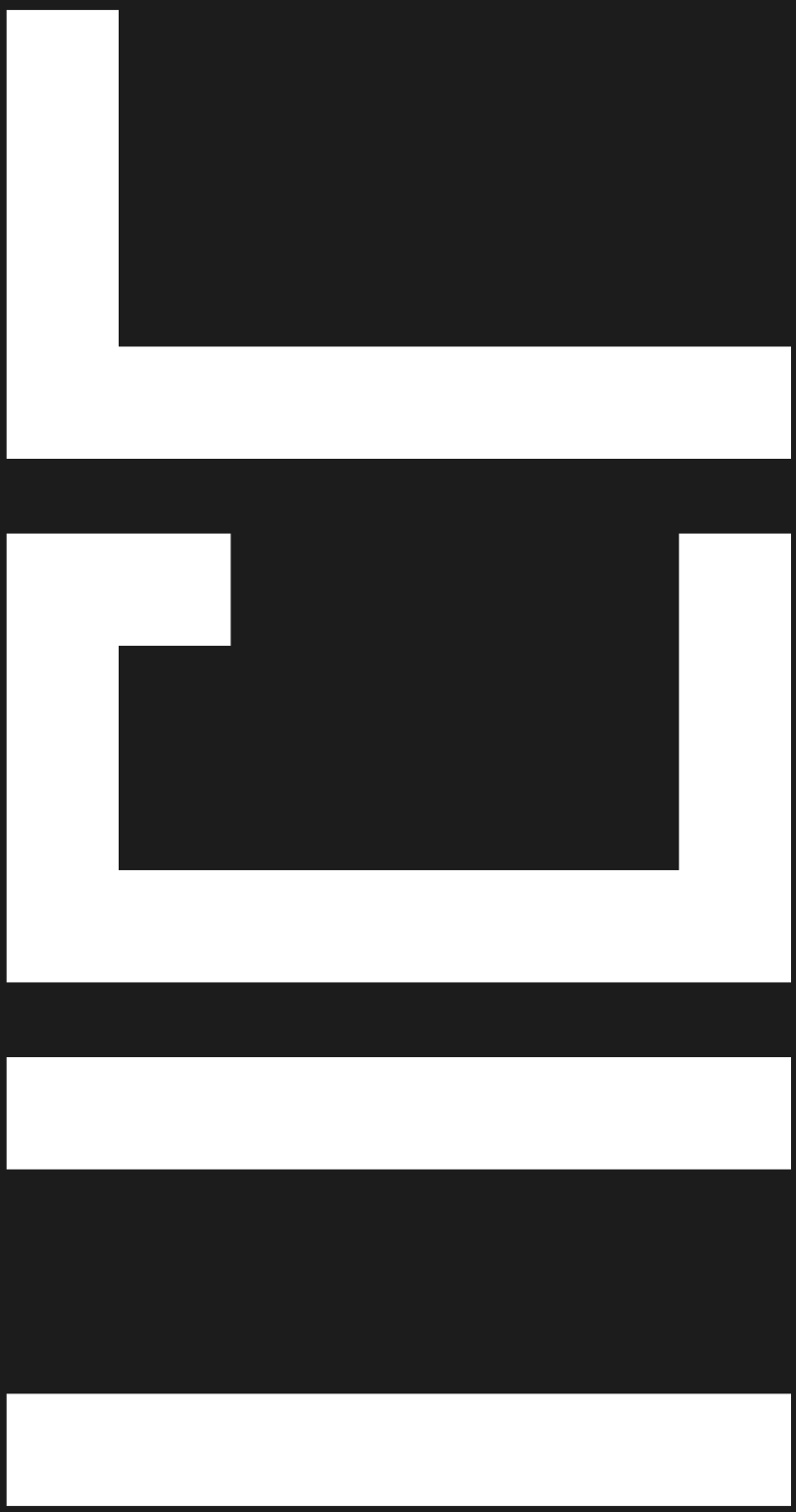

7

Measurements of right ventricular volumes and function in the PROSTAVA study

Hendrik G. Freling
Ymkje J. van Slooten
Joost P. van Melle
Barbara J.M. Mulder
Arie P.J. van Dijk
Hans L. Hillege
Marco C. Post
Gertjan Tj. Sieswerda
Monique R.M. Jongbloed
Tineke P. Willems
Petronella G. Pieper

Abstract

Background Data on long-term complications in adult patients with congenital heart disease (ACHD) and a prosthetic valve are scarce. Moreover, the influence of prosthetic valves on quality of life (QoL) and functional outcome in ACHD patients with prosthetic valves has not been studied.

Objectives The primary objective of the PROSTAVA study is to investigate the relation between prosthetic valve characteristics (type, size and location) and functional outcome as well as QoL in ACHD patients. The secondary objectives are to investigate the prevalence and predictors of prosthesis-related complications including prosthesis-patient mismatch.

Methods The PROSTAVA study, a multicentre cross-sectional observational study, will include approximately 550 ACHD patients with prosthetic valves. Primary outcome measures are maximum oxygen uptake during cardiopulmonary exercise testing and quality of life. Secondary outcomes are the prevalence and incidence of valve-related complications including prosthesis-patient mismatch. Other evaluations are medical history, physical examination, echocardiography, MRI, rhythm monitoring and laboratory evaluation (including NT-proBNP).

Implications Identification of the relation between prosthetic valve characteristics in ACHD patients on one hand and functional outcome, QoL, the prevalence and predictors of prosthesis-related complications on the other hand may influence the choice of valve prosthesis, the indication for more extensive surgery and the indication for re-operation.

** Addendum added to "Prosthetic valves in adult patients with congenital heart disease: Rationale and design of the Dutch PROSTAVA study"*

Neth Heart J. 2012 Oct;20(10):419-24.

Background

Due to the improved survival of children with congenital heart disease (CHD), the number of adults with CHD has increased and adult patients with CHD now outnumber children [1]. Prosthetic valves, mechanical or biological, are part of the treatment in many patients with CHD. Mechanical prosthetic valves may negatively influence quality of life because of the necessity for anticoagulation therapy, which can hamper the active lifestyle of young adult patients with CHD and which prevents women from going through untroubled and safe pregnancies [2]. Biological prosthetic valves are an alternative, but they have their own disadvantages, the most important of which is their high deterioration rate, especially in young patients and during pregnancy, inevitably leading to re-operation [3].

Both types of valves share another complication: prosthesis-patient mismatch (PPM). PPM is present when the effective orifice area (EOA) of the inserted prosthetic valve is too small in relation to body size. In adults with acquired heart disease, PPM is associated with increased morbidity and mortality [4]. The prevalence of PPM is probably high in adult patients with CHD, both with biological and with mechanical valves, because of somatic growth of patients after implantation of a small valve during childhood. A few small series have investigated mid- and long-term complications of prosthetic valves including PPM in children [5,6]. However, the prevalence of PPM and its consequences in adult patients with CHD are unknown.

Adult patients with CHD and a prosthetic valve differ from patients with acquired valve disease in terms of age, lifestyle and underlying disease. Additionally, the prevalence of tricuspid and pulmonary prosthetic valves is higher in adult patients with CHD. These differences may lead to a different outcome in terms of functional capacity and quality of life as well as to a distinct spectrum of long-term complications associated with prosthetic valves. However, the influence of prosthetic valves on quality of life and functional outcome in adult patients with CHD has not been studied, and data on long-term complications are scarce [7]. We intend to study these issues in an adult population with CHD and prosthetic valves. In this article we introduce the study design and describe the rationale of the 'Functional outcome and quality of life in adult patients with congenital heart disease and prosthetic valves (PROSTAVA) study'.

Methods

Study objectives

The primary objective of this multicentre cross-sectional observational study is to investigate the relationship between characteristics of valve prostheses (type, size, location) and functional outcome as well as quality of life in adult patients with CHD (objective 1). The secondary objectives of this study are to investigate the prevalence and predictors of PPM (objective 2) and the incidence of prosthesis-related complications (objective 3) in an adult CHD population.

Study population

Inclusion and exclusion criteria for objectives 1, 2 and 3 are shown in Table 1. All patients in the Dutch national CONCOR ('CONgenital CORvitia') database with valve prostheses (homografts, heterografts and mechanical valves) are eligible to participate in this study. Of the 900 identified patients, 702 were eligible for prospective investigation; by 15 February 2012, 406 of these patients with 424 valves were included in the PROSTAVA study (Fig. 1).

Table 1 Inclusion and exclusion criteria PROSTAVA

Inclusion criteria	Exclusion criteria
All objectives	All objectives
Included in the CONCOR database	Patient aged < 18 years
Prosthetic valve	
Objectives 1, 2	Objective 1, 2
Patients able to understand the study procedures	Pregnant or < 3 months after pregnancy
Patients willing to provide informed consent	Inability to complete QoL questionnaire
	Inability to perform cardiopulmonary aerobic capacity testing

CONCOR = CONgenital CORvitia; QoL = quality of life

Main procedures

Objective 1

Characteristics of valve prostheses (type, size and location) will be obtained from the medical records and from echocardiographic examination. For the evaluation

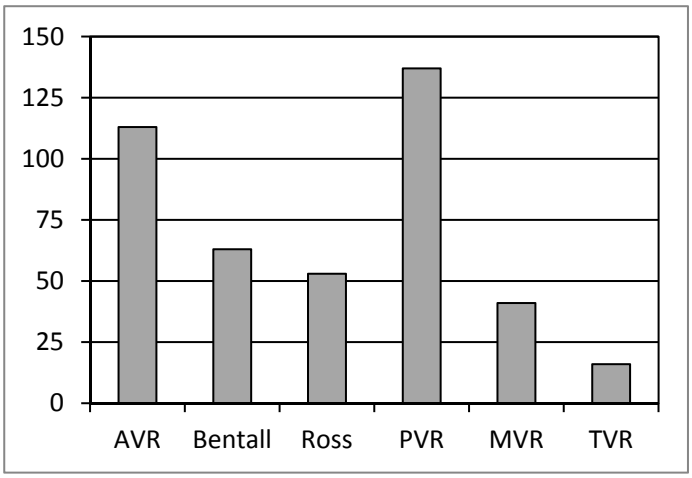

Figure 1. *Prosthetic valves included in the prospective part of the study by 15 February 2012. AVR = aortic valve replacement, PVR = pulmonary valve replacement, MVR = mitral valve replacement, TVR = tricuspid valve replacement*

of functional outcome and quality of life, cardiopulmonary aerobic capacity testing (CACT), New York Heart Association functional class and the SF-36 quality of life questionnaire will be used as primary outcome measures. Confounders which may influence the quality of life and functional outcome, such as ventricular function, native valve dysfunction and rhythm disorders, will be recorded using echocardiography, magnetic resonance imaging (MRI) and 24-hour Holter recording.

Objective 2

To investigate the prevalence and degree of PPM, echocardiography will be used to measure the EOA and calculate the indexed EOA (iEOA = EOA/Body Surface Area). Consequences of PPM including the presence and degree of ventricular hypertrophy, ventricular and atrial volumes, and pulmonary pressures will be measured with MRI and/or echocardiography. Possible predictors of PPM will be identified from the medical records, such as underlying heart disease, type of cardiac surgery, type and size of valve prosthesis and age at implantation.

Objective 3

The inventory of the patient's past medical history and present medical status (including current medical history and physical examination) will be used to record the incidence of prosthesis-related complications. Published guidelines will be used for the registration of complications [8]. To ensure completeness of data collection a patient interview will be used to check if any data were missed by studying the medical files; however, data that can not be verified from medical files are not qualified for entry in the database.

Laboratory evaluations will be performed to obtain information on heart failure and haemolysis. To detect rhythm disorders, ventricular hypertrophy and intraventricular conduction delays, electrocardiogram and 24-hour Holter monitoring will be used. Ventricular volumes, mass and function and prosthetic valve function will be assessed using echocardiography and MRI.

Cardiopulmonary aerobic capacity testing

The parameters to be recorded are: expected and achieved VO_2max, respiratory quotient, anaerobic threshold, blood pressure at rest and during exercise, and heart rate at rest and during exercise.

Quality of life questionnaire

Quality of life will be assessed using the short-form 36 health survey questionnaire. This questionnaire consists of 36 items to measure health and quality of life using a multi-item scale for eight different aspects: physical functioning, role of limitations due to physical problems, role of limitations due to emotional problems, social functioning, mental health, pain, energy/vitality and general health. Furthermore, there is a single item on changes in respondents' health over the past year.

Echocardiography

Two-dimensional echocardiography will be performed according to current guidelines to assess the function of prosthetic and native valves, to quantify chamber dimensions and left ventricular mass, and to assess chamber function. Pulmonary artery systolic pressure will be estimated and disease-specific evaluation performed. The EOA will be determined by the continuity equation using continuous and pulsed wave Doppler. For prosthetic valves, moderate PPM in the aortic and pulmonary valve position is defined as an iEOA of 0.65 – 0.85 cm^2/m^2 and severe PPM as iEOA ≤ 0.65 cm^2/m^2. For the mitral and tricuspid position, we will consider moderate PPM to be present when the iEOA is ≤ 1.25 cm^2/m^2 and severe PPM when the iEOA is ≤ 0.95 cm^2/m^2 [9,10].

Magnetic resonance imaging

Systemic and pulmonary ventricular function, volume and mass will be determined with a steady-state free precession cine sequence in the short-axis plane. Flow dynamics, including the regurgitation fraction of the aortic and pulmonary valve, will be assessed by using velocity-encoded MR imaging distal to the prosthetic

valve. It is expected that approximately 25% of the patients will have a contraindication for MRI (i.e. pacemaker).

Statistical and ethical considerations

Sample size Because this is an explorative study in a population where the prevalence of both valve characteristics (e.g. PPM) and the values for outcome measures are yet unknown, an appropriate sample calculation is not possible. However, the populations we expect to include are sufficiently large for all valve locations; therefore, meaningful outcomes can be expected.

Statistical analysis

Continuous variables will be expressed as mean and standard deviation when normally distributed or as median with interquartile ranges in case of non-normal distribution. Categorical variables will be presented as absolute numbers and percentages.

Groups will be compared by using independent Student's t-test for normally distributed continuous variables. Mann-Whitney U test will be used for comparisons of non-normally distributed continuous variables, and χ^2 test or Fisher's exact test for comparison of categorical variables. Univariate and multivariate logistic regression analysis will be performed to identify independent predictors for main outcome measures. All statistical analyses will be performed using the statistical software package SPSS version 16.0 or higher (SPSS Inc., Chicago, IL). All statistical tests are two-tailed and a P-value of <.05 is considered statistically significant.

Ethical considerations

The PROSTAVA study has been approved by the Medical Ethics Committee of all the participating hospitals (METc2009/270; NL29965.042.09). The study will be conducted in accordance with the Helsinki Declaration. Subjects will be asked to participate and sign a written informed consent form after having received written as well as oral information about the study.

Discussion

In the proposed PROSTAVA study, we will assess the implications of prosthetic valves in adult patients with CHD. We will have the opportunity to relate prosthetic valve characteristics to functional outcome and quality of life in a unique large-scale patient cohort. In addition we will investigate the incidence of complications related to prosthetic valve type, size and location in this adult population with CHD.

Valve type: biological or mechanical valve prosthesis

In children and young adults, biological valves are often implanted to avoid the disadvantages of oral anticoagulation therapy. The rate of structural valve degeneration is, however, high at young age. Structural valve deterioration results in progressive prosthesis dysfunction which will impair functional capacity and which ultimately leads to valve replacement. The influence of the amount and prospect of re-operations on quality of life in patients with CHD has only been studied in a relatively small population and seems to be limited [11]. However, parameters reflecting functional status are associated with satisfaction with life and perceived health [12]. Therefore we expect that structural valve deterioration in adult patients with CHD will influence quality of life through its impact on functional outcome, which we will elucidate in the PROSTAVA study.

Structural valve deterioration and re-operations can be avoided by use of mechanical prostheses. The risk of thromboembolic complications warrants the need for anticoagulation therapy resulting in an increased risk of bleeding complications. The cumulative risk of bleeding complications during life may well be high in young adults with CHD because of their long life expectancy after valve replacement. The risk of bleeding complications may be increased by the active lifestyle of many young adult patients with CHD. Frequent international normalised ratio (INR) controls are needed with anticoagulant therapy and patients are prevented from participating in risky sports activities. Poor compliance with warfarin therapy, which is not uncommon in adolescents, can increase the risk of thromboembolic complications. Pregnancy in women with mechanical valves bears the risk of foetal loss and embryopathy when oral anticoagulants are continued throughout pregnancy, while substitution with heparin increases the risk of thromboembolic complications [13,14]. Therefore, the impact of anticoagulation therapy is probably high in this young population. Our study will provide insight into the incidence and predictors of biological and

mechanical prosthesis-related complications in adult patients with CHD as well as the consequences for quality of life and functional outcome.

Valve size: the impact of PPM

When valve replacement is necessary in childhood, implantation of an adult-sized prosthetic valve is often not possible. With somatic growth in children, the iEOA decreases steadily until they reach adulthood. Therefore we expect that in our study population the prevalence of PPM will be high.

A few small series have investigated PPM in children [15]. However, in adult patients with CHD the prevalence and consequences of PPM are unknown. In patients with acquired valve disease, aortic PPM is associated with less improvement in symptoms and exercise capacity, less regression of left ventricular hypertrophy, more cardiac events and higher mortality [4,9,16]. Mitral PPM is associated with recurrence of congestive heart failure, pulmonary hypertension and decreased survival [10]. We expect that PPM in adult patients with CHD will further diminish the already compromised ventricular function and exercise capacity. This reduction in exercise capacity may negatively influence quality of life by limiting these patients in their daily activities. Our study will provide a comprehensive database with a long follow-up to present us with useful information on the incidence, predictors and consequences of PPM in adult CHD patients.

Valve location: right-sided versus left-sided prostheses

Prevalence of tricuspid and pulmonary prosthetic valves is relatively high in adult patients with CHD compared with patients with acquired valve disease. In right-sided mechanical prostheses thromboembolic risk is presumed to be higher compared with left-sided mechanical prostheses due to lower pressures and flow velocities in the right heart. Therefore, biological valves are the preferred valve type in the tricuspid and pulmonary position in most centres. Several recent studies have reported satisfactory results in pulmonary mechanical prostheses with aggressive anticoagulation, INR 3.0-4.5 [17,18]. However, data concerning long-term survival, and thromboembolic and bleeding complications are still limited. Available studies are small and the only large study with more than 30 patients has a short median follow-up of only 2 years. The proposed study gives the possibility to compare complications of pulmonary mechanical valves in a relatively large cohort (54 patients) and a cohort of patients with biological valves, with a long median follow-up duration of more than 6 years.

Limitations

A limitation of our study is the presence of multiple confounding factors such as the heterogeneity of patients with CHD, multiple types and locations of prosthetic valves and differences in ventricular function. Regression analysis will partially overcome this limitation. As patients who are not able to complete the CACT and quality of life questionnaire will be excluded from the prospective study, the study population will not entirely representative for adult patients with CHD and a prosthetic valve.

Another limitation comes with the use of the CONCOR database. This database started including patients with CHD in 2001. Patients who died before this date are not included, which will limit the possibility to investigate long-term mortality.

Conclusion

The PROSTAVA study is the first study to investigate the influence of prosthetic valve characteristics on functional outcome and quality of life in adult congenital heart disease patients. Our results may influence the choice of valve prosthesis, the indication for more extensive surgery and the indication for re-operation in patients with prosthesis patient mismatch.

Addendum

Magnetic resonance imaging

MRI is performed at least 6 months after valve implantation. Systemic and pulmonary ventricular function, volume and mass are determined with a steady-state free precession cine sequence in the short-axis plane for the left ventricle. Flow dynamics, including regurgitation fraction of the aortic and pulmonary valve, are assessed by using velocity-encoded MR imaging distal to the prosthetic valve. No contrast agent is given. Function and flow are quantitatively analyzed by the department of Radiology of the University Medical Center of Groningen using a commercial software package (QMass version, Medis, Leiden, The Netherlands). The end-systolic and end-diastolic frames were selected by visual assessment independently for the left and right ventricle. The basal slice was selected with aid of long-axis cine view images. The basal slice of the left ventricle was defined as the most basal slice surrounded for at least 50% by the left ventricular myocardium. When the pulmonary valve was visible in the right ventricular basal slice, only the portion of the right ventricular outflow tract below the level of the pulmonary valve was included. The inflow part of the right ventricle was included in the right ventricular volume. The right ventricular inflow part was distinguished from the right atrium by recognizing the trabeculated and thick right ventricular wall compared to the thin right atrial wall. Contours were drawn manually by tracing the endocardial and epicardial borders in every slice in end-systole and end-diastole. Contour tracing was aided by reviewing the multiple phase scans in the movie mode.

Discussion

We expect PPM to be uncommon in pulmonary prosthetic valves as most of these patients received relatively large prosthetic valves in their dilated right ventricular outflow tracts. However, almost all pulmonary and tricuspid valve replacements are performed using biological prosthetic valves. The main complication of this valve type is structural valve deterioration resulting in a combination of stenosis and regurgitation. Mechanical pulmonary valve prostheses show no substantial increase in gradient and regurgitation with time. Three years after pulmonary valve replacement, mechanical valve prostheses have a superior hemodynamic performance compared to homografts. With our study we can investigate whether patients with mechanical valve prosthesis also benefit in terms of right and left ventricular volumes and function, exercise capacity and quality of life. Furthermore, recent studies reported in patients without a pulmonary valve

replacement that combined right ventricular outflow tract obstruction and pulmonary regurgitation results in smaller right ventricular volumes and better ejection fraction compared to patients with isolated pulmonary regurgitation. We can investigate whether similar findings are present in patients with biological pulmonary valve replacements and structural valve deterioration.

References

[1] Marelli AJ, Mackie AS, Ionescu-Ittu R, et al., (2007) Congenital heart disease in the general population: changing prevalence and age distribution. Circulation 115:163-72.

[2] Drenthen W, Boersma E, Balci A, et al., (2010) Predictors of pregnancy complications in women with congenital heart disease. Eur Heart J 31:2124-32.

[3] Rahimtoola SH, (2010) Choice of prosthetic heart valve in adults an update. J Am Coll Cardiol 55:2413-26.

[4] Tasca G, Mhagna Z, Perotti S, et al., (2006) Impact of prosthesis-patient mismatch on cardiac events and midterm mortality after aortic valve replacement in patients with pure aortic stenosis. Circulation 113:570-6.

[5] Karamlou T, Jang K, Williams WG, et al., (2005) Outcomes and associated risk factors for aortic valve replacement in 160 children: a competing-risks analysis. Circulation 112:3462-9.

[6] Masuda M, Kado H, Ando Y, Shiose A, et al., (2008) Intermediate-term results after the aortic valve replacement using bileaflet mechanical prosthetic valve in children. Eur J Cardiothorac Surg 34:42-7.

[7] Oosterhof T, Meijboom FJ, Vliegen HW, et al., (2006) Long-term follow-up of homograft function after pulmonary valve replacement in patients with tetralogy of Fallot. Eur Heart J 27:1478-84.

[8] Akins CW, Miller DC, Turina MI, et al., (2008) Guidelines for reporting mortality and morbidity after cardiac valve interventions. J Thorac Cardiovasc Surg 135:732-8.

[9] Pibarot P, Dumesnil JG, (2000) Hemodynamic and clinical impact of prosthesis-patient mismatch in the aortic valve position and its prevention. J Am Coll Cardiol 36:1131-41.

[10] Pibarot P, Dumesnil JG, (2007) Prosthesis-patient mismatch in the mitral position: old concept, new evidences. J Thorac Cardiovasc Surg 133:1405-8.

[11] Loup O, von Weissenfluh C, Gahl B, et al., (2009) Quality of life of grown-up congenital heart disease patients after congenital cardiac surgery. Eur J Cardiothorac Surg 36:105,11; discussion 111.

[12] Moons P, Van Deyk K, De Geest S, et al., (2005) Is the severity of congenital heart disease associated with the quality of life and perceived health of adult patients? Heart 91:1193-8.

[13] Pieper PG, Balci A, Van Dijk AP, (2008) Pregnancy in women with prosthetic heart valves. Neth Heart J 16:406-11.

[14] Pieper PG, (2008) Expected and unexpected cardiac problems during pregnancy. Neth Heart J 16:403-5.

[15] Masuda M, Kado H, Tatewaki H, et al., (2004) Late results after mitral valve replacement with bileaflet mechanical prosthesis in children: evaluation of prosthesis-patient mismatch. Ann Thorac Surg 77:913-7.

[16] Tasca G, Brunelli F, Cirillo M, et al., (2005) Impact of valve prosthesis-patient mismatch on left ventricular mass regression following aortic valve replacement. Ann Thorac Surg 79:505-10.

[17] Waterbolk TW, Hoendermis ES, den Hamer IJ, et al., (2006) Pulmonary valve replacement with a mechanical prosthesis. Promising results of 28 procedures in patients with congenital heart disease. Eur J Cardiothorac Surg 30:28-32.

[18] Stulak JM, Dearani JA, Burkhart HM, et al., (2010) The increasing use of mechanical pulmonary valve replacement over a 40-year period. Ann Thorac Surg 90:2009,14; discussion 2014-5.

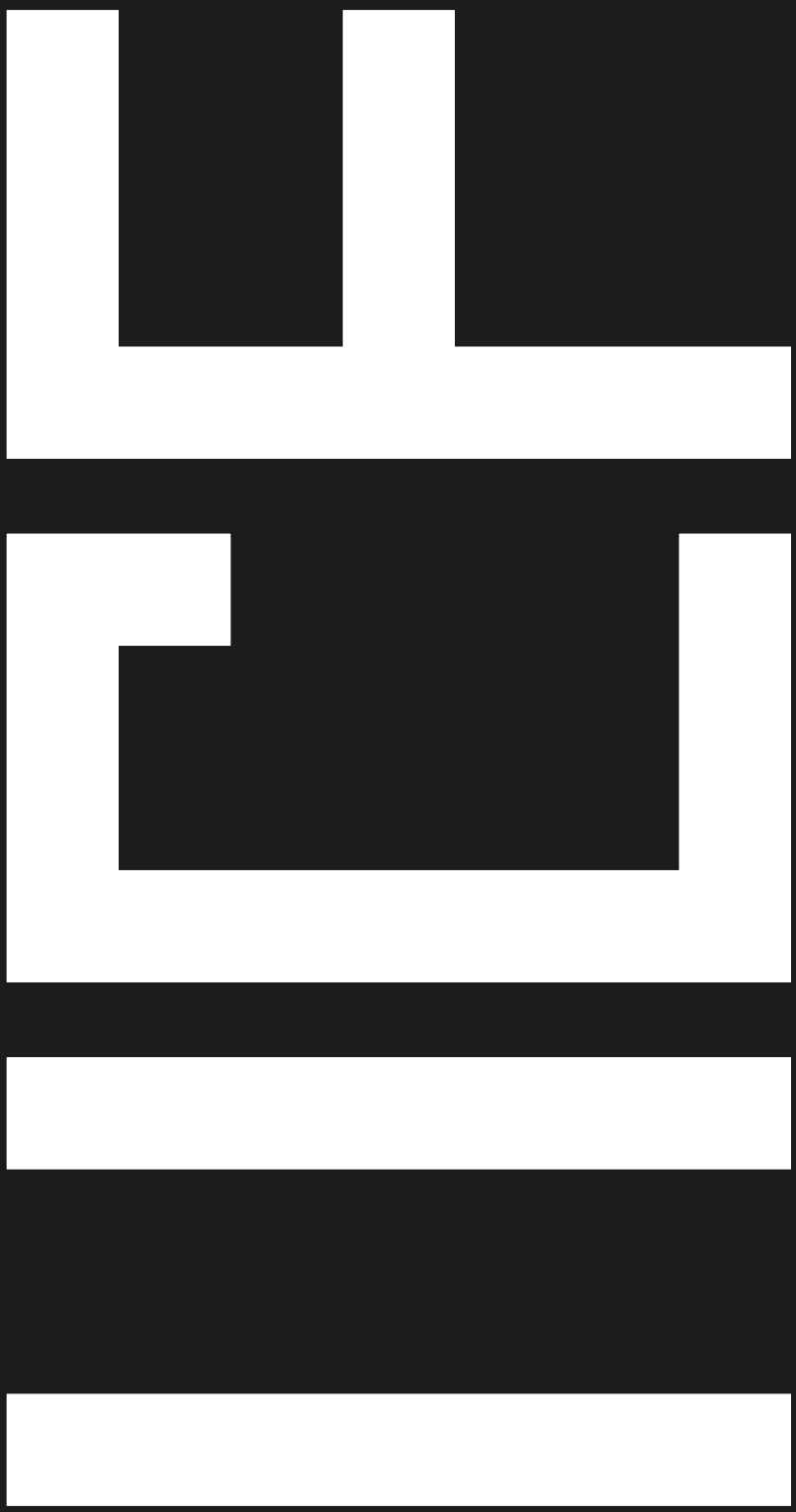

8

Summary

The introduction of palliative surgery led to an increased number of patients with complex congenital heart disease surviving into adulthood. At the same time sophisticated invasive and non-invasive imaging modalities became available. However, most patients develop long-term complications involving the right ventricle. The combination of a large group of patients with a dysfunctional right ventricle and new imaging modalities boosted our understanding of anatomy, physiology and pathophysiology of the right heart as well as improved care for patients with right sided congenital heart disease. Nowadays, imaging is considered a cornerstone in the follow-up of patients with congenital heart disease. Cardiac magnetic resonance is considered the gold standard for evaluation of cardiac volumes and function. Measurements of right ventricular volumes and function do not rely on assumptions of geometry but uses slice summation to calculate volumes, which are highly accurate and reproducible. However, knowledge on the used methodology and patient characteristics is essential for interpreting right ventricular volume measurements.

In **Chapter 1** a general introduction on the right ventricle is provided with a focus on imaging. **Chapter 2** evaluated the influence of independent selection of the end-systolic and end-diastolic frame for the right and left ventricle on cardiac magnetic resonance derived right ventricular volume measurements in patients with tetralogy of Fallot. Dyssynchrony resulting from a right bundle branch block in these patients significantly extends duration of right ventricular contraction and delays timing of right ventricular end-systole compared to the left ventricle. Additionally, timing of right ventricular ejection and end-diastole may be delayed in patients with tetralogy of Fallot. In some centers all right ventricular volumes are routinely measured in the left ventricular end-systolic and end-diastolic frame. We examined to what extent this result in a misrepresentation of right ventricular volumes. Right ventricular end-systolic volume using the right ventricular end-systolic instead of left ventricular end-systolic frame was smaller. Using the right ventricular end-systolic and end-diastolic frame hardly affected right ventricular end-diastolic volumes, while increasing the ejection fraction. QRS duration correlated positively with the changes in the right ventricular end-systolic volume and right ventricular ejection fraction when using the right ventricular instead of the left ventricular end-systolic and end-diastolic frame. We conclude that for clinical decision making in patients with tetralogy of Fallot and a right bundle branch block, right ventricular volumes should be measured in the end-systolic frame of the right ventricular and not of the left ventricle.

Current clinical practice is to include papillary muscles and trabeculae in the blood volume which introduces a bias in the measured volumes and ejection

fraction. This bias is generally accepted, as manually excluding the papillary muscles by drawing non-convex endocardial contours is even more time consuming and has demonstrated a higher intra- and inter-observer variability. An automated segmentation of blood and muscle could not only provide faster and more objective analysis, but may also yield more accurate estimations of cardiac volumes and function than the manual method. In **Chapter 3** we validated a novel semi-automatic threshold-based segmentation algorithm in an anthropomorphic heart phantom, and the left ventricle of twelve subjects with normal cardiac function. The semi-automatic threshold-based segmentation software we developed classified voxels within the epicardial contour as either blood or muscle according to their signal intensity, taking into account spatial variations in signal intensity. We showed that this semi-automatic method could exclude left ventricular endoluminal muscular structures from the blood volume with significantly improved intra- and inter-observer variabilities in function measurements compared to the conventional, manual method, which includes endoluminal structures in the blood volume.

Chapter 3 was limited to the left ventricle. Therefore, we used the same software in **Chapter 4** to measure trabecular volume of the right ventricular in adult patients with repaired tetralogy of Fallot. The main complication after repair for tetralogy of Fallot is right ventricular volume overload due to pulmonary regurgitation. Furthermore, many patients have some amount of pressure overload caused by residual outflow tract obstruction, stenosis of a pulmonary artery branch or stenosis of a valve prosthesis. These residual lesions result in right ventricular dilatation and hypertrophy. Consensus is lacking on whether to consider trabeculae and papillary muscles as part of measured right ventricular volumes. In healthy subjects and patients without congenital heart disease, the influence of trabeculae and papillary muscle on right ventricular volumes is too small to be of clinical importance. However, in patients with repaired tetralogy of Fallot the increase in papillary muscles and trabeculae can be large. As timing of re-operations is guided by right ventricular volumes, the effect of including papillary muscles and trabeculae in the right ventricular blood volume is of clinical importance. We showed that the semi-automatic threshold-based segmentation software provided a reproducible method to differentiate right ventricular myocardium from blood. Compared to including papillary muscle and trabeculae from the right ventricular blood volume, exclusion of the papillary muscle and trabeculae in the right ventricular blood volume resulted in clinical significantly decreased end-systolic and end-diastolic volumes and increased ejection fraction and mass.

In **Chapter 5** the impact of trabeculae and papillary muscles on right ventricular volumes and function was assessed in different patient groups with pressure overloaded right ventricles using the same software as in Chapters 3 and 4. As already shown in Chapter 4, exclusion of trabeculae and papillary muscles from the right ventricular blood volume result in significant and potentially clinically relevant differences in right ventricular volumes, right ventricular ejection fraction and right ventricular mass. Furthermore the impact of trabeculae on right ventricular volumes and function differed markedly depending on the underlying etiology of right ventricular pressure overload.

Chapter 6 evaluated the effects of right ventricular outflow tract obstruction on exercise capacity, right ventricular volumes, function and mass in adult patients with tetralogy of Fallot and volume overload due to pulmonary regurgitation. Recent studies demonstrated that patients with tetralogy of Fallot and combined pulmonary regurgitation and right ventricular outflow tract obstruction have smaller right ventricular volumes and higher ejection fraction compared to patients with isolated pulmonary regurgitation. New York Heart Association functional class was not different between both patient groups. However, since functional class is known to be poorly correlated with objective exercise capacity, it remained unclear what the effect of right ventricular outflow tract obstruction is on exercise capacity. We were the first to show that patients with combined right ventricular outflow tract obstruction and pulmonary regurgitation have reduced exercise capacity despite more favourable right ventricular volumes at rest compared to patients without right ventricular outflow tract obstruction. Furthermore, peak pressure gradient across the right ventricular outflow tract was the only independent predictor of percentage of predicted peak oxygen uptake. Therefore, exercise testing as well as cardiac magnetic resonance imaging should be interpreted in conjunction with the presence of right ventricular outflow tract obstruction.

Due to the improved survival of children with congenital heart disease, the number of adults with congenital heart disease has increased and adult patients with congenital heart disease now outnumber children. Many of these patients have prosthetic valves as part of their treatment. The influence of prosthetic valves on quality of life and functional outcome in adult patients with congenital heart disease has not been studied, and data on long-term complications are scarce. Therefore, the multicenter cross-sectional observational study described in **Chapter 7** will assess the implications of prosthetic valves in adult patients with congenital heart disease.

Future directions

Imaging is becoming more and more important in medicine, especially in the care for grown-ups with congenital heart disease. The main purpose of this thesis on imaging of the right ventricle is to improve care for patients with congenital heart disease as decisions to re-operate or initiate medical therapy are increasingly based on cardiac volumes and function. In the (near) future budgets for research are more likely to decrease than increase. Therefore, improving care for patients with congenital heart disease will become more dependent on retrospective studies. To make these future retrospective studies a success, standardisation in clinical management is the key. Currently, in many patients echocardiography, magnetic resonance imaging, exercise testing and biomarkers are not performed at regular intervals or combined with each other. Therefore, to boost the number and size of future retrospective studies we should put more effort in developing protocols for examining patients with congenital heart disease and especially in the compliance to these protocols.

Important in this setting is also a thorough description of the used methodology (e.g. inclusion or exclusion of trabeculae) as methods change during time. We showed that methodology can have a profound impact on the measurements of right ventricular volumes and function. Interpretation of studies which used different methodologies is difficult or even impossible when the used methodology is not clearly described. To guarantee high accuracy and reproducibility of cardiac volume and function measurements, post-processing should be easy and uniform. Independent selection of the end-systolic phase can be implemented in clinical practice with great ease. Furthermore, the semi-automatic threshold-based software described in this thesis is currently being implemented in commercial software. Widespread application of this software may be a step forward in the direction of achieving uniformity of right ventricular volume measurements, which would be of great importance for research and cooperation between centers.

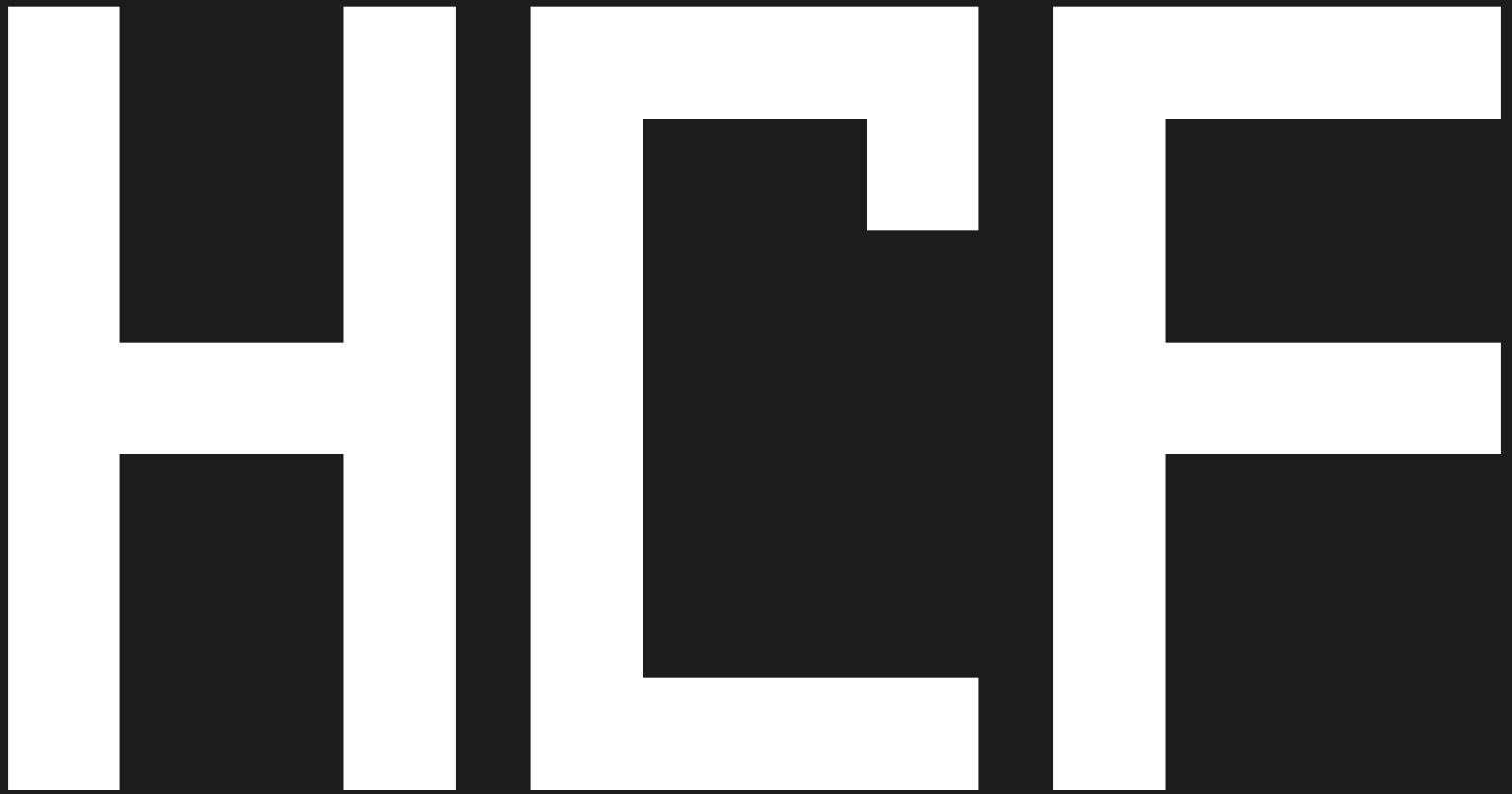
HCF

9

Nederlandse samenvatting

De afgelopen decennia zijn er twee belangrijke ontwikkelen geweest die nog steeds gaande zijn. Door nieuwe operatietechnieken en verbeterde zorg op de kinder en volwassen leeftijd is de levensverwachting van patiënten met een complexe aangeboren hartafwijking sterk toegenomen. Daarnaast zijn er nieuwe invasieve en non-invasieve methoden ontwikkeld om het hart af te beelden. Bij patiënten met een aangeboren hartafwijking wordt hier veelvuldig gebruik van gemaakt aangezien veel patiënten op volwassen leeftijd complicaties krijgen van de rechter kamer van het hart. De combinatie van een grote groep patiënten met problemen van de rechter kamer en nieuwe beeldvormende technieken heeft geleid tot een sterke toename in kennis over anatomie, fysiologie en pathofysiologie van de rechter kamer alsmede verbeterde zorg voor patiënten met rechtszijdige aangeboren hartafwijkingen. Tegenwoordig is beeldvorming een van de hoekstenen in de zorg voor patiënten met een aangeboren hartafwijking. MRI van het hart wordt hierbij beschouwd als de gouden standaard voor het bepalen van de hartvolumes en functie. MRI is erg nauwkeurig en reproduceerbaar doordat er geen aannames worden gedaan over de vorm van de rechterkamer maar gebruik maakt van 'slice summation', dat wil zeggen dat hartvolumes van iedere gescande plak bij elkaar worden opgeteld. Van belang is hierbij dat men weet hoe er gemeten is aangezien de meetmethode van grote invloed kan zijn op de gemeten volumes. Daarnaast is bij de interpretatie van de gevonden volumes informatie over de patiëntenkarakteristieken onmisbaar.

In **Hoofdstuk 1** word een algemene introductie gegeven over de rechter kamer met een focus op de beeldvorming. In **Hoofdstuk 2** hebben we middels MRI de volumes van de rechter hartkamer gemeten in de eind-systolische en eind-diastolische fase van zowel de rechter als linker kamer bij volwassen patiënten met een gecorrigeerde tetralogie van Fallot. Vrijwel al deze patiënten hebben een rechter bundeltakblok waardoor de rechter kamer langzamer samentrekt en het moment van de eind-systole later valt vergeleken met de linker kamer. Daarnaast valt mogelijk ook de eind-diastolische fase later. In sommige ziekenhuizen is het de gewoonte om alle rechter kamervolumes te meten in de eind-systolische en eind-diastolische fase van de linker kamer. Wij laten zien dat rechter kamer volumes gemeten in de eind-systolische en einddiastolische fase van de rechter kamer in plaats van de linker eind-systolische en eind-diastolische fase resulteerde in kleinere rechter kamer eind-systolische volumes, hogere ejectie fracties en vrijwel geen verschil in eind-diastolische volumes. Bij een toename in QRS duur namen deze verschillen toe voor wat betreft eind-systolisch volume en ejectie fractie. Wij concluderen dat het klinisch relevant kan zijn om bij patiënten met een tetralogie

van Fallot en een rechter bundeltakblok, de rechter kamervolumes te meten in de eind-systolische fase van de rechter kamer en niet die van de linker kamer.

Vaak worden de papillairspieren en trabeculae tot het bloedvolume gerekend bij het meten van hartvolumes middels MRI waardoor er te grote bloedvolumes worden gemeten. Deze meetfout wordt over het algemeen geaccepteerd omdat handmatig excluderen van alle papillairspieren en trabekels door het tekenen van extra contouren zeer veel tijd kost en slecht te reproduceren is. Semi-automatische segmentatie van bloed en spier zou de hartvolumes niet alleen sneller en objectiever kunnen bepalen, maar ook nog eens accurater kunnen zijn dan handmatig de volumes te bepalen. In **Hoofdstuk 3** valideren we een nieuwe semi-automatische methode in een hartfantoom en twaalf linker kamers bij personen met een normale hartfunctie. Het algoritme classificeert voxels binnen de epicardiale hartcontour als bloed of als spier afhankelijk van de signaal intensiteit waarbij rekening wordt gehouden met spatiële variaties in de signaalintensiteit. Wij laten zien dat deze semi-automatische methode trabekels en papillairspieren uit het bloedvolume kan excluderen met een significant verbeterde intra- en interobserver reproduceerbaarheid vergeleken met de conventionele manuele methode waarbij deze structuren tot het bloedvolume worden gerekend.

Hoofdstuk 3 beperkte zich tot de linker kamer. Daarom hebben we in **Hoofdstuk 4** dezelfde software gebruikt om het volume van trabekels en papillairspieren te meten in de rechter kamer van volwassen patiënten met een gecorrigeerde tetralogie van Fallot. De belangrijkste complicatie na correctie van een tetralogie van Falot is rechter kamer volumeoverbelasting door pulmonaalklepinsufficiëntie. Daarnaast hebben veel patiënten enige mate van drukoverbelasting door een resterende uitstroombaan obstructie, stenose van een pulmonalistak of stenose van een kunstklep. Deze resterende afwijkingen resulteren in rechter ventrikel dilatatie en hypertrofie. Er is geen consensus bij het meten van de rechter kamer of de trabekels en papillairspeieren gerekend moeten worden tot de ventrikel bloedvolumes of spiermassa. Bij gezonde vrijwilligers en patiënten zonder aangeboren hartafwijking is de invloed van trabekels en papillairspieren op de gemeten rechter ventrikel volumes te klein om van klinisch belang te zijn. Echter, bij patiënten met een aangeboren hartafwijking kan de toename in trabekels en papillairspieren groot zijn. Aangezien het moment van opereren gedeeltelijk bepaald wordt door de gemeten rechter kamervolumes kan het van klinisch belang zijn om te weten wat het effect is van papillairspieren en trabekels te includeren in de gemeten bloedvolumes. Wij laten zien dat de semi-automatische software een reproduceerbare methode is om spier van bloed te

scheiden. Exclusie vergeleken met inclusie van papillairspieren en trabekels in het rechter kamervolume resulteert in significant kleinere eind-systolische en eind-diastolische volumes en grotere rechter kamer massa en ejectiefractie welke klinisch significant zouden kunnen zijn.

In **Hoofdstuk 5** wordt met behulp van dezelfde software als in Hoofdstuk 3 en 4 de invloed van inclusie of exclusie van trabekels en papillairspieren op rechter kamer volumes en functie onderzocht bij groepen patiënten met een verschillende mate van drukoverbelasting van de rechter kamer. Net als bij de patiënten in hoofdstuk 4, resulteerde exclusie van trabekels en papillairspieren tot significante en mogelijk klinische relevante verschillen in rechter ventrikel volumes, ejectiefractie en massa. De invloed van trabekels op de rechter kamer metingen waren sterk afhankelijk van het onderliggend ziektebeeld.

In **Hoofdstuk 6** wordt het effect bekeken van rechter kamer uitstroombaanobstructie op inspanningsvermogen, rechter kamervolumes, functie en massa bij volwassen patiënten met een gecorrigeerde tetralogie van Fallot en volumeoverbelasting door pulmonalisklepinsufficientie. Recente onderzoeken hebben laten zien dat patiënten met een gecorrigeerde tetralogie van Fallot en gecombineerde pulmonalisinsufficientie en rechter kamer uitstroombaan obstructie kleinere rechter kamervolumes en een hogere ejectie fractie hebben vergeleken met patiënten met geïsoleerde pulmonalisinsufficientie. New York Heart Association functionele klasse was niet verschillend tussen beide patiëntengroepen. Van deze functionele klasse is echter bekend dat er een slechte correlatie is met het objectief gemeten inspanningsvermogen. Daarom is het onduidelijk wat de invloed is van rechter ventrikel uitstroombaanobstructie op het inspanningsvermogen. Wij laten zien dat patiënten met een gecombineerde rechter ventrikel uitstroombaanobstructie en pulmonalisklepinsufficiëntie vergeleken met patiënten met een geïsoleerde pulmonalisklepinsufficientie een verminderd objectief bepaald inspanningsvermogen hebben ondanks betere rechter ventrikel volumes in rust. Daarnaast was de piekdrukgradient over de rechter uitstroombaan de enige onafhankelijke voorspeller van het percentage van voorspelde piek zuurstofopname. Daarom zou zowel inspanningsonderzoek als rechter kamer metingen geïnterpreteerd moeten worden met kennis over de aanwezigheid van een rechter kamer uitstroombaanobstructie.

Door de verbeterde overleving van kinderen met een aangeboren hartafwijking is het aantal volwassen patiënten met een aangeboren hartafwijking sterk toegenomen en is het aantal volwassen patiënten inmiddels groter dan het aantal kinderen. Veel van deze volwassen patiënten hebben een nieuwe hartklep gekregen als onderdeel van hun behandeling. De invloed van nieuwe hartkleppen

op kwaliteit van leven en inspanningsvermogen bij volwassen patiënten met een aangeboren hartafwijking is nog niet onderzocht, en gegevens over lange termijn complicaties zijn schaars. Daarom zal het multicenter cross sectionele observationele onderzoek beschreven in **Hoofdstuk 7** de gevolgen van kunstkleppen onderzoeken in volwassen patiënten met een aangeboren hartafwijking. In dit proefschrift wordt de rol van beeldvorming van de rechter kamer in dit onderzoek uitgelicht.

Toekomst

Beeldvorming wordt steeds belangrijker in de geneeskunde, vooral bij het bepalen van het beleid bij volwassenen met een aangeboren hartafwijking. Het belangrijkste doel van dit proefschrift over beeldvorming van de rechter hartkamer is daarom ook het verbeteren van deze zorg aangezien het besluit te re-opereren of andere therapie te starten vaak gebaseerd wordt op metingen van het hart middels MRI. In de (nabije) toekomst is het waarschijnlijk dat financiering van onderzoek onder druk komt te staan. Daarom zal retrospectief onderzoek steeds belangrijker worden. Om ervoor te zorgen dat er in de toekomst goede retrospectieve onderzoeken gedaan kunnen worden is het nu al belangrijk om veel onderzoeken gestandaardiseerd uit te voeren. In de huidige praktijk is het vaak zo dat patiënten een echo hart, MRI hart, inspanningsonderzoek en biomarkers niet met een vaste regelmaat of gecombineerd worden uitgevoerd. Om het aantal en de grootte van toekomstige retrospectieve onderzoeken te bevorderen zouden we meer inspanningen moeten leveren om protocollen te ontwikkelen voor patiënten met een aangeboren hartafwijking en zich ook aan de protocollen te houden.

Belangrijk in deze setting is om de gebruikte methode nauwkeurig te beschrijven (b.v. inclusie of exclusie van trabekels) aangezien methodes veranderen gedurende de jaren. Interpretatie van onderzoeken die andere methodes hebben gebruikt is vaak moeilijk of zelfs onmogelijk wanneer het niet goed beschreven is. Om een hoge mate van nauwkeurigheid en reproduceerbaarheid te garanderen moet analyseren van de MRI beelden makkelijk en uniform zijn uit te voeren. Onafhankelijke selectie van de eind-systolische plak is makkelijk te implementeren in de klinische praktijk. Daarnaast wordt de semi-automatische software die gebruikt is in dit proefschrift op moment van schrijven geïmplementeerd in reeds bestaande commercieel verkrijgbare software. Wijdverspreid gebruik van deze software kan een eerste stap zijn richting het uniform meten van rechter hartkamer volumes waardoor makkelijker samen onderzoek te doen valt met andere medische centra.


HGF

10

Dankwoord
About the author
List of publications

Dankwoord

Vader worden, verhuizen, toetreden tot TR125, beginnen met de opleiding tot radioloog. Dit zijn allemaal gebeurtenissen die grote invloed hebben (gehad) op mijn leven de afgelopen jaren. Mijn promotietraject is nu ten einde en hoort ook in dit rijtje thuis. Maar dit proefschrift is niet alleen mijn verdienste. Zonder de bijdrage van velen was het nooit zover gekomen of waren de afgelopen jaren lang niet zo gezellig geweest. Een aantal personen wil ik graag in het bijzonder bedanken.

Allereerst wil ik mijn promotor, Dirk Jan, bedanken. Hoewel mijn proefschrift uiteindelijk vrijwel geheel gericht is op de radiologische kant van mijn werk de afgelopen jaren waren jouw suggesties wat betreft de opbouw en boodschap van artikelen van onschatbare waarde.

Tineke, mijn co-promotor, zonder jou was dit proefschrift zeker niet mogelijk geweest. Jouw enthousiasme en grote betrokkenheid hebben mij er mede van overtuigd om toch door te gaan met het onderzoek nadat ik eigenlijk besloten had te stoppen. Daarnaast zit je altijd barstensvol goede onderzoeksideeen waarvan we er vele hebben uitgewerkt.

Els, mijn tweede co-promotor, ik ben je dankbaar dat ik samen met Ymkje de PROSTAVA studie heb mogen uitvoeren. Ik heb heel veel van je geleerd.

Joost, hoewel je niet mijn co-promotor was, was je samen met Els de tweede begeleider van PROSTAVA. Mede dankzij jouw inzet en gedrevenheid hebben we een groot aantal patiënten kunnen includeren.

Petra en Martijn, mijn kamergenoten, wil ik graag bedanken voor de gezellige tijd die we hebben gehad. Petra, zonder jou had ik niet kunnen promoveren. Jij bent een keiharde werker die mij altijd met raad en daad terzijde stond als ik ergens niet uit kwam. Daarnaast stel ik jouw oprechtheid en persoonlijke interesse erg op prijs. Martijn, wat hebben wij een plezier beleefd aan het spelen van Bomberman in de pauze. Maar het meest heb ik nog genoten van ‘Promoveren in een gekkenhuis’ dat wij samen gemaakt hebben voor Petra. Daarvan heb ik nog wel het meest geleerd dat je samen meer bereikt dan in je eentje.

Ymkje, mijn PROSTAVA maatje, wil ik graag bedanken voor de vele gezellige en nuttige momenten. Ik ben blij dat ik samen met jou dit project heb mogen doen.

Iedereen op de researchafdeling van de radiologie bedanken voor de prettige sfeer en de samenwerking. Karolien wil ik met name bedanken voor de samenwerking aan de artikelen over semi-automatische software. Martijn van Swieten, bedankt voor het doen van vele inter-observermetingen. Stella, als researchcoordinator ben jij onmisbaar voor iedereen die onderzoek doet bij de radiologie. Je kunt goed luisteren en geeft praktische adviezen wanneer nodig. Hoewel mijn vaste werkplek op de radiologie was wil ik ook graag de onderzoekers op de cardioresearch bedanken. Als ik er was, was het altijd gezellig. De secretaresses van de cardiologie, Alma en Audrey, wil ik graag bedanken voor alle hulp gedurende mijn promotietraject. Anna en Philemon, de studenten van Ymkje en mij, zonder jullie was de data nooit op tijd binnen geweest. De segmentatie methode is ontwikkeld door Medis. Daarom wil ik in het bijzonder Kees bedanken voor het schrijven van de software. David, ik vond het altijd erg leuk om te zien hoe enthousiast jij bezig was met het verbeteren van jullie producten en dat ik veel van mijn input ook terug zag in nieuwe versies. Alle co-auteurs van mijn artikelen wil ik graag bedanken voor hun bijdrage aan dit proefschrift. Graag wil ik ook alle mensen bedanken in de centra waar ik vanwege de PROSTAVA studie ben geweest. Mieke wil ik in het bijzonder bedanken, jij hebt mij veel werk uit handen genomen in Utrecht.

Graag wil ik ook alle andere die ik nog niet genoemd heb, maar wel op de één of andere manier betrokken zijn geweest bij dit proefschrift.

Lieve Gienke, bedankt voor je eindeloze liefde, begrip en support. Ik weet niet wat ik zonder jou zou moeten. Jochem en Stijn, jullie doen mij beseffen wat echt belangrijk is in het leven.

About the author

Hendrik Freling was born on 24th of February, 1985 in IJsselstein, the Netherlands. He grew up in Maastricht and Hoogeveen. He attended high school at the Roelof van Echten College in Hoogeveen, where he graduated in 2003. In September 2003 he started to study Medicine at the University of Groningen. He went to the Scheper Ziekenhuis Emmen for his internships. In 2003 he started his senior internship at the department of Radiology in the University Medical Center Groningen and at the department of Cardiology in the Isala Clinics Zwolle. He graduated as Medical Doctor in September 2009.

After his graduation, he started working in a research position at the department of Radiology at the University Medical Center Groningen. After one year he also started working for the department of Cardiology on a project of the Netherlands Heart Foundation. He presented his research topics at various international congresses, including the Radiological Society of North America, European Congress of Radiology and the European Society of Cardiac Radiology. In July 2013, he started his residency in Radiology at the University Medical Center Groningen.

List of publications

[1] Freling HG, van Slooten YJ, van Melle JP, Mulder BJ, van Dijk AP, Hillege HL, Post MC, Sieswerda GT, Jongbloed MR, Willems TP, Pieper PG; PROSTAVA investigators. (2012) Prosthetic valves in adult patients with congenital heart disease: Rationale and design of the Dutch PROSTAVA study. Neth Heart J. 20(10):419-24.

[2] Freling HG, Pieper PG, Vermeulen KM, van Swieten JM, Sijens PE, van Veldhuisen DJ, Willems TP. (2013) Improved cardiac MRI volume measurements in patients with tetralogy of Fallot by independent end-systolic and end-diastolic phase selection. PLoS One.8(1):e55462.

[3] Freling HG, van Wijk K, Jaspers K, Pieper PG, Vermeulen KM, van Swieten JM, Willems TP. (2013) Impact of right ventricular endocardial trabeculae on volumes and function assessed by CMR in patients with tetralogy of Fallot. Int J Cardiovasc Imaging. 29(3):625-31.

[4] Jaspers K, Freling HG, van Wijk K, Romijn EI, Greuter MJ, Willems TP. (2013) I mproving the reproducibility of MR-derived left ventricular volume and function measurements with a semi-automatic threshold-based segmentation algorithm. Int J Cardiovasc Imaging. 29(3):617-23.

[5] van Slooten YJ, Freling HG, van Melle JP, Mulder BJ, Jongbloed MR, Ebels T, Voors AA, Pieper PG. (2013) Long-term tricuspid valve prosthesis-related complications in patients with congenital heart disease. Eur J Cardiothorac Surg. [Epub ahead of print]

[6] Freling HG, Willems TP, van Melle JP, van Slooten YJ, Bartelds B, Berger RFM, van Veldhuisen DJ, Pieper PG. Effect of right ventricular outflow tract obstruction on right ventricular volumes and exercise capacity in patients with repaired tetralogy of Fallot. Accepted in Am J Cardiol

[7] Driessen MMP, Baggen VJM, Freling HG, Pieper PG, van Dijk AP, Doevendans PA, Snijder RJ, Post MC, Meijboom FJ, Sieswerda GTj, Leiner T, Willems TP. Pressure overloaded right ventricles: a multicenter study on the importance of trabeculae in right ventricular function measured by CMR. Accepted in Int J Cardiovasc Imaging